

Forensic Electrochemistry: Developing Electrochemical Sensors for the Detection of Illicit Compounds

Jamie P Smith

*Submitted in partial fulfilment of the requirements of Manchester
Metropolitan University for the degree of Doctor of Philosophy*

2015

School of Science and the Environment

Division of Chemistry and Environmental Science

Manchester Metropolitan University



**Manchester
Metropolitan
University**

Abstract

The following thesis reports the development of novel electrochemical protocols to further expand the niche research area of *Forensic Electrochemistry*. 0 introduces the key fundamental concepts within electrochemistry detailing why it is a significant analytical tool. Also described within this chapter are prior examples of electrochemistry used within in a forensic environment to further justify the use of such techniques in this work setting a solid foundation for the development of electrochemical sensors for previously undetected (electrochemically) materials.

Chapter 2 focuses on the growing epidemic of “*Legal Highs*” formally known as “*Novel (New) Psychoactive Substances*” (NPSs) that, at the time of this research is a major concern for drug authorities. Highlighted within is the multitude of existing techniques to analyse NPSs yet unable to simultaneously detect in-the-field with great sensitivity.

Chapter 3 provides a summation of the materials employed in this research in addition to the experimental procedures. Furthermore, a brief synopsis of the screen-printing methodology is provided in order to deliver further understanding of the novel electrochemical sensors that are used throughout the thesis.

Chapter 4 explores the use of screen-printed electrodes) as a novel electrochemical sensor for illicit compounds; with a particular focus on the NPS *mephedrone* (4-MMC; MKat; the most commonly abused NPS). The common ‘date-rape’ drug Rohypnol® (flunitrazepam) is also detected using screen-printed electrodes for the first time.

The concept of screen-printed electrodes as a novel detector for illicit materials is expanded within Chapter 5 exploring different carbon materials utility as a sensor as well as the avant-garde field of study “*Regal Electrochemistry*” which utilises British Currency (GBP) to successfully quantify 4-MMC. Finally, Chapter 6 provides a summary and conclusion of the presented work highlighting the societal impact of such research whilst also posturing future work to ensure the field of *Forensic Electrochemistry* continues to grow.

Aims and Objectives

The principal aim of this thesis is the development of a novel sensing protocol towards illicit compounds and in particular, *Novel Psychoactive Substances* (NPSs) to tackle the growing epidemic postured by such compounds and expand the field of *Forensic Electrochemistry*.

The key objectives of this study were:

- Compare and contrast existing methodologies for the detection of illicit compounds (particularly NPSs) and evaluate their utility for in-the-field detection.
- Utilise graphite screen-printed electrodes (useful in light of their portability and low production cost) towards the detection of illicit compounds.
- Application of the novel sensing protocol in 'real' samples (i.e. seized street samples and/or spiked samples) such as those encountered within routine forensic casework.
- Exploration and evaluation of new materials towards the sensing of commonly used/abused NPSs (see above).

Acknowledgements

Like guiding Scunthorpe United to promotion, a great task is seldom complete by one's self – the completion of this PhD was no different and necessitated a wealth of support that thankfully, I had.

First and foremost, I would like to thank my supervisory team comprising of Professor Craig Banks and Dr Oliver Sutcliffe. Throughout the years of my study I was continually pressed to reach higher, work harder, and delve deeper – because of this, I feel I have grown tremendously as a person and this would not have been possible without these mentors.

There have been a great number of peers that I have encountered throughout the duration of this degree that I would be happy to count amongst friends. In no particular order: Dr Dimitrios Kampouris, Dr Jonathan Metters, Dr Dale Brownson, Dr Edward Randviir, Dr Athanasios Kolliopoulos and Joanna Kamieniak have all supported me in one way or another – from explaining technical nuances to carousing, they could always be counted on and their support (*and camaraderie*) cannot go understated.

None of this would have been possible were it not for the studentship provided by the School of Chemistry and the Environment, affording me the opportunity to continue my learning, experience a profound personal development and live in what I believe to be the greatest city in the world.

Lastly, it would be wrong of me to not mention my parents. They brought me into this world, kept me relatively out of trouble and have always believed in me. A sturdy foundation goes a long way and I hope to one-day repay all the faith that has been placed in me to succeed.

Thank you all, sincerely.

"Gatsby believed in the green light, the orgastic future that year by year recedes before us. It eluded us then, but that's no matter -- tomorrow we will run faster, stretch out our arms farther... And one fine morning -- So we beat on, boats against the current, borne back ceaselessly into the past."

NICK CARRAWAY, THE GREAT GATSBY

Table of Contents

Abstract.....	i
Aims and Objectives.....	ii
Acknowledgements.....	iii
List of Figures	4
List of Schemes.....	10
List of Tables.....	11
Glossary of Terms.....	12
Chapter 1 Forensic Electrochemistry.....	18
1.1 Dynamic Electrochemistry.....	18
1.1.1 Voltammetric Methods.....	19
1.1.2 Mass Transport	23
1.1.3 Electric Double Layer.....	26
1.1.4 Cyclic Voltammetric Systems	28
1.1.5 Electroanalysis.....	30
1.2 Forensic Electrochemistry in the Field	33
1.2.1 Poisons	34
1.2.2 Gunshot Residue (GSR)	35
1.2.3 Fingerprinting.....	38
1.2.4 DNA	39
Chapter 2 What are Novel Psychoactive Substances?	41
2.1 Introduction.....	41
2.2 Synthetic Cathinones.....	45

2.3	Synthetic Cannabinoids	55
2.4	Miscellaneous.....	66
2.4.1	Piperazines	66
2.4.2	Aminoindanes	68
2.4.3	Salvinorin A (<i>Salvia Divinorum</i>)	70
2.4.4	Mitragynine (<i>Kraton</i>).....	71
2.5	Conclusions and Future Challenges.....	74
Chapter 3	Experimental Methods.....	76
3.1	Chemicals and materials.....	76
3.2	Voltammetric Procedures	76
3.3	Electrode Polishing	77
3.4	Screen-Printing	77
3.5	Characterisation	80
Chapter 4	Detection of Illicit Compounds.....	81
4.1	The electroanalytical sensing of synthetic cathinone-derivatives and their accompanying adulterants in “legal high” products via electrochemical oxidation	81
4.1.1	Direct Electrochemical Oxidation of Methcathinone.	82
4.1.2	Direct Electrochemical Oxidation of Methcathinone Derivatives	88
4.2	Forensic Electrochemistry Applied to the Sensing of New Psychoactive Substances: Electroanalytical Sensing of Synthetic Cathinones and Analytical Validation in the Quantification of Seized Street Samples	97
4.2.1	Exploring In-Situ Mercury and Bismuth Film Modified Screen-Printed Electrodes.....	98
4.2.2	Direct electrochemical reduction of NPSs 4-MMC and 4-MEC	102
4.2.3	HPLC and LC-MS analysis of seized street samples.....	108
4.2.4	Application of the proposed electroanalytical protocol	109

4.3	The electroanalytical sensing of Rohypnol® (Flunitrazepam) using Screen-Printed Graphite Electrodes without Recourse for Electrode or Sample Pre-treatment	117
4.3.1	Electrochemical Behaviour of Rohypnol®	118
4.3.2	Application of the Proposed Electroanalytical Protocol	124
Chapter 5	Exploration of New Materials for Electrochemical Detection	131
5.1	Exploring Graphene as an Alternative Screen-Printed Electrode Material	131
5.2	<i>Regal Electrochemistry</i> : Exploring British Currency as a novel electrochemical sensor	138
Chapter 6	Conclusions and Future Work	144
6.1	Conclusions	144
6.2	Future Work	146
	Bibliography	148
	Appendix	161
6.1	The following experimental was performed by a 3 rd party:	161
6.1.1	Characterisation	161
6.1.2	Chromatography	162
6.1.3	Synthesis	163

List of Figures

Figure 1-1 A: Typical screen-printed setup that allows a route to point-of-care electrochemistry, which is a development of a typical laboratory-based setup in B: WE: Working Electrode; CE: Counter Electrode; RE: Reference Electrode.	20
Figure 1-2 A: Potential-time profile for a cyclic voltammetric experiment B: An example of a cyclic voltammogram (in this case a reversible system).	21
Figure 1-3 Cyclic square-wave voltammogram for a mixture of trace metals and explosives constituents of GSR: 2 ppm Zn, 2 ppm Pb, 20 ppm Sb, and 200 ppm Diphenylamine (DPA). Square wave parameters: E_{step} , 4 mV; amplitude, 25 mV; frequency, 25 Hz; and t_{accum} , 120 s; (reduction) $E_{\text{start,accum}}$ 1.2 V and E_{stop} , -1.3 V; (oxidation) $E_{\text{start,accum}}$, -1.3 V; E_{stop} , 1.2 V; and t_{accum} , 120 s. Electrolyte, acetate buffer (pH = 4.5). Reproduced from reference 28.	
.....	37
Figure 1-4 Electrolysis-etched fingerprint on a bullet. Reproduced from Reference 30 with permission from the International Association for Identification.	39
Figure 2-1 A graphical representation of new psychoactive substances notified to the EWS between 2005-2014. Reproduced with permission from the EMCDDA.	43
Figure 2-2 Characterisation of galvanic displacement. The optical image (top left) shows a clean British 2p coin, with silver deposited onto its surface. (A) shows an SEM of the rough surface of the two pence after cleaning. The SEM in (B) shows the silver dendritic structures that are formed on the coins surface. The fern like structures are magnified in (C) and show that secondary crystalline domains grow perpendicular from a primary silver backbone. Recreated from reference 86.	53
Figure 2-3 Visual representation of synthetic cannabinoid presumptive test.	62
Figure 2-4 Microcrystals formed with mercury chloride and (a) mephedrone (bi) MDAI freebase (bii) MDAI hydrochloride and (c) BZP. Recreated from reference 147.	70

Figure 3-1 A: Schematic diagram of the Regal Electrochemistry experimental cell PTFE 'housing' unit used to hold the 1 pence sensor in place for analysis and accurately defines the working electrode area. B: Cross sectional diagram of assembled PTFE 'housing' unit with a retrofitted 1p-sensor in place which is then inserted into the solution under investigation.....78

Figure 3-2 A shows an image of the overview GSPE used in this work along with an SEM image (B) of the electrode surface.79

Figure 4-1 Voltammetric profiles observed at a boron-doped (solid line), glassy carbon (dashed line) and SPE (dotted line) electrode in a solution of 500 $\mu\text{g mL}^{-1}$ methcathinone in a pH 12 PBS buffer. Scan rate: 100 mV s^{-1} . vs. SCE (BDD, GC) Ag/AgCl (SPE).83

Figure 4-2 Voltammetric profiles observed at a SPEs of blank pH 12 PBS buffer (solid line), and 500 $\mu\text{g mL}^{-1}$ methcathinone (dotted line) in a solution of in a pH 12 PBS buffer. Scan rate: 100 mV s^{-1} . vs. Ag/AgCl.84

Figure 4-3 A: Cyclic voltammetric responses (A) of methcathinone obtained in phosphate buffer solution at different pHs. B: Plot of peak potential as a function of pH for the electrochemical oxidation of methcathinone Scan rate: 100 mV s^{-1} . vs. Ag/AgCl. The responses shown in (B) represent are an average response (squares) with corresponding error bars ($N = 3$).....85

Figure 4-4 Plot of the square root of scan rate against peak current for 500 $\mu\text{g mL}^{-1}$ methcathinone in pH 12 buffer solution.86

Figure 4-5 A typical calibration plot corresponding to the addition of methcathinone into a pH 12 phosphate buffer solution over the range 31.3 – 200.0 $\mu\text{g mL}^{-1}$ using a new SPE for each addition. The responses shown are an average response (squares) with corresponding error bars ($N = 3$).....87

Figure 4-6 A: Voltammetric profiles for both 4-MMC (dotted line) and 4-MEC (dashed line) compared to methcathinone (solid line) in a pH 12, 500 $\mu\text{g mL}^{-1}$ aqueous buffer solution using SPEs. Scan rate: 100 mV s^{-1} , vs. Ag/AgCl. B: *For Reference*, Background Voltammetric profiles for both 4-MMC (solid line) and 4-MEC (dashed line) in pH 12 aqueous buffer solution using SPEs. Scan rate: 100 mV s^{-1} , vs. Ag/AgCl.

.....	89
Figure 4-7 A: Cyclic voltammetric responses 4-MMC obtained in phosphate buffer solution at pH 2 (solid line), pH 6 (dashed line) and pH 12 (dotted line). B: Cyclic voltammetric responses of 4-MEC obtained in phosphate buffer solution pH 2 (solid line) pH 6 (dashed line) and pH 12 (dotted line). Scan rate: 100 mV s ⁻¹ vs. Ag/AgCl.....	90
Figure 4-8 Typical calibration plots corresponding to 4-MEC (solid line) over the range 95.2 to 1000.0 µg mL ⁻¹ and 4-MMC (dotted line) over the range 39.2 to 666.7 µg mL ⁻¹ into a pH 12 aqueous buffer. The responses shown are an average response with the corresponding error bars (N = 3).....	91
Figure 4-9 Typical calibration plot corresponding to the addition of 4-MEC (A) and 4-MEC (B) into a pH 2 phosphate buffer solution over the range 16.1 – 300 µg mL ⁻¹ using a new SPE for each addition. The responses shown are an average response (squares) with corresponding error bars (N = 3).	94
Figure 4-10 Voltammetric profiles of both caffeine (solid line) and benzocaine (dashed line) at pH 12 in 500 µg mL ⁻¹ obtained using SPE. Scan rate: 75mV s ⁻¹ vs. Ag/AgCl.	95
Figure 4-11 Comparison of the voltammetric profiles of 4-MMC (solid line), 4-MEC (dashed line), caffeine (dotted line) and benzocaine (dashed-dotted line) in 500 µg mL ⁻¹ pH 2 buffer solution. Scan rate: 100mV s ⁻¹ vs. Ag/AgCl.	96
Figure 4-12 Cyclic voltammetric background responses in the absence (solid) and presence of mercury (II) (dashed line) and bismuth (III) (dotted line) recorded in an pH 4.3 acetate buffer using SPEs. The voltammetric scan is ran cathodically inducing the electrochemical deposition of mercury and bismuth metals (separately), visible as anodic peakss at ~ +0.1 V (vs. Ag/AgCl) and ~ -0.3 V (vs. Ag/AgCl) respectively. Scan rate: 50 mV s ⁻¹ (vs. Ag/AgCl).	99
Figure 4-13 A: Voltammetric responses of acetate buffer in the presence of 4-MMC (solid line) using the <i>in-situ</i> formed mercury(II) (dashed line) and bismuth(III) film modified SPEs (dotted line) recorded in a pH 4.3 acetate buffer. Scan rate: 50 mV s ⁻¹ (vs. Ag/AgCl) B: Typical calibration resulting from the analysis of the voltammetric signatures obtained in (A) in the form of a plot of peak height against 4-MMC concentration using SPEs in a pH 4.3	

acetate buffer(triangles) and with the <i>in-situ</i> film formed mercury (squares) and bismuth (circles) over a linear range of 100 - 400 $\mu\text{g mL}^{-1}$. <i>Note</i> : a new SPE was utilised with each scan/addition. Scan rate: 50 mVs^{-1} (vs. <i>Ag/AgCl</i>).....	101
Figure 4-14 Typical cyclic voltammetric profiles recorded using SPEs in the presence (dashed line) and the absence (solid line) of 47.62 $\mu\text{g mL}^{-1}$ 4-MMC. Experimental conditions: pH 4.3 Acetate buffer; Scan rate: 50 mV s^{-1} (vs. <i>Ag/AgCl</i>).....	102
Figure 4-15 Cyclic voltammetric profiles recorded using a boron-doped (dotted), glassy carbon (dashed line) and SPEs (solid line) in 90.91 $\mu\text{g mL}^{-1}$ 4-MMC, pH 4.3 acetate buffer. Scan rate: 50 mV s^{-1} (vs. <i>Ag/AgCl</i>).....	103
Figure 4-16 A calibration plot corresponding to the addition of 4-MMC into a model pH 4.3 acetate buffer solution over the concentration range 0.00 – 200.00 $\mu\text{g mL}^{-1}$ using a <i>new</i> SPE upon each addition. Also included are error bars ($N = 3$).....	104
Figure 4-17 A calibration plot corresponding to the addition of 4-MEC into a model pH 4.3 acetate buffer solution over the concentration range 0.00 – 200.00 $\mu\text{g mL}^{-1}$ using a <i>new</i> SPE upon each addition. Also included are error bars ($N = 3$).....	105
Figure 4-18 Cyclic voltammetric profiles recorded using an SPE in the absence (dashed) and presence of 90.91 $\mu\text{g mL}^{-1}$ 4-MMC (solid) and 90.91 $\mu\text{g mL}^{-1}$ 4-MEC (dotted line), pH 4.3 acetate buffer. Scan rate: 50 mV s^{-1} (vs. <i>Ag/AgCl</i>).....	106
Figure 4-19 Effect of common adulterants on the electrochemical response of pH 4.3 acetate buffer using SPEs. A: With (dashed line) and without (solid line) the presence of 1000 $\mu\text{g mL}^{-1}$ benzocaine. B: With (dashed line) and without (solid line) the presence of 1000 $\mu\text{g mL}^{-1}$ caffeine. Scan rate: 50 mV s^{-1}	107
Figure 4-20 Cyclic voltammetric profiles recorded using SPEs in the presence of A: 12.35 $\mu\text{g mL}^{-1}$ B: 148.94 $\mu\text{g mL}^{-1}$ C: 200.00 $\mu\text{g mL}^{-1}$ 4-MMC following being degassed with N_2 (solid line), un-changed (dashed) and saturated with O_2 (dotted). Scan rate: 50 mV s^{-1} (vs. <i>Ag/AgCl</i>).....	110
Figure 4-21 Typical cyclic voltammetric profiles of 1 mg mL^{-1} NRG-2-B (caffeine 34.21% w/w, benzocaine 68.77% w/w) in pH 4.3 acetate buffer + 20% methanol (to dissolve benzocaine) and 1 mg mL^{-1} NRG-2-D (caffeiene 76.03% w/w, 4-MEC 19.16% w/w) in pH 4.3 acetate buffer. Scan rate: 50 mV s^{-1} (vs. <i>Ag/AgCl</i>).....	113

Figure 4-22 Cyclic voltammetric responses obtained in pH 6 phosphate buffer solution in the absence (dotted line) and presence (solid line) of 50 $\mu\text{g mL}^{-1}$ Rohypnol[®] using a SPE. Scan rate: 100 mV s^{-1}119

Figure 4-23 A: A plot of peak potential, E_p (A1), as a function of pH for the electrochemical oxidation of 125 $\mu\text{g mL}^{-1}$ Rohypnol[®] using a SPE and the. Scan rate: 100 mV s^{-1} . B: A plot of peak height, I_p (A1), as a function of pH for the electrochemical oxidation of 125 $\mu\text{g mL}^{-1}$ Rohypnol[®] using a SPE and the. Scan rate: 100 mV s^{-1}120

Figure 4-24 Cyclic voltammetric responses obtained in pH 6 phosphate buffer solution in the absence (dotted line) and presence (solid line) of 0.3 $\mu\text{g/mL}$ 7-aminoflunitrazepam using a SPE. Scan rate: 100 mV s^{-1} 122

Figure 4-25 Cyclic voltammetric responses obtained in pH 6 phosphate buffer solution in the absence (dotted line) of Rohypnol[®] and in the presence (solid line) of Rohypnol[®] ranging from 1 $\mu\text{g mL}^{-1}$ to 95.2 $\mu\text{g mL}^{-1}$ (39.2, 76.9 and 95.2 $\mu\text{g mL}^{-1}$ depicted) using a *new* SPE upon each addition. Scan rate: 100 mV s^{-1} B: Typical corresponding calibration plot with error bars ($N = 3$).....123

Figure 4-26 A calibration plot corresponding to the addition of Rohypnol[®] into an unmodified Coca Cola[™] solution over the concentration range 1 – 245.6 $\mu\text{g mL}^{-1}$ using a *new* SPE upon each addition. Also included are error bars ($N = 3$).125

Figure 4-27 A calibration plot corresponding to the addition of Rohypnol[®] into an unmodified WKD alcopop solution over the concentration range 1 – 245.6 $\mu\text{g mL}^{-1}$ using a *new* SPE upon each addition. Also included are error bars ($N = 3$).129

Figure 5-1 A: The cyclic voltammetric responses in PBS pH 7 for GSPE (solid line), GSPE A (dashed line), and GSPE B (dotted line). Scan rate 50 mV s^{-1} (*vs. Ag/AgCl*). B: The electrochemical oxidation of 10 mM hydrazine at the GSPE (solid line), GSPE A (dashed line), and GSPE B (dotted line) where oxidation peaks are evident at +0.8, +1.1, and +0.2 (*vs. Ag/AgCl*) respectively. Scan rate 50 mV s^{-1} . C: Observed electrochemical response for Fe(II) modified GSPE in the absence (solid line) and presence (dashed line) of 10 mM hydrazine. Scan rate 50 mV s^{-1} (*vs. Ag/AgCl*). Inset: Voltammetric profiles of Mn(II) (solid line) and Fe(III) (dashed line) modified GSPE in the presence of 10 mM hydrazine. Scan rate 50 mV s^{-1} (*vs. Ag/AgCl*).134

Figure 5-2 A: SEM Image of the GSPE B surface at $\times 200 \mu\text{m}$ B: The SEM-EDX “map” of the iron impurities present on the GSPE B surface; relative intensities of iron present is represented by brightness of the dot at $\times 200 \mu\text{m}$	136
Figure 5-3 Calibration plots for both the GSPE A (Squares) and GPSE B (Triangles) electrodes response to hydrazine over the linear range 400 - 3900 μM . Scan rate 50 mV s^{-1} (vs. <i>Ag/AgCl</i>)	137
Figure 5-4 Typical cyclic voltammograms using a 1 pence electrochemical sensor in the absence (black) and presence of 4-MMC (red) and 4-MEC (blue) in pH 8.5 acetate buffer. Scan rate: 50 mV s^{-1} (vs. SCE).....	139
Figure 5-5 A: Typical voltammetric responses between the range -0.5 and $+0.1$ V as a result of increasing concentrations of 4-MMC using the 1p-sensor recorded in a pH 8.5 acetate buffer. Scan rate 50 mV s^{-1} (vs. SCE), using the oxidative peak at approximately -0.1 V as the analytical peak. Inset: typical voltammetric responses (full voltammetric range) as a result of increasing concentrations of 4-MMC. B: Typical calibration resulting from the analysis of voltammetric signatures obtained in the form of a plot of peak height (current) against 4-MMC concentration using a 1p-sensor in a pH 8.5 acetate buffer over a linear range of $0.01\text{--}0.10 \mu\text{g mL}^{-1}$. Scan rate: 50 mV s^{-1} (vs. SCE) ($N = 3$ – average and standard deviation is plotted).	140
Figure 5-6 SEM of a A: British 1 pence coin minted pre-1992 and B: British 1 pence coin minted post-1992.....	141
Figure 5-7 EDX spectra obtained from a pre-1992 (red) and post-1992 (black) British 1 pence coin following analysis.	142

List of Schemes

Scheme 2-1 The structure of mephedrone, centrepiece of the research conducted within the thesis.....	42
Scheme 2-2 Key structure of synthetic cathinones	45
Scheme 2-3 Comparison of a) Tetrahydrocannabinol (THC), the active component in cannabis against b) JWH-018, aminoalkylindole synthetic cannabinoid.....	56
Scheme 2-4 Chemical structures of synthetic cannabinoids found in herbal products such as the Spice range.	59
Scheme 2-5 Chemical structures of synthetic cannabinoids discovered after legislative bans were introduced: cyclopropylindoles e.g. UR-144, XLR-11 and adamantylindoles (APICA and APINACA).....	64
Scheme 2-6 Benzylpiperazine and other piperazines derivatives which have been historically abused.	66
Scheme 2-7 Structures of 2-aminoindane and its derivatives, all of which have been found in “legal high” samples.....	68
Scheme 4-1 Proposed mechanism for the oxidation of methcathinone at the electrode surface.....	92
Scheme 4-2 Chemical structure of Rohypnol® (Flunitrazepam).....	118

List of Tables

Table 2-1 List of the most common synthetic cathinones, emphasis given to the most prevalently abused globally.	47
Table 4-1 LC-MS and HPLC analysis of the purchased NRG-2 “street” samples.....	111
Table 4-2 Direct comparison between quantification data collected from HPLC and the new proposed electrochemical protocol proposed for the analytical quantification of synthetic cathinones composition in a selection of seized street samples.....	114
Table 4-3 Comparison of the analytical methods for the detection of 4-MMC, emphasis added to the method presented in this thesis.	115
Table 5-1 De-convolution of the functional group percentages <i>via</i> XPS for the fabricated graphene electrodes, presented as % totals. ²⁵³	135

Glossary of Terms

3-MPPP	3'-Methyl-A-Pyrrolidinopropiophenone
3-TFMPP	3-(Trifluoromethyl)Phenylpiperazine
4-MBC	4'-Methyl- <i>N</i> -Benzylcathinone
4-MEC	4-Methylethcathinone
4-MMC	4-Methylmethcathinone; Mephedrone
4 β -MDEA	Ethylone
5-IAI	5'-Iodo-2-Aminoindane
α -PVP	<i>N</i> -Pyrrolidinovalerophenone
β k-MBDB	(\pm)-Butylone
β k-MDMA	3,4-Methylenedioxy- <i>N</i> -Methylcathinone; Methylone
β k-PMMA	4-Methoxymethcathinone; Methedrone
CPK	Creatine Phosphokinase
CSEW	Crime Survey For England And Wales
CVD	Chemical Vapour Deposition
DART-MS	Direct Analysis In Real Time Mass Spectrometry
DME	Dropping Mercury Electrode

DNA	Deoxyribonucleic Acid
DPA	Diphenylamine
EC	N-Ethylcathinone,
EMCDDA	European Monitoring Centre For Drugs And Drug Addiction
EU	European Union
EWS	Eu Early Warning System
FDA	United States Food And Drug Administration
FMC	N-Fluoromethcathinone
FPIA	Fluorescence Polarization Immunoassay
FTIR	Fourier Transform Infrared Spectroscopy
GBP	British Pound
GC	Glassy Carbon
GC-FID	Gas Chromatography - Flame Ionisation Detection
GC-HRMS	Gas Chromatograph - High Resolution Mass Spectrometry
GC-MS	Gas Chromatography - Mass Spectrometry
GSPE	Graphene Screen-Printed Electrode
GSR	Gunshot Residue
HPLC	High Performance Liquid Chromatography

HPLC-UV	High Performance Liquid Chromatography - Ultra Violet
ICP-MS	Inductively Coupled Plasma - Mass Spectrometry
IHP	Inner Helmholtz Plane
IMS	Ion Mobility Spectrometry
IR	Infrared Spectroscopy
IRMS	Isotope Ratio Mass Spec
JWH	John W. Huffman
LC-ESI-MS	Liquid Chromatography-Electrospray Ionization- Mass Spectrometry
LC-MS	Liquid Chromatography–Mass Spectrometry
LC-MS/APCI	Liquid Chromatography-Mass Spectrometry Atmospheric Pressure Chemical Ionization
LC-MS/MS	Liquid Chromatography - Tandem Mass Spectrometry
LLOQ	Lower Limit Of Quantification
LOD	Limit Of Detection
LOQ	Limit Of Quantification
MCPP	Meta-Chlorophenylpiperazine
MDAI	5', 6'-Methylenedioxy-2-Aminoindane
MDMA	3',4'-Methylenedioxymethamphetamine
MDMAI	5', 6'-Methylenedioxy- <i>N</i> -Methyl-2-Aminoindane

MDPV	3',4'-Methylenedioxypropylvalerone
MMAI	5'-Methoxy-6'-Methyl-2-Aminoindane
MS/MS	Tandem Mass Spectrometry
NMR	Nuclear Magnetic Resonance
NPS	Novel Psychoactive Substance
NQS	2'-Naphthoquinone-4-Sulphonate
OHP	Outer Helmholtz Plane
PBS	Phosphate-Buffered Saline
PFPA	Pentafluoropropionic Anhydride
PTFE	Polytetrafluoroethylene
RE	Reference Electrode
RRF	Relative Response Factor
RSD	Relative Standard Deviation
SA	Salvinorin A
SCE	Saturated Calomel Electrode
SECM	Scanning Electrochemical Microscopy
SEM	Scanning Electron Microscope
SEM-EDX	Scanning Electron Microscope - Energy-Dispersive X-Ray Spectroscopy

SERS	Surface Enhanced Raman-Spectroscopy
SPE	Graphite Screen-Printed Electrode
THC	Tetrahydrocannabinol
TLC-DESI-MS	Thin Layer Chromatography Desorption Electrospray Ionization Mass Spectrometry
TLC-GC-MS	Thin Layer Chromatography Gas Chromatography-Mass Spectrometry
TOF	Time Of Flight
TOF-MS	Time Of Flight - Mass Spectrometry
UHPLC-HRMS	Ultra-High Performance Liquid Chromatography - High Resolution Mass Spectrometry
UHPLC-UV	Ultra-High Performance Liquid Chromatography - Ultra Violet
UK	United Kingdom
USA	United States Of America
UV	Ultra-Violet
WE	Working Electrode
XPS	X-Ray Photoelectron Spectroscopy

Publications featured in this thesis:

J.P Smith, E. P. Randviir and C. E. Banks, in *Forensic Science – Multidisciplinary Approach*, Wiley-VCH, 2016.

L. R. Cumba, C. W. Foster, D. A. C. Brownson, J. P. Smith, J. Iniesta, B. Thakur, D. R. do Carmo and C. E. Banks, *Analyst*, 2016, **141**, 2791-2799.

F. Tan, J. P. Smith, O. B. Sutcliffe and C. E. Banks, *Anal. Methods*, 2015, **7**, 6470-6474.

J. P. Smith, O. B. Sutcliffe and C. E. Banks, *Analyst*, 2015, **140**, 4932-4948.

J. P. Smith, J. P. Metters, C. Irving, O. B. Sutcliffe and C. E. Banks, *Analyst*, 2014, **139**, 389-400.

J. P. Smith, J. P. Metters, O. I. G. Khreit, O. B. Sutcliffe and C. E. Banks, *Anal. Chem.*, 2014, **86**, 9985-9992.

J. P. Smith, C. W. Foster, J. P. Metters, O. B. Sutcliffe and C. E. Banks, *Electroanalysis*, 2014, **26**, 2429-2433.

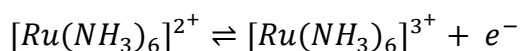
J. P. Smith, J. P. Metters, D. K. Kampouris, C. Lledo-Fernandez, O. B. Sutcliffe and C. E. Banks, *Analyst*, 2013, **138**, 6185-6191.

Chapter 1 Forensic Electrochemistry

This chapter covers an introduction to dynamic electrochemistry and its application to analytical chemistry whilst also covering the role electrochemistry has, to-date, in *Forensic Electrochemistry*.

1.1 Dynamic Electrochemistry

Electrochemistry is the study of chemical reactions taking place in solution between an electrolyte and electrode at a solid/liquid interface;¹ these reactions typically involve the transfer of an electron between a reduction and oxidation species and, as such, they can be imagined as a set of 'Redox Reactions'. Archetypally, these redox reactions may be depicted in the form of two 'half reactions' offering a more in depth depiction of occurrences at the solid/liquid interface. For instance, consider the redox behaviour of well-known reversible redox-couple ruthenium hexamine during an electrochemical reaction.¹



During an electrochemical reaction, the observed chemistry occurs upon the working electrode surface that is a part of a 'three-electrode' set-up working in tandem with both a counter and reference electrode.² The working electrode is the circuit component that interacts with the solution and is where measured oxidation and reduction processes take place. The counter electrode is incorporated into the circuit to allow current to flow by providing electrons (or holes) for reaction with the oppositely charged species than the reaction occurring at the working electrode.¹ Nonetheless, the potential of the reactions occurring are arbitrary without a point of reference, therefore, a reference electrode provides a well-defined redox couple (such as the Saturated Calomel Electrode; SCE) with a fixed potential.^{1, 3} The potential of oxidation and reduction is thus compared to the potential of the reactions occurring at the reference electrode.^{1, 3} It is a combination of these potentials and currents studied analytically that make the field of electrochemistry

highly interesting for the purposes of analytical chemistry. The focus of this Chapter will be primarily upon voltammetric methods, a common subset of dynamic electrochemical measurements procured by analytical chemists forming the basis for a vast array of electrochemical sensors.

1.1.1 Voltammetric Methods

A voltammetric method involves utilising a potentiostat and most typically, the previously mentioned three-electrode electrolytic cell - depicted in Figure 1-1, which can either be employed using more recently developed screen-printed electrode technology (Figure 1-1A) or a more classical approach (Figure 1-1B). The most widely used technique is cyclic voltammetry³ and is the technique that forms the foundation of the work compiled within this thesis. In a cyclic voltammetric experiment, a potential ramp with a fixed potential step (known as the scan rate) is applied to an electrolytic cell. The electric field created at the working electrode surface forces the surface to interact with the immediate solution (or sample) environment, stimulating the exchange of electrons between the working electrode surface and the sample.²

This exchange of electrons is measured as a current. Currents of this ilk are known as Faradaic currents (see later). However, like in normal chemical reactions, the exchange of electrons will only take place when a sufficiently high activation barrier is achieved, therefore, the potential ramp must approach a high enough value to stimulate such exchange processes. When the voltage ramp is reversed, the current response decreases, and the reverse half-cell reaction will occur (reduction). The current is plotted as a function of the voltage and presented as a voltammogram. The waveform profile is also presented in Figure 1-2A.

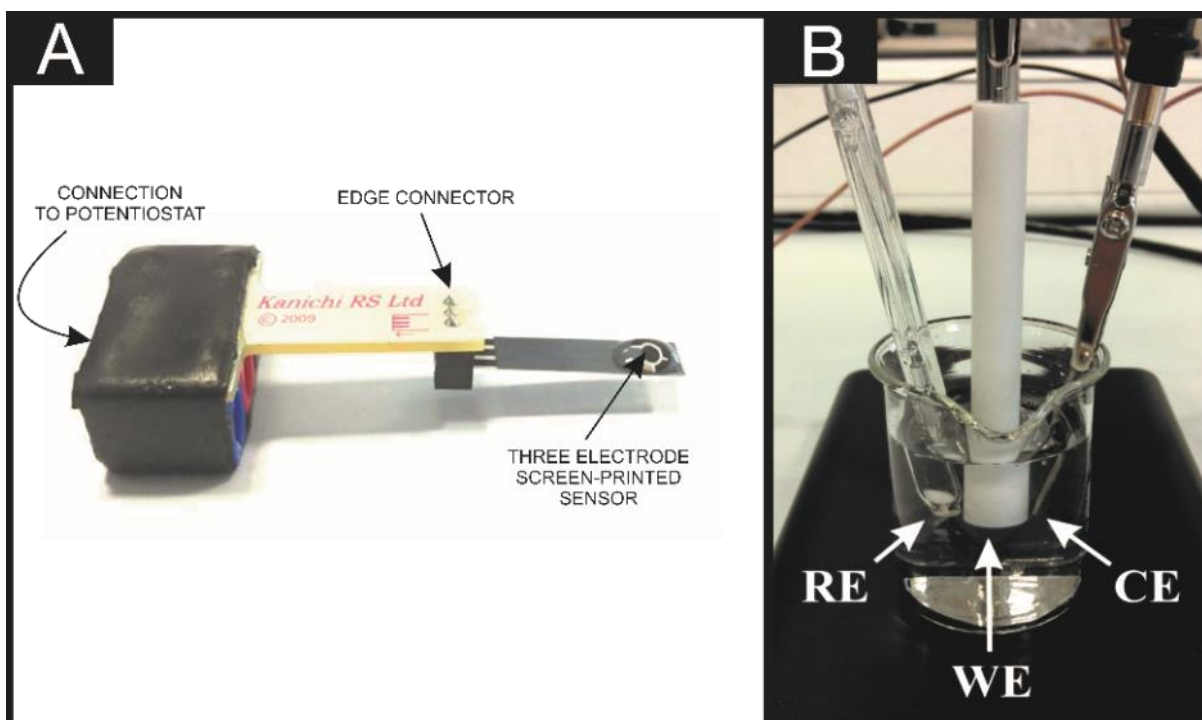


Figure 1-1 A: Typical screen-printed setup that allows a route to point-of-care electrochemistry, which is a development of a typical laboratory-based setup in B: WE: Working Electrode; CE: Counter Electrode; RE: Reference Electrode.

The resultant current-potential plot, such as the one depicted in Figure 1-2B, is interpreted by electrochemists in order to determine concentrations of specific analytes. An electrode, at equilibrium with the electrolyte, will have a potential that remains constant over time; which is thermodynamically related to the chemical composition of the electrolyte solution. In the electrolyte solution, for example, species '*Ox*' is reduced to species '*Red*' at the solid/liquid interface of the electrode via a reversible reaction with electrons: $Ox + ne^- \leftrightarrow Red$. Therefore, in a system that is controlled by the laws of thermodynamics, the measured potential at the electrode can determine the concentration of the electroactive species, $[Ox]$ and $[Red]$ for oxidised and reduced forms respectively at the surface (*i.e.* distance from surface ($x = 0$) with the Nernst equation,^{1, 2, 4} (Equation 1-1):

Equation 1-1

$$E = E^0 + \frac{2.3RT}{nF} \log \frac{[Ox]}{[Red]}$$

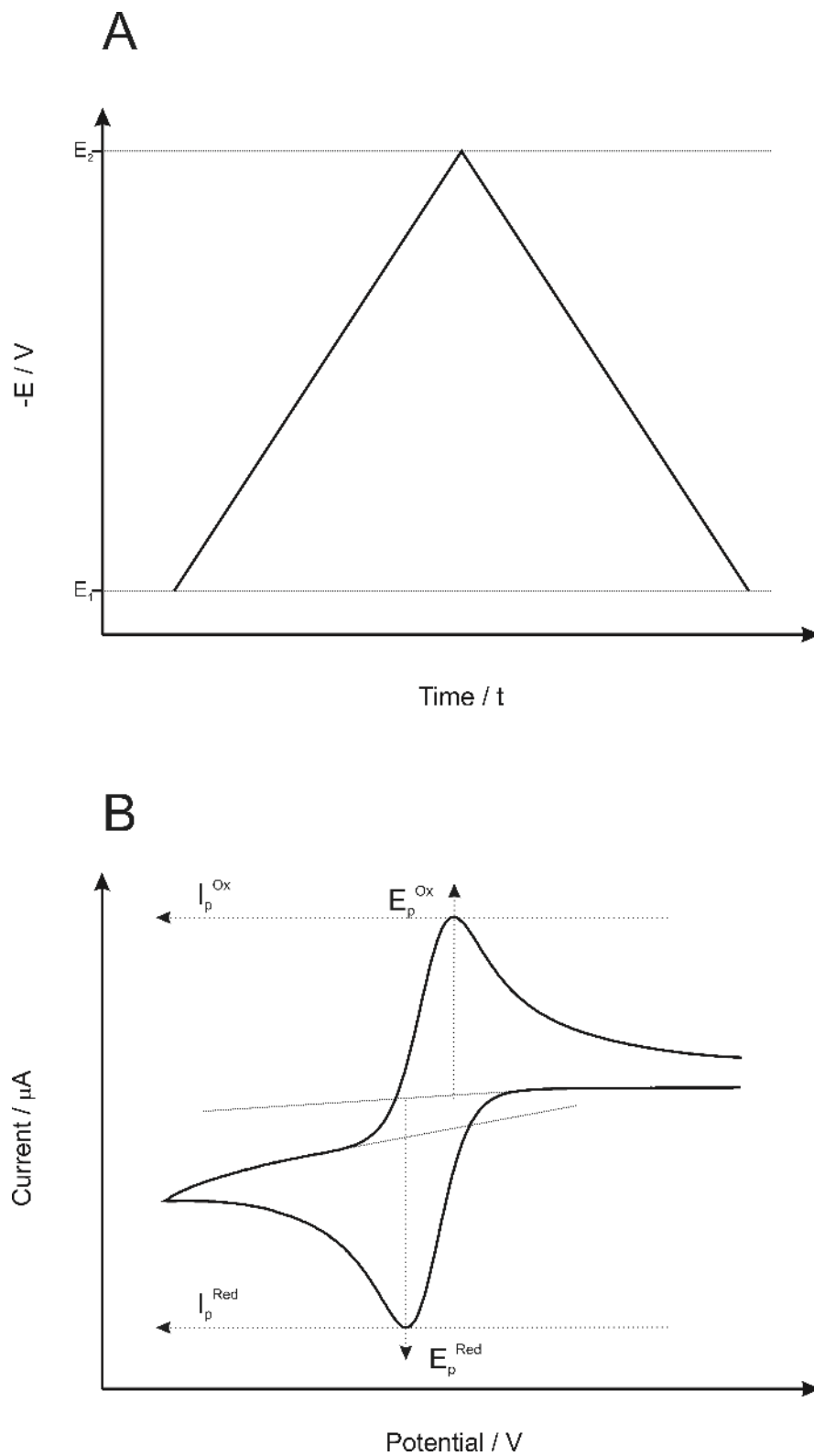


Figure 1-2 A: Potential-time profile for a cyclic voltammetric experiment B: An example of a cyclic voltammogram (in this case a reversible system).

Where E is the measured potential, E^0 is the standard potential of the reaction, R is the universal gas constant ($8.314 \text{ J K}^{-1} \text{ mol}^{-1}$), T is temperature (K), F is the Faraday constant ($96,485.33 \text{ C mol}^{-1}$) and n is the number of electrons transferred during the reaction. The concentrations used in the Nernst equation assumes ideal solutions, however activities of the species can be taken into account using the following form of the Nernst equation:⁴

Equation 1-2

$$E = E^0 + \left(\frac{RT}{nF}\right) \ln\left(\frac{a_p}{a_r}\right)$$

Where a_p and a_r are the standard activities of the products and reactants respectively.

Voltammetric methods, such as cyclic voltammetry, use the variance in the ratio of $[Ox]$ and $[Red]$ as a function of potential as their foundation. The Nernst equation assumes the reaction of $Ox + ne^- \leftrightarrow Red$ as being fast in both directions and as a result the concentration at the electrode surface changes almost immediately with changes in potential.^{2, 4} Consequently, observed currents in a voltammetric experiments are useful because they are proportional to the concentration of the desired species and which is described through use of the Randles-Ševčík equation as given in Equation 1-3.²⁻⁴

Equation 1-3

$$I_p = 269,000 n^{\frac{3}{2}} A D^{\frac{3}{2}} C v^{\frac{1}{2}}$$

Where I_p is the current, n is the number of electrons transferred, F is the Faraday constant, A is the surface area of the working electrode, C is the concentration of the target species, v is the scan rate, D is the diffusion coefficient, R is the molar gas constant, and T is the temperature. As described in Equation 1-3, the peak current in a voltammetric process is equal to approximately 10^5 (269,000) times the concentration of the target analyte under standard conditions (assuming all the other parameters are constant).³ This unique relationship allows electrochemical determination of target species at extremely low concentrations by monitoring the Faradaic current, while providing similar or better sensitivities over other methods such as optical, fluorescence, and so on. In light of this, electrochemistry finds itself particularly useful for its ability to detect low concentrations

such as those present in forensic cases, whilst negating the need for large and expensive equipment. Chemistry is seldom without complication and electrochemistry is no exception to the rule. Throughout experimentation there are various factors that contribute to electrochemical response and demand consideration.

1.1.2 Mass Transport

The movement of mater in solution from one location to another is labelled as ‘mass transfer’. In electrochemical experiments this involves electroactive species being transported to the electrode surface. There are three different types of mass transfer in electrochemical systems, these are: diffusion, migration and convection – each one of these is a contributor to the overall current detected in the system ($i_{tot} = i_d + i_m + i_c$).¹

1.1.2.1 Diffusion

In a concentration gradient, species will move from an area of high concentration to an area of low concentration; this is according to Fick’s law. Fick’s first law, in electrochemical terms, is used to relate the diffusive flux (j) of the species to be oxidised (Ox) to the concentration of ‘ Ox ’ assuming the steady state approximation is in effect.^{1, 2} In a one dimensional model, where D_{ox} the diffusion coefficient ($cm^2 s^{-1}$) of is Ox and x is the distance from the electrode surface is given in Equation 1-4:^{1, 2}

Equation 1-4

$$j_{ox} = - D_{ox} \frac{\partial[Ox]}{\partial x}$$

Fick’s second law (Equation 1-5) describes how diffusion can cause the concentration to change over time:^{1, 2}

Equation 1-5

$$\frac{\partial[Ox]}{\partial t} = D_{ox} \frac{\partial^2[Ox]}{\partial x^2}$$

Species being either produced or diminished at the electrode surface form a concentration gradient between the electrode and the 'bulk' solution in a zone called the 'diffusion layer'.^{1,4}

The thickness of the diffusion layer, δ , is a result of extrapolation of the concentration profile assuming it remained linear to the point where bulk concentration is reached; corresponding with the tangent of the actual concentration profile - this is also known as the 'Nernst diffusion layer'.⁴ Knowing the value of δ allows the estimation of flux at the electrode surface and hence the calculation of the current (Equation 1-6) where $[Ox]_{x=0}$ is the concentration at the electrode surface:¹

Equation 1-6

$$\frac{\partial[Ox]_{x=0}}{\partial x} = \frac{[Ox]_{bulk} - [Ox]_{x=0}}{\delta} \rightarrow i_{Ox} = nFAD_{Ox} \frac{[Ox]_{bulk} - [Ox]_{x=0}}{\delta}$$

1.1.2.2 Migration

Diffusion involves the movement of species due to a concentration gradient; Migration on the other hand involves the movement of charged species (i) with a charge (z) due to a potential gradient. The occurrence of flux due to migration is estimated by Equation 1-7:²

Equation 1-7

$$j_{Ox} = -\frac{z_{Ox}F}{RT} D_{Ox}[Ox] \frac{\partial E}{\partial x}$$

However, interactions in the diffuse layer and ion solvation effects make the calculation of this value difficult to calculate in actual solutions. For many electrochemical systems, to ensure the reaction is not effected by migration effects, an excess of inert background electrolyte is added to the solution.¹ As well as significantly removing the effects of migration a background electrolyte can also help with conduction in the electrochemical system.

1.1.2.3 Convection

A physical force applied to a solution cause the 3rd form of mass transport – Convection. These physical forces can either be natural or forced and each has significantly different magnitudes.^{1, 4} Natural convection however, is also present in every chemical system; it is caused by small differences in temperature or density and can even be caused by gravity - these contributions cause the solution to mix.^{1, 4} In electrochemical experiments these effects of natural convection can be avoided by ensuring an experiment takes no longer than ≈ 20 s.⁴ Applying an external physical force to the system (pumping, bubbling, stirring or hydrodynamic flow) is known as forced convection. Forced convection is several orders of magnitude larger than natural convection and is able to ‘dominate’ and effectively remove the ‘random’ trait incurred by said natural convection and its effect on experimental measurements (as well as improve the previously mentioned mass transport).¹ Nevertheless, this removal of the random aspect in experimental measurements can only occur if the forced convection is brought into the system via a quantitative manner. Studying these effects has led to the construction of the Nernst-Planck equation (Equation 1-8) to predict the changing behaviour in one dimension, where v_x is the hydrodynamic velocity of species Ox (cm s^{-1}), adapted to describe convective mass transport in electrochemical systems:^{1, 4}

Equation 1-8

$$j_{Ox} = -D_{Ox} \frac{\partial[Ox]}{\partial x} - \frac{Z_{Ox}F}{RT} D_{Ox}[Ox] \frac{\partial E}{\partial x} + v_x[Ox]$$

The aforementioned scan rates can span from any chosen value between mere millivolts per second to a sizeable million volts per second although these do come with their own problems.² The lower scan rates (in the millivolts per second) as well as taking an exceptionally long time to perform are also subject to a substantial amount of natural convection leading to irreproducible mass transport. Upper scan rates although faster in nature, are constrained by capacitive charging (section below 1.1.3) thus disguising the faradaic current.^{1, 2, 4} Therefore, the conditions in which cyclic voltammetry are performed ensure that diffusion is the main form of mass transport. Because of this mass transport for

the overall reaction at the interfacial surface can be described by Fick's second law of diffusion (Equation 1-5 and Equation 1-9):⁴

Equation 1-5

$$\frac{\partial[Ox]}{\partial t} = D_{ox} \frac{\partial^2[Ox]}{\partial x^2}$$

Equation 1-9

$$\frac{\partial[Red]}{\partial t} = D_{Red} \frac{\partial^2[Red]}{\partial x^2}$$

A cyclic voltammogram is dependent on both the rate of mass transport by diffusion and electron transfer kinetics. Because of this a system can either be reversible or non-reversible depending on the intensities of the rate of diffusion or electron transfer kinetics.

1.1.3 Electric Double Layer

At the interface of the electrode and electrolyte there are interactions between the two. If a potential is applied to the electrode there will no longer be electroneutrality in the solution and thus, as a result, there will be strong interactions between ions and the electrode surface.¹ This area of interaction between the electrode surface and ions in the electrolyte solution is known as the 'electric double layer'. The nature of these interactions is important and should be taken into consideration when on the subject of using electrochemical methods for analysis. There have been several models suggested to try and explain this region and the behaviour of the molecules involved.¹

In 1853 Helmholtz⁵ predicted that a "double layer" would exist from excess charge on the electrode being neutralized by a layer of ions of opposite charge to that of the electrode, however the model did not take into consideration the random motion of ions.⁵ The Gouy-Chapman "diffuse-layer model" describes the distribution of overall charge near the surface which lessens the further away from the interfacial region.⁶ The model predicts a diffuse layer of charge as a result of the random movement of ions wherein there is a higher concentration of counter ions nearer the surface of the electrode which gradually declines until there is a homogeneous distribution of charged species.¹ It wasn't until Stern⁶ proposed a model shortly after for this region consisting of a Helmholtz double layer in

tandem with the Gouy-Chapman diffuse-layer model that a wholly suitable model was created.⁶ The Gouy-Chapman-Stern model contains a layer of desolvated ions directly adsorbed onto the electrode surface, this is the inner Helmholtz plane (IHP) and is the location of electrostatic and chemical interactions between the electrode and ion.^{1, 2, 4} A build-up of anions exceeds the positive charge of the electrode and approximately 1nm from the electrode surface solvated cations form a sheet of ionic charge, this is the outer Helmholtz plan (OHP).⁴ The OHP is the presumed to be the site of electron transfer; it is where an electroactive species undergoes oxidation/reduction by electron transfer between the electrolyte solution and electrode.^{1, 2, 4} A diffuse layer (Gouy-Chapman layer) exists after the OHP containing excess ions distributed in such a way that charge dissipates over increasing distance from the electrode. The oxidation or reduction i.e. the heterogeneous reaction of electrons between electrode and solution is an observable current.^{1, 2, 4} This current is also known as a 'Faradaic Current' and its magnitude is calculated with Equation 1-10:

Equation 1-10

$$i = nFAj$$

Where n the number of transferred electrons and j is the diffusion flux and A is the electrode area.

Changes to the structure of the electrode/electrolyte solution interface add a non-Faradaic component to the observed current which is induced by the applied potential. Under these conditions the interface acts as a capacitor (storing an electric charge, Q , due to movement of ions in the double layer). Double layer capacitance, C_d , is calculated with Equation 1-11 where E is an applied potential:¹

Equation 1-11

$$C_d = \frac{Q}{E}$$

A potential is applied to an electrode at a constant scan rate, v , with a starting potential, E_1 , leads to Equation 1-12:

Equation 1-12

$$E = E_1 + vt$$

Where t is time after the start of the scan, and given that current is the charge passed over time (Equation 1-13):

Equation 1-13

$$i = \frac{dQ}{dt}$$

It can therefore be said that the non-Faradaic component for charging is proportional to the scan rate (Equation 1-14):¹

Equation 1-14

$$i_{cap} = C_d v$$

And consequently, voltammetry performed at high scan rates can be dominated by the capacitive current.^{1, 2, 4}

1.1.4 Cyclic Voltammetric Systems

1.1.4.1 Reversible Systems

If the effect from kinetics of electron transfer far outweighs the rate of mass transport via diffusion then the electrochemical system is said to be reversible. This means that there is a Nernstian equilibrium (also known as the boundary condition; Equation 1-15) at the electrode surface meaning:²

Equation 1-15

$$E = E_f^0 + \frac{RT}{nF} \ln \frac{[Ox]_{x=0}}{[Red]_{x=0}}$$

Where E_f^0 is the formal potential and the concentrations are that of when they are at the electrode surface ($[Ox]_{x=0}$, $[Red]_{x=0}$).

When studying the cyclic voltammogram of a reversible system, the key features are the peak currents at both the anode and cathode as well as the corresponding peak potential of each peak current. It must be remembered that the anodic reaction is an oxidation, i_p^{ox} , just as the reaction at the cathode is a reduction, i_p^{red} .²

In these instances, the Randles-Sevcik equation can also be used to explain diffusion in the system using the peak currents of the reversible system as a function of the scan rate (Equation 1-16):¹⁻⁴

Equation 1-16

$$i_p = \pm 0.4463 \left(\frac{F^3}{RT} \right)^{1/2} n^{3/2} A D_{ox}^{1/2} [Ox]_{bulk} v^{1/2}$$

This form of the equation takes into account the bulk concentration of the oxidation species before the reduction species is present, $[Ox]_{bulk}$.¹⁻⁴

In cyclic voltammetry, when the potential is decreased from its initial value, E_1 , to a more negative potential there is electron transfer at the electrode surface reducing Ox into Red and henceforth reducing the concentration of the Ox bulk solution, $[Ox]_{x=0}$, which creates an increase in the flux (due to an ever increasing concentration gradient). An increase of flux (the movement of ionic species) therefore equates to an increase in current. Continuation of decreasing the potential over time will result in the value of $[Ox]_{x=0}$ eventually becoming zero – when this occurs the flux can no longer increase (and therefore the current).^{2, 4}

Upon reversing the scan to go from a more positive potential back to E_1 the inverse of what previously occurred happens.^{2, 4} Because now there is a high concentration of Red now at the electrode surface (as opposed to Ox) the increasing current causes flux in the opposite direction and thus a current. Potential is increased and eventually the value of $[Red]_{x=0}$ becomes zero and the oxidative current reaches its peak. Increases in scan rate will increase the peak current as the decrease in time will give the diffusion layer less relaxation time; because of this, the higher the scan rate the smaller the diffusion layer and therefore an increase in the rate of flux (and therefore an increase in the current) at the electrode/electrolyte interface.^{2, 4}

1.1.4.2 Non-Reversible Systems

In the case where the rate of diffusion far exceeds the electrode kinetics, this is a non-reversible electrochemical system. In non-reversible electrochemical system there is no equilibrium at the electrode/electrolyte interface rather than a Nernstian boundary condition a kinetic boundary condition exists in the system which includes a rate constant for the reduction, k_c , as described in Equation 1-17:¹

Equation 1-17

$$j = D_{Ox} \left(\frac{\partial [Ox]}{\partial x} \right) = k_c [Ox]_{x=0}$$

Because the standard exchange constant, k_0 , is so small in an irreversible system a sizeable potential difference between applied and standard electrode potential, overpotential, is required to force the electrolysis.¹⁻⁴

1.1.4.3 Quasi-Reversible Systems

Systems can exist wherein it is neither reversible nor irreversible - it is a quasi-reversible system. Quasi-reversible systems are the intermediate; at lower scan rates it has a system that appears to be reversible however upon increasing the scan rate, the Nernstian boundary condition cannot be upheld due to a sub-sufficient rate of electron transfer resulting in greater peak to peak separation.

1.1.5 Electroanalysis

Employing cyclic voltammetry for electroanalysis typically involves studying the current that is the result of an electrochemical reaction occurring at the electrode surface/solution interface. In particular, the peak height (I_p) that arises at a specific voltammetric potential (E_p) following the oxidation/reduction of the target analyte can be a reliable analytical signal. For example, in a typical electrochemical system, such as that postured with the

widely utilised redox- couple ruthenium hexamine – an increase in analyte would result in a proportional increase in peak height.³ The concentration range wherein an increase in analyte has a directly proportional effect on the measured peak height is known as the analytical linear range.⁷ As with the techniques regularly discussed within the analytical chemistry community, concentrations outside of this linear range no longer increase the measured signal in a proportional fashion and can no longer be considered a reliable, accurate measurement.⁷ A common reason for this in analytical electrochemistry is saturation of the electrode surface (to say, there is physically no space for an analyte to interact with the electrode surface) – this is observed on an analytical curve by a plateau at higher concentrations.³

As previously mentioned (section 1.1.1), the peak current in a voltammetric process is equal to approximately 10^5 times the concentration of the target analyte. It is this unique relationship that allows electrochemistry to be such a powerful tool. However, variations to the electrochemical system (i.e. the solution containing both analyte and electrode system) can have an effect on the analytical signal for instance, pH.² Changes in pH can affect or even dictate the electrochemistry, for example, the analysis of metals in basic solutions is unfeasible just as exchanges mechanisms that require an exchange of protons are heavily influenced by pH either positively or negatively (dependant on whether acidic or basic) effecting the magnitude of measured current (E_p).²

A common theme for analytical electrochemists is the improvement of analytical signals though changes to the electrode material,⁸⁻¹² modifications to the surface¹³⁻¹⁷ or sometimes both – this is a superlative way of increasing sensitivity whilst not compromising on the rapid speeds offered by electrochemistry. A measure of selectivity can also be introduced with modification to the electrode surface,¹⁸ this is key in particularly complex matrices, such as blood, where the ability to detect ultra-low concentrations is vital. The work detailed within later chapters of this thesis employs some of these approaches using a variety of carbon-based materials in addition to modifying existing materials with heavy metals mercury and bismuth in an attempt to improve electroanalytical responses.

A critical value for any analytical protocol is the limit of detection.⁷ This is the lowest value that can be measured within a certain confidence level, it is common practise for this to be

set at the 3-sigma (3σ) level⁷ and is used within this thesis. The 3σ significance level is the lowest confidence level that is typically believed as to being a true result within the analytical community rather than merely noise - essentially, it is a measure of probability relating to the mean and standard deviation of a normal distribution.^{7,19} A simple approach to calculating this value is analysing a minimum of three replicates and calculating the standard deviation – multiplying this by three will result in the limit of detection at a 3σ level. The assurance this leaves is that, when referred to a Standard Normal Z-table, a 3σ confidence level 99.87% chance the result is not due to random fluctuations in the measured signal but a correct recording.^{7,19}

1.2 Forensic Electrochemistry in the Field

The objective examination of a crime scene using scientific methods has aided judiciary systems across the world for decades, and there are no words too emphatic to describe the impact that analytical procedures have had upon Forensic Science. In some cases, forensic evidence becomes so important that it is the contributing factor to the final decision of a jury; and conversely, forensic evidence derived from analytical techniques have returned not guilty verdicts and even overturned convictions. However, the power of analytical forensic evidence in the courtroom notwithstanding – it would be prudent to approach such cases with a degree of caution. There is evidence to suggest that DNA (deoxyribonucleic acid) evidence can quite easily be fabricated, for example,²⁰ leading to suspicions that analytical scientists could potentially have involvements in criminal cases. This means that any person undertaking a forensic procedure requiring the removal of samples from a crime-scene is subject to cross-examination in the courtroom to ascertain potential conflicts of interest within that particular case. Such caution could be eliminated, or at least made less open to interpretation, if objective analytical measurements were made at the scene of a crime instead of evidence taken away. This way the sampling is monitored independently at the scene and there is less room for accusation of falsifying data through chemical manipulation in the lab, or sample damage due to the transfer of material. The importance of on-site forensic methods has therefore never been higher.

The choice of analytical procedure is never a simple decision, because there are more factors that need to be considered than simply the determination of a chemical component. One example may be the determination of cyanide in blood; the complex sample matrix limits highly accurate chromatographic methods, so optical measurements or mass spectrometry may be preferred.²¹ The limits of detection may also be too low in some cases, so it stands to reason that spectroscopic methods may be replaced by Inductively Coupled Plasma – Mass Spectrometry (ICP-MS). In fact, there is probably no such thing as an all-encompassing analytical technique, method, or procedure and consequently, a combination of methods would generally be implemented to determine trace substances present at a crime scene. Such as the examination of smaller fragments, fibres, or shards, a microscopic instrument would typically be employed, whereas the

separation of mixtures or elemental analysis may require chromatographic methods to be utilized. That said, electrochemical methods have made some enormous strides towards offering an all-encompassing technique. That is, electrochemistry in some cases can offer the required selectivity, portability, and sample versatility needed in order to detect substances at the scene of a crime without the need for a lengthy sample pre-treatment step.^{22, 23} The term “Forensic Electrochemistry” therefore describes the use of electrochemical methods in order to quantify any chemical species present at the scene of a crime in a variety of matrices.

The versatility of electrochemistry is rarely celebrated in scientific literature, but there is no doubt that it ranks highly amongst all analytical methods when it comes to the range and scope of its use. As a consequence of the continual evolution of both electrochemistry and Forensic Science,²⁴ it seems almost inevitable that a synergy between the two would eventually be formed. The application of electrochemical methods to Forensic Science spans a range of areas. There are obvious applications, such as the detection of poisons and drugs, yet there are some less obvious ways to implement electrochemical methods into Forensic Science. Few people could imagine using electrodes to probe gunshot residues, and fewer would think that electrochemistry could detect fingerprints. Indeed, the focus of this thesis is primarily towards the utilisation of screen-printed electrodes for the detection of illicit compounds (and in particular, *Novel Psychoactive Substances*) however, this section explores the origin of forensic electrochemistry as a concept and its widely used applications within the literature to further understanding of this niche subject area.

1.2.1 Poisons

There is no exact date when Forensic Electrochemistry was coined, but it was used as a phrase by Ramdani *et al.* in their paper regarding the electrochemical detection of atropine.²⁵ The case in point in Ramdani’s work related to Dr Paul Agutter, who in 1995 was convicted of attempted murder after attempting to poison his wife by spiking her gin and tonic with atropine.²⁶ The story caused a national outcry in Scotland because he had attempted to cover his tracks by placing atropine-contaminated bottles of tonic on the shelves of a local supermarket. Unfortunately for Mrs Agutter, in 1995 Ramdani’s work

wasn't even in the thoughts of researchers. However, if such an accusation was made today the method would have the ability to electrochemically determine concentrations of atropine in tonic at the scene of the incident, through the use of screen-printed carbon electrodes.²⁵ In this case, electrochemistry could speed up the process of returning an objective result.

In the original research article, atropine was dissolved in both laboratory model buffer solutions and Diet Coke™ and tested electrochemically, using a voltammetric method (*see above*). The electrochemical reaction between atropine and the SPE was demonstrated to occur at a potential of +0.82 V in pH 10 model buffer solution and it was also proved that atropine could be monitored in Diet Coke™ within a linear range of 5 – 50 μM. The results for Diet Coke™ were actually more analytically reliable than the laboratory buffers because the alkalinity of the buffer solutions interfered detrimentally with the electrochemical response. Solutions such as tonic water, however, had to be compared more carefully as tonic water normally contains quinine as a flavour enhancer, an electroactive molecule exhibiting voltammetric waves at similar potentials to atropine! The application of SPEs to this process allows a potential route towards taking the lab into the field for onsite analysis, effectively reducing waiting times for result feedback as well as reducing the risk of sample contamination between sites. This method therefore developed the concept of Forensic Electrochemistry by applying potentials across a screen-printed three electrode cell to determine the concentration of a specific molecule. The advantage of the printed electrode setup is the miniaturisation of electrochemical methods using cheap and disposable, yet reproducible, electrodes that do not require pre-treatment in the lab prior to analysis. Many applications of Forensic Electrochemistry exploit screen-printed electrodes. These advantages avoid expensive and time-consuming lab-based techniques such as high performance liquid chromatography and gas chromatography with mass spectrometry.

1.2.2 Gunshot Residue (GSR)

Researchers in America however may be quick to dispute the origins of Forensic Electrochemistry; particularly if the above example was cited as the originator of the concept. Although Ramandani *et al.* were the first to use the phrase academically, the Royal Society of Chemistry takes some of the credit for when they reported work from the

University of California in 2012.²⁷ Such work reported an exciting and innovative approach towards the electrochemical detection of gunshot residues. The article was quickly publicised by scientific news outlets and they were quick to suggest that gunshot residues could be electrochemically detected. Actually the work was, in-fact, simply laying the foundation for such applications as the method was designed to only electrochemically detect the organic propellants and heavy metals associated with gunshot residues (of course, in a courtroom scenario, it would be the job of the prosecution to find out the exact origins of such materials). The beauty of the work reported by Vuki *et al.* is that their method detects not one, but several components that are associated with gunshot residues such as dinitrotoluene, nitroglycerin, antimony, zinc, barium, and lead.²⁸ In the introductory arguments, the authors provide a view that the singular detection of these compounds/ions/elements can be inconclusive in criminal investigations because many are not unique to gunshot residues. Their method consequently is designed to detect several components from gunshot residue in tandem, as it is less likely that these would appear together at the scene of a crime *without* being fired from a gun.

In forensic cases, the required detection levels of nitroglycerin and lead are in the ppm range or less. Therefore, the method specifically operates utilising a square-wave voltammetry procedure; such procedures are normally employed when the user requires detection limits to be lower than a than a typical voltammetric method, such as cyclic voltammetry. In a single measurement, the method has the ability to detect no fewer than four common components of gunshot residues - this was achieved by holding the cell at a high potential of +1.2 V for 120 seconds to accumulate electroactive species at the electrode surface.²⁸ This step allows the absorption of oxidation species upon the electrode surface. Following this the cell was ramped from a high to low potential (+1.2 - -1.3 V) in order to instigate the electrochemical reduction processes and then once more held at -1.3 V for a period of 120 seconds to accumulate a high concentration of the reduction species at the electrode surface. Subsequently the cell is then ramped from a low to a high potential (-1.3 - +1.2 V) and the current signals produced are plotted as a function of applied electrode potential.²⁸ An example is shown in Figure 1-3.²⁸

The method was found to have the ability to qualitatively determine the presence of at least four different components of gunshot residues including: antimony, lead,

nitroglycerin, and dinitrotoluene. In one measurement, this method has the potential ability to determine whether these species coexist at the scene of a crime. The coexistence of such materials provides a strong case for the use of a firearm and may potentially lead to conviction or acquittal. The present methods for detecting such particles are highly expensive and require skilled personnel. For example, a scanning or transmission electron microscope would normally be utilised to image the gunshot

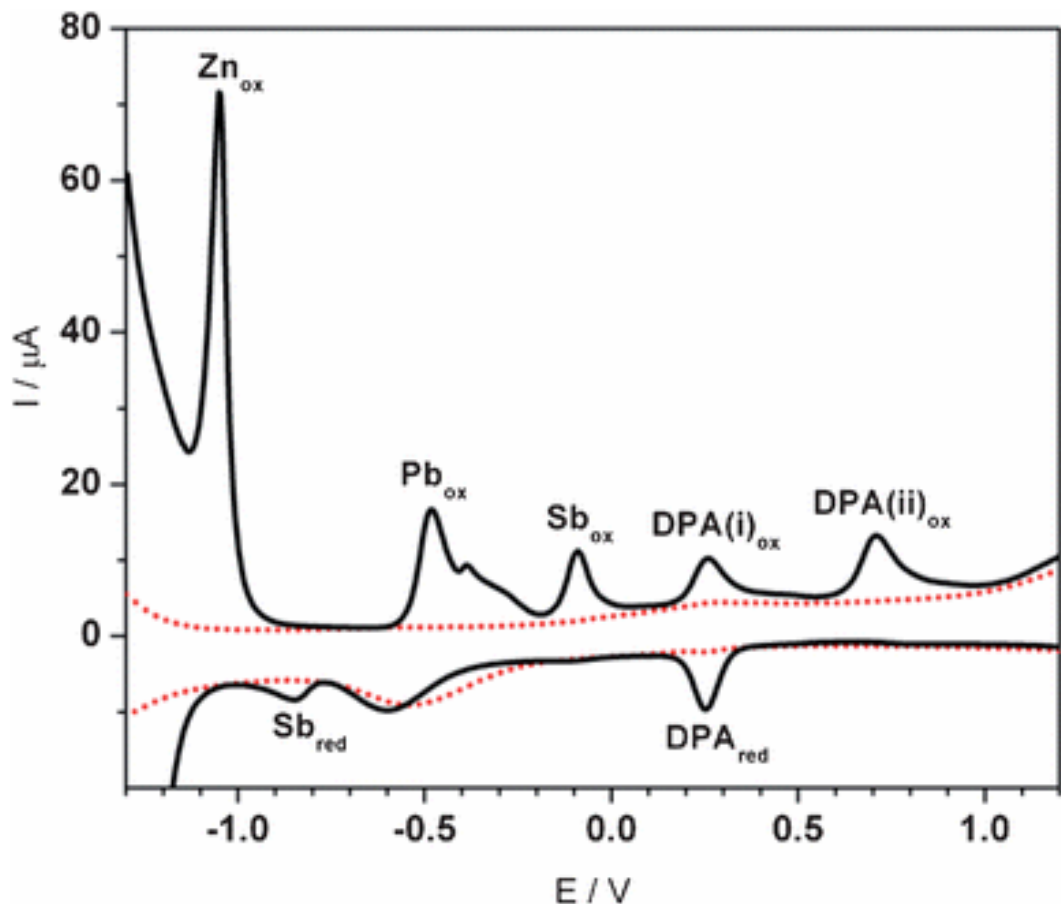


Figure 1-3 Cyclic square-wave voltammogram for a mixture of trace metals and explosives constituents of GSR: 2 ppm Zn, 2 ppm Pb, 20 ppm Sb, and 200 ppm Diphenylamine (DPA). Square wave parameters: E_{step} , 4 mV; amplitude, 25 mV; frequency, 25 Hz; and t_{accum} , 120 s; (reduction) $E_{\text{start,accum}}$ 1.2 V and E_{stop} , -1.3 V; (oxidation) $E_{\text{start,accum}}$, -1.3 V; E_{stop} , 1.2 V; and t_{accum} , 120 s. Electrolyte, acetate buffer (pH = 4.5). Reproduced from reference 28.

particle, and a chromatographic method would be used to determine the chemical species. A combination of these techniques is highly expensive and time-consuming; electrochemistry can solve these issues. Such work could have been implemented for famous criminal cases such as the murder of UK journalist Jill Dando in 1999, whose

murderer still hasn't been found and could have perhaps avoided the false sentencing of Barry George who served 8 years for her murder.²⁹

1.2.3 Fingerprinting

Electrochemistry can also be used forensically for fingerprinting using some highly innovative methods. One literature report describes how the corrosion rates of a metal surface are different when a surface has come into contact with a fingerprint.³⁰ The paper utilises electrolysis to "create" a fingerprint on a metal surface by immersing a metal surface into a solution of hydrochloric acid. The fingerprint acts as a barrier to corrosion, essentially meaning that the kinetics of corrosion are much faster for the uncovered parts of the metal than the fingerprinted parts. When a reductive voltage is applied to the metal, electrochemical reactions are forced, which gently corrode the surface, etching a fingerprint into the metal. The concept was expanded further by applying the method to a bullet fired from a gun. The authors argue that this is necessary because the high temperatures and pressures subjected upon the bullet can be highly destructive to fingerprints to the point where they are not detectable through conventional methods. Their method does come with a degree of success, as seen in Figure 1-4; the reduced metal sections have clearly been discoloured and have effectively etched the fingerprint into the bullet after only 5 minutes of electrolysis. This method would be very simple to apply in the field, using dilute hydrochloric acid and a handheld potentiostat.

The fingerprint shown in Figure 1-4 could potentially be used to support a criminal prosecution or defence in the event that conventional fingerprint methods are unsatisfactory. Scanning Electrochemical Microscopy (SECM) is another electrochemical-based method that has potential for fingerprint analysis,³¹ though the size of the equipment may limit its use in the field. Such a method uses gold nanoparticles to stick to fingerprints.³⁰



Figure 1-4 Electrolysis-etched fingerprint on a bullet. Reproduced from Reference 30 with permission from the International Association for Identification.

1.2.4 DNA

The next topic discussed in this Chapter is the application of electrochemical methods for the detection of DNA, which by no means is a new type of technology. There are a plethora of DNA-related papers reporting the electrochemical oxidation of DNA bases, the detection of specific DNA strands, and electrochemical coding technology for multiple DNA bases.³²⁻

³⁵

Work reported by Wang³⁵ in 2003 and has become a highly cited research article.³⁵ The work incorporated the use of several quantum dots, such as CdS, ZnS and PbS, that are used as labels on single stranded DNA.³⁵ The quantum dot tagged single stranded DNA is hybridized with a known base sequence; such hybridization events only occur with complimentary DNA bases. Adsorptive stripping voltammetry can then be applied to electrochemically detect a specific DNA strand because the quantum dot labels can uniquely interact with electrode surfaces and strip from the surface at finite electrode

potentials. This way, several DNA fragments can be differentiated and such a method is potentially useful for the analysis of mixed DNA fragments at crimes scenes.³⁵

The use of nanotechnology for DNA sequencing saw a rapid boost after the aforementioned works. Researchers turned to gold nanoparticles for DNA detection in forensic applications; an example of this was reported by Li.³⁶ Their work took a dual nanotechnology approach, by incorporating dendrimers and gold nanoparticles into their methodological design. Such methods act as a signal amplification and an electrochemical detection strategy, eliminating the needs for lab-based procedures such as the polymerase chain reaction.

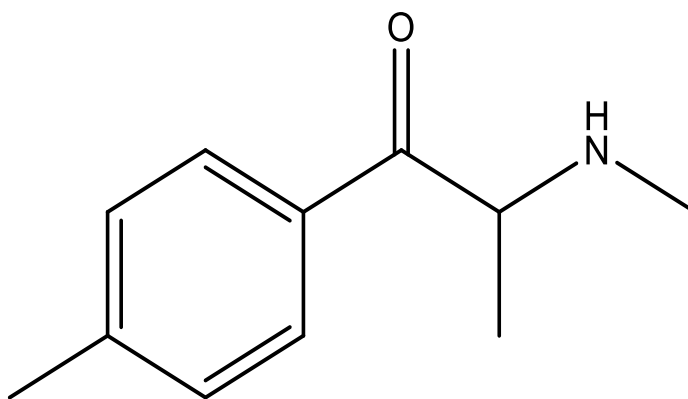
The work presented in this chapter formed the basis of the chapter: J.P Smith, E. P. Randviir and C. E. Banks, in *Forensic Science – Multidisciplinary Approach*, Wiley-VCH, 2016.²³ The next chapter addresses the growing Novel Psychoactive Substance epidemic by reviewing the current analysis techniques available and appraises what a pertinent course of action would be to aid the necessary authorities.

Chapter 2 What are Novel Psychoactive Substances?

A major issue that is addressed by this thesis is the growing epidemic postured by Novel Psychoactive substances (NPSs) and the detection thereof. The following chapter is a critical review on the existing methodologies for the detection of the array of Novel Psychoactive Substances whilst also evaluating how these techniques can be applied to 'in-the-field' analysis to aid nationwide drug law enforcement.

2.1 Introduction

A Novel Psychoactive Substance (NPS) is an umbrella term to refer to substances which mimic the effects of common illicit materials (for example, methamphetamine and cannabis) but are not controlled by drug legislation such as the Misuse of Drugs Act in the United Kingdom and other similar controls internationally. Designed, in some cases deliberately, to evade international control, NPSs may pose a significant danger to the health and safety of the public. As with controlled substances, NPSs are understood to have potentially negative short-term side effects such as paranoia, psychosis and seizures however these may not always be fully understood on account of the materials often being fairly new and understudied, as such their long term health risks are also not always clearly understood.³⁷ The United Nations Office on Drugs and Crime (UNODC) and European Monitoring Centre for Drugs and Drug Addiction (EMCDDA) standardised the term "*New Psychoactive Substance(s)*" and detailed the following sub-categories: Synthetic cannabinoids, Synthetic cathinones, Ketamine, Phenethylamines, Piperazines, Plant-based substances: khat, kratom, salvia divinorum and Miscellaneous: aminoindanes, phencyclidine, tryptamines.³⁸



Scheme 2-1 The structure of mephedrone, centrepiece of the research conducted within the thesis

Given the nature of NPSs underhanded production, purposely designed to evade international drug legislation, they are intrinsically marketed and sold as “*legal highs*”. Easily available at ‘head shops’ (a commercial outlet selling cannabis and tobacco paraphernalia), market stalls and the internet; vendors of NPSs are often operating on the edge of legality by being both vague and creative in their description of the products contents and its purported uses. NPSs may be sold as research chemicals, plant food, bath salts, exotic incenses *etc* together with slightly more telling descriptors such as: party pills, herbal highs and smoking blends although these names can often be mercurial, for example, mephedrone (a synthetic cathinone) pre-control was plant food whereas after becoming a controlled substance it was referred to as a ‘research chemical’.

Although given these nondescript aliases, NPSs products often have brand names; examples of “*legal high*” brand names are ‘Benzo Fury’, ‘Afghan Incense’, ‘NRG-1’ and ‘NRG-2’. The name or description given to a NPSs or “*legal high*” product may not always pertain to what is the actual psychoactive substance present, for example mephedrone was detected in products sold as naphyrone or NRG-1 in the UK even after its ban,³⁹ another survey found 70% of NRG-1 and NRG-2 products examined contained mixtures of substituted cathinones and not, at the time uncontrolled, naphyrone.⁴⁰ Clearly there are no assurances to the customer of these NPS products that the contents are the same as advertised, furthermore they may be unwittingly violating drug legislation as the contents within are controlled substances.

Abuse of NPSs has been reported to be increasing since *ca.* 2009 and has continued to be an ever growing market⁴¹ emerging at an unprecedented rate something also reflected in the online marketplace with the number of online vendors in the UK increasing by more than 300% between 2010 and 2011.⁴² New materials made available for abuse appear rapidly and, at times, can gain a ‘foothold’ in the market – such as mephedrone. In 2014, 101 new substances were reported for the first time to the EU early warning system (EWS) run by the EMCDDA, up from 81 in 2013 which is also an increase from the 74 substances notified in 2012.⁴³ Of the findings of the EWS synthetic cannabinoids are the most frequently discovered with 102 detected between 2005 and 2013. A graphical representation of NPSs notified to the EWS between 2005-2014 is shown in Figure 2-1.⁴³

The media has reported on numerous deaths related to “*legal highs*” and given the wide variety of NPS and the ever-changing composition of existing products, a completely new field of research has emerged in the continual development of analytical techniques along

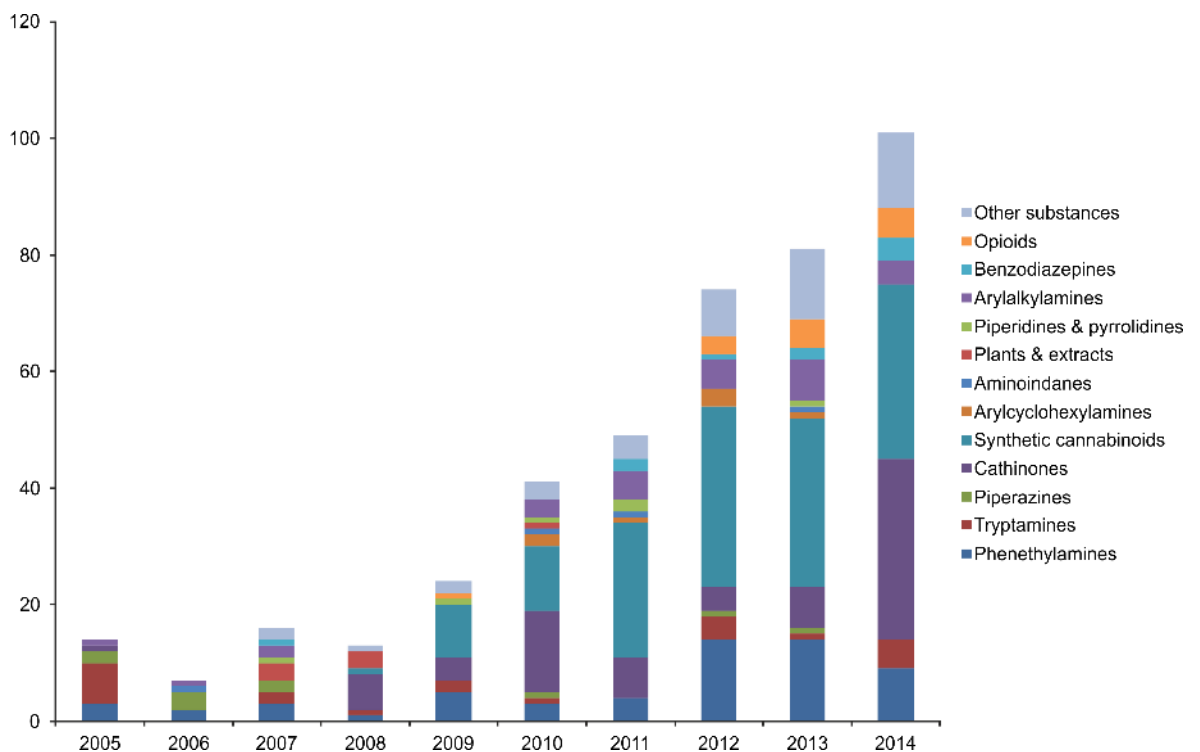


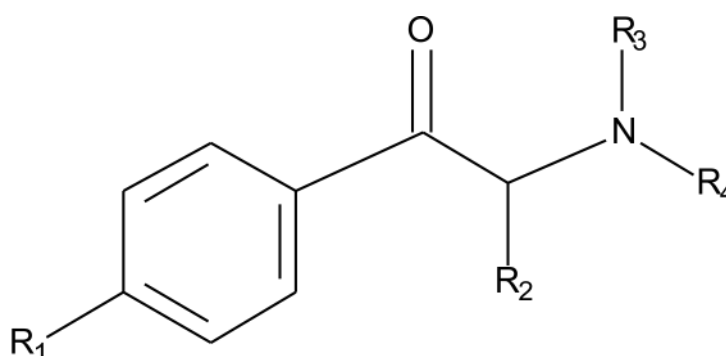
Figure 2-1 A graphical representation of new psychoactive substances notified to the EWS between 2005-2014. Reproduced with permission from the EMCDDA.

with presumptive tests and in-the-field sensors. In this review of the literature, a thorough overview of this new analytical field of NPSs is provided. Covered within are: synthetic cannabinoids (most frequently discovered NPS by the EWS), synthetic cathinones; particularly mephedrone, observable in Scheme 2-1, (amidst reports by the Crime Survey for England and Wales [CSEW] detailing mephedrone as the most prevalent of abused NPSs) and in lesser detail pieces of interesting research of the other NPSs notified to the EWS (visible in Figure 2-1).⁴³

2.2 Synthetic Cathinones

Synthetic cathinones are an amphetamine-like cheap alternative to Ecstasy derived from cathinone; an organic stimulant found in Khat – a plant native to East Africa and the Middle-East and they possess pharmacological similarity to the phenethylamine class of psychoactives (*e.g.* amphetamine and methamphetamine) all sharing a common structure that is observed in Scheme 2-2. The effects of synthetic cathinones on the body are reported to have both cardiovascular and neurological side-effects; believed to block the reuptake of norepinephrine, dopamine and serotonin⁴⁴ whilst there are also reports that they also induce the release of more dopamine⁴⁵ suggesting synthetic cathinones act like both methamphetamine and cocaine synchronously.⁴⁴⁻⁴⁸

Internationally there has been a tightening of the legislation regarding synthetic cathinone derivatives, for example, cathinones are illegal in the UK as well as Germany, The United States, Canada and many others.^{49, 50} The European Monitoring Centre for Drugs and Drug Addiction's (EMCDDA) Early Warning System (EWS) has reported 74 new synthetic cathinones between 2005 and 2014, with 30 new substances discovered in the year 2014 alone (Figure 2-1). Clearly, the epidemic initiated by synthetic cathinones is showing no signs of cessation within the near future, hence the development of methods for their detection and quantification is timely and urgently required. Mephedrone in particular, since it's availability for abuse, is popular amongst users of "legal high"



Scheme 2-2 Key structure of synthetic cathinones

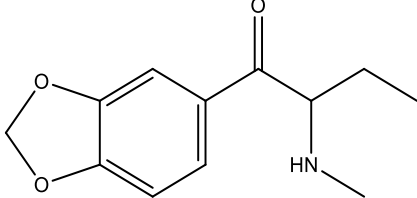
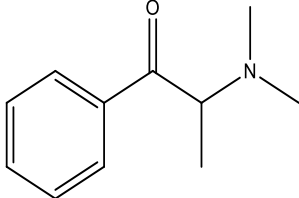
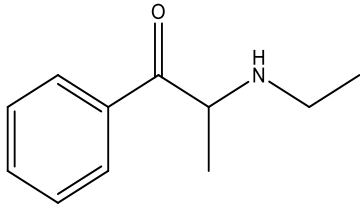
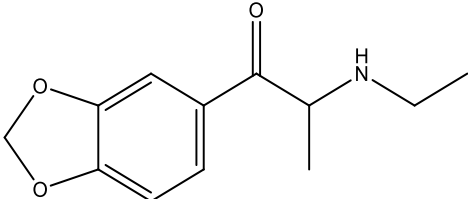
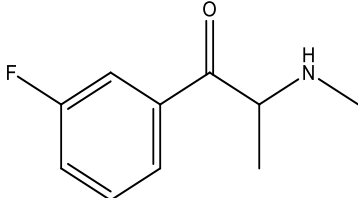
products and despite its classification in 2009 reports from the Crime Survey for England and Wales (CSEW) reveal mephedrone was still being abused in England and Wales in 2014.

Popularly known as ‘bath salts’, ‘research chemicals’ or ‘plant food’, synthetic cathinones are sold under, often mercurial, non-descript brand names such as ‘Energy’ (NRG), Blizzard and Ivory Snow containing warning labels such as ‘not for human consumption’ or ‘not tested for hazards or toxicity’ in an attempt to bypass legislative controls. The active component in a “*legal high*” product can vary wildly, even within the same brand name;^{39, 46, 51} there are no clear assurances to the customer of these NPS products that the contents are the same as advertised (see above).

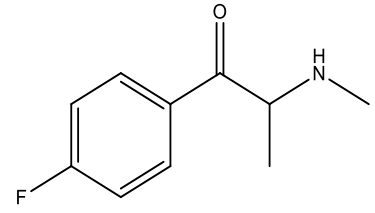
The list of case reports concerning synthetic cathinone-induced intoxication is extensive and ever increasing. In the United States the number of calls to emergency centres, as a result of synthetic cathinone abuse, increased from 303 to 6,100 between 2010 and 2011. A plethora of case reports are reported in the literature and media spanning a sizeable age range, including both of the sexes and include fatalities and the curious report of the murder of a goat whilst dressed in lingerie.⁵² For instance, a female aged 15 had symptoms of nausea, vomiting, altered mental status, euvoelaemic hypo-osmotic hyponatremia with encephalopathy and increased intracranial pressure – mephedrone metabolites were found in her urine.⁵³ A male aged 31 after admitting to taking three 1500 mg packets of “bath salts” and was reported to have hallucinations, paranoia, agitation; elevated serum creatine phosphokinase (CPK) level, hyperkealemia, dehydration, rhabdomyolysis and acute renal failure.

Considering all the synthetic cathinones discovered, there can be no assertions to which are the being abused but what is evident from the literature is that the most prominent synthetic cathinones found within “*legal high*” products globally are mephedrone (4'-methylmethcathinone; 4-MMC) and 3',4'-methylenedioxypropylone (MDPV).⁵¹ Mephedrone is more prevalent in Europe and MDPV in the United States;⁵¹ a list of some of the most prevalent cathinone derivatives (with corresponding structures)⁵⁴ abused worldwide can be found in Table 2-1, although the main focus of the chapter (and

Table 2-1 List of the most common synthetic cathinones, emphasis given to the most prevalently abused globally.

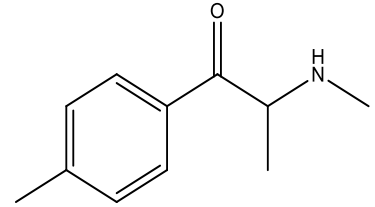
Common name and abbreviation	Chemical structure
(±)-Butylone (βk-MBDB)	
<i>N,N</i> -Dimethylcathinone, (methamfepramone)	
<i>N</i> -Ethylcathinone, (EC)	
Ethylone, (4β-MDEA)	
3-Fluoromethcathinone (3-FMC)	

4-Fluoromethcathinone (4-FMC)



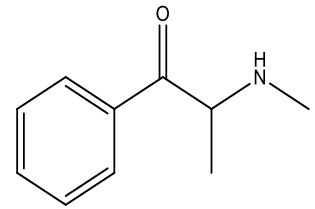
Mephedrone,

(4-methylmethcathinone; 4-MMC)



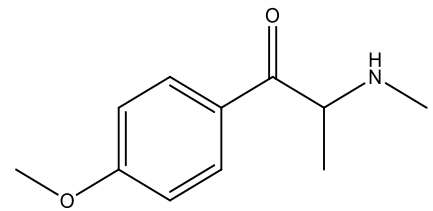
(±)-Methcathinone,

(ephedrone)



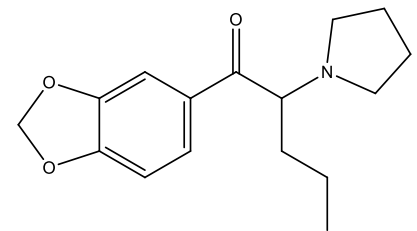
Methedrone,

(4-methoxymethcathinone, βk-PMMA)



3,4-Methylenedioxypropylvalerone,

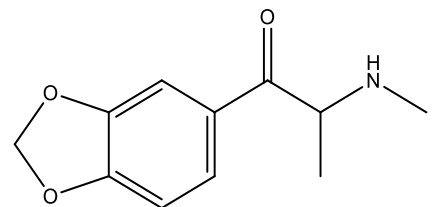
(MDPV)



Methylone,

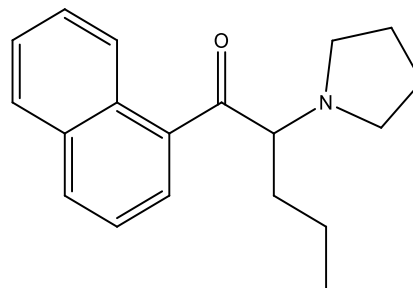
(3,4-methylenedioxy-N-methylcathinone;

βk-MDMA)

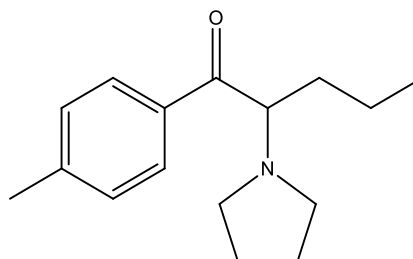


(±)-Naphyrone

(naphylopyrovalerone)



Pyrovalerone



subsequent work within the thesis) will apply generally towards the detection and quantification of mephedrone. Studying the patterns of NPS abuse can be difficult as it is frequently based upon self-reported user surveys.⁵⁵ This is potentially problematic as in many instances users are, due to poorly labelled products (see earlier), not in fact aware of the substances they are taking. In light of this, numerous groups are making advances towards screening the current NPSs being abused. A number of revered groups using a range of chromatographic techniques including high performance liquid chromatography (HPLC) and gas chromatography with mass spectrometric detection (GC-MS), with liquid chromatography–mass spectrometry (LC-MS) methods seemingly the preferred and established technique of choice, have published exhaustively upon the laboratory-based analysis of synthetic cathinones,^{39, 56-76} phase I and II metabolites^{77, 78} and more recently, in light of the often nonenantioselective NPS synthesis, chiral separation of racemic mixtures.⁷⁹

In 2014 Archer *et al.*⁵⁵ analysed urine samples collected from a night club over one weekend. The manuscript with its real and imaginative title, “*Taking the Pissoir – a novel and reliable way of knowing what drugs are being used in nightclubs*”, reported the detection of classical recreational drugs and NPSs such as: mephedrone, 3’-(trifluoromethyl)phenylpiperazine and 2-aminoindane using various chromatographic and

mass spectrometric methods.⁵⁵ Furthermore parent drug/metabolites were also detected for amphetamine, cocaine, ketamine, 3',4'-methylenedioxyamphetamine (MDMA), mephedrone and 3-(trifluoromethyl)phenylpiperazine (3-TFMPP); this is important as it indicates drugs were being used and not simply discarded into the urinal.⁵⁵ In the same year, Leffler et al.⁸⁰ (located in the United States) analysed 14 separate street samples wherein 10 synthetic cathinones were identified employing a variety of techniques, including gas chromatography with mass spectrometric detection (GC-MS) and flame ionization (GC-FID).⁸⁰ HPLC direct infusion tandem mass spectrometry (MS/MS) was also used to identify compounds which were not available as reference materials. Out of the synthetic cathinones detected: 3',4'-methylenedioxypropylvalerone (MDPV), 3',4'-methylenedioxy- α -pyrrolidinobutiophenone (MDPBP), 4'-fluoromethcathinone (4-FMC), butylone, mephedrone, naphyrone, 4'-methylethcathinone (4-MEC), ethcathinone, α -pyrrolidinopentiophenone (α -PVP), and 3'-methyl- α -pyrrolidinopropiophenone (3-MPPP), MDPV was the most prevalent, found in five of the 14 samples and ranging from 11% to 73% (w/w) between samples.⁸⁰

Earlier reports in Denmark, Pedersen *et al.*⁷¹ presented an automated solid-phase extraction (SPE) and ultra-high-performance liquid chromatography (UHPLC) with time of flight mass spectrometry (TOF-MS) screening method for 256 illicit compounds in blood and 95 of these compounds were validated with regard to matrix effects, extraction recovery, and process efficiency with the limit of detection (LOD) ranging from 0.001 to 0.1 mg kg⁻¹.⁷¹ Application of the technique to the analysis of 1335 forensic traffic cases revealed 992 cases (74%) were positive for one or more traffic-relevant drugs above the Danish legal limits. Commonly abused drugs such as amphetamine, cocaine, and frequent types of benzodiazepines were the major findings. Nineteen less frequently encountered drugs were detected: buprenorphine, butylone, cathine, fentanyl, lysergic acid diethylamide, *m*-chlorophenylpiperazine, MDPV, mephedrone, 4'-methylamphetamine, *p*-fluoroamphetamine, and *p*-methoxy-*N*-methylamphetamine.⁷¹

Even as early as 2011, there have been numerous attempts at constructing screening methods for substituted cathinones in a number of different matrices, Bell and co-workers⁶⁵ reported a rapid multi-analyte direct urinalysis Liquid Chromatography - Tandem

Mass Spectrometry (LC-MS/MS) screening method being able to detect eight analytes including; 4'-methylmethcathinone (mephedrone), 3',4'-methylenedioxy methcathinone (β k-MDMA, 'methylone'), 4'-methoxymethcathinone (β k-PMMA, 'methedrone') and 3', 4'-methylenedioxypropylone (MDPV).⁶⁵ Using a dilution of 1 part urine to 4 mobile phase to reduce matrix effects and although not all compounds were completely chromatographically resolved, there was sufficient specificity to allow target analyte identification. All the analytes were readily detected at a concentration of 500 ng mL⁻¹ offering an attractive method for the routine screen of NPSs.⁶⁵ The global impact of synthetic cathinones is compounded when substances such as mephedrone and MDPV have been detected following sewage-based epidemiology in Chinese 'megacities'.⁸¹

In terms of quantification, Santali *et al.* provided the first fully validated HPLC method for the quantification of mephedrone⁵⁸ where limits of detection and quantification of 0.1 and 0.3 μ g mL⁻¹ respectively were reported. Khreit *et al.* further refined this method enabling the detection of both mephedrone and two novel derivatives, 4'-methyl-N-ethylcathinone (4-MEC) and 4'-methyl-N-benzylcathinone (4-MBC), in seized samples of "NRG-2". In this case the limits of detection and quantification were reported as 0.03 and 0.08 for 4-MEC and 0.05 and 0.14 μ g mL⁻¹ for 4-MBC both in their pure form and in the presence of common adulterants such as caffeine and benzocaine.^{39, 59} There has also been work using chromatographic methods on the detection of cathinone based "legal highs" in biological matrices^{60, 73} in which Beyer *et al.* were able to detect and quantify 25 designer cathinones in a validated LC-MS/MS method.⁷³

Other work⁶² has seen an attempt to screen chronic abuse of mephedrone through GC-MS analysis of hair. The hair was first decontaminated in methylene chloride and incubated overnight in a pH 7 buffer in the presence of deuterated MDMA at 40 degrees Celsius. The work saw 67 hair specimens tested for mephedrone with 13 yielding positive results of concentrations ranging from 0.2 - 313.2 ng mg⁻¹.⁶² The work showed that like other stimulant drugs, mephedrone is well incorporated into hair and the analytical method reported appears sensitive enough to reveal occasional to regular use of mephedrone.⁶²

Recently direct analysis in real time mass spectrometry (DART-MS) has been utilised to quantify and characterise the multitude of new and emerging NPSs.⁸² Solid synthetic

cathinone samples (2-FMC, 2-MEC, 2-FEC and 2-EEC) were sampled directly without pre-treatment and positive ion mass spectra were acquired using a DART-SVP™ ion source interfaced to an AccuTOF™ mass spectrometer. Further advancements in this methodology by the same authors⁸³ has seen the application of a time-of-flight (TOF) mass analyzer along with in-source collision-induced dissociation (CID) spectra to provide data for presumptive analysis of various synthetic cathinones in a similar fashion to GC-MS analysis.⁸³ The authors scope for this work is to provide a rapid screening method to quickly respond to the rapid evolution of designer drugs and the consequent testing backlogs that develop.^{82, 83} Ion mobility spectrometry (IMS) has also been applied to the screening of an array of NPSs within the literature with acceptable results.^{84, 85}

Interesting developments in the detection of synthetic cathinone derivatives with the use of surface enhanced Raman-spectroscopy (SERS) have also been reported.^{86, 87} In this novel approach, the usually required thin metallic surface (typically gold or silver) was provided by galvanising a British two pence coin with silver (created by spotting 10 µL of a 0.1 M silver nitrate solution onto the coin's surface at room temperature; 23 °C).⁸⁶ Note that a pre-1992 two pence coin (97% Copper) is required as post-1992 two pence coins are composed of copper-plated steel and have an undefined composition.⁸⁶ Figure 2-2 shows the concept when dendritic structures are evident on the two pence surface, providing proof of concept for SERS detection of mephedrone, MDMA and aminoindane 5',6'-methylenedioxy-2-aminoindane

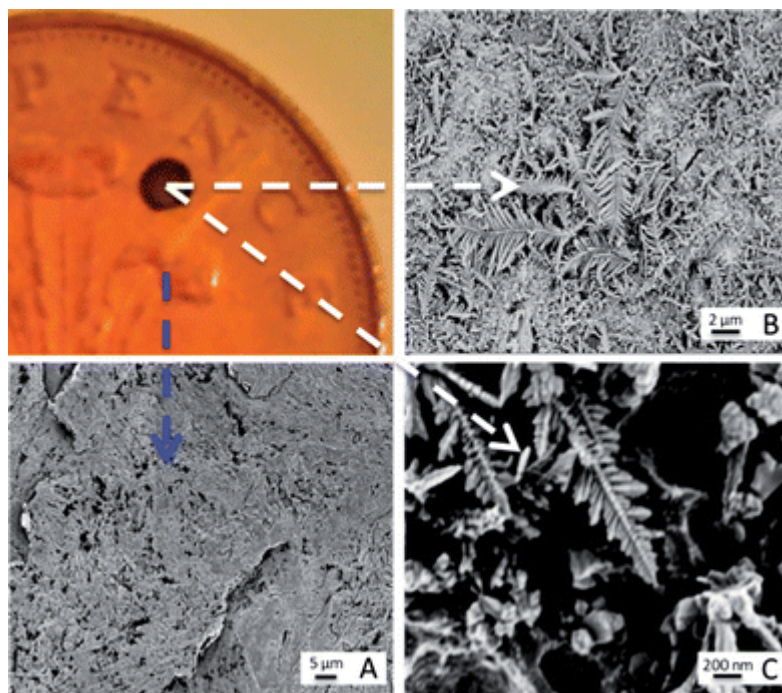


Figure 2-2 Characterisation of galvanic displacement. The optical image (top left) shows a clean British 2p coin, with silver deposited onto its surface. (A) shows an SEM of the rough surface of the two pence after cleaning. The SEM in (B) shows the silver dendritic structures that are formed on the coins surface. The fern like structures are magnified in (C) and show that secondary crystalline domains grow perpendicular from a primary silver backbone. Recreated from reference 86.

(MDAI) was demonstrated.⁸⁶ Further developments saw the researchers working towards a new optimization strategy for the SERS detection of mephedrone using a portable Raman system employing a fractional factorial design approach to significantly reduce the statistical experiments whilst maintaining statistical integrity.⁸⁷ Furthermore, four optimised SERS protocols for which the reproducibility of the SERS signal and the limit of detection of mephedrone were established with an estimated limit of detection of $1.6 \mu\text{g mL}^{-1}$.⁸⁷ Another alternative to the well-established chromatographic methods, NPS detection has been reported with the use of immunochemistry, Paillet-Loilier *et al.*⁵⁴ noted the use of this technique to test the cross-reactivity of some synthetic cathinones using the semi-quantitative AxSYM amphetamine/methamphetamine II assay in tandem with Fluorescence Polarization Immunoassay (FPIA). Evaluating the responses from aqueous solutions of 14 substituted cathinones at 1 mg L^{-1} , 10 mg/L and 100 mg L^{-1} , the authors observe pentedrone, pentylone, α -pyrrolidinovalerophenone (α -PVP) and

3',4'-methylenedioxypropylamphetamine (MDPV) did not react with the protocol. Some synthetic cathinones, however, reacted in the assay at 10 mg L⁻¹: ethylone, mephedrone, methylone, methedrone, and 4'-methylethcathinone (MEC) scrutiny of this reveals that each of these that did react had the least substitutions on the ethylamine chain suggesting the method has limitations to larger molecules.⁵⁴ Commercially available enzyme-linked immunosorbent assays have been used to analyse eight synthetic cathinone derivatives amongst 30 designer drugs.⁸⁸ The test demonstrated cross-reactivity at concentrations as low as 0.15 mg L⁻¹ when tested against the Randox Mephedrone/Methcathinone ELISA kit (RANDOX Toxicology, Crumlin, UK), a protocol recently developed for forensic specific cathinone screening in urine and blood specimens.⁸⁸

Presumptive testing of cathinone derivatives was carried out by Nic Daeid and colleagues⁷⁶ as per United Nations recommended guidelines. Various presumptive tests were investigated, however results suggested the Zimmerman test, which relies on the presence of a carbonyl group in close proximity to a methyl group on the same molecule and reaction with 2', 4'-dinitrobenzene to form a Meisenheimer reddish-purple colour, was the most consistently effective test method. A small amount of each test sample was placed into a well of a spotting tile and 2 drops of 1% 2', 4'-dinitrobenzene in methanol followed by 2 drops of 15% potassium hydroxide in water were added. Any colour change or other noticeable effect occurring immediately on addition of the reagents was noted and observations were made again after 5 minutes; Specific colour changes were observed in all cases apart from bupropion. Nic Daeid *et al.* have also reported using stable isotopic fractionation/profiling (isotope ratio mass spectrometry; IRMS), to provide a potentially quantifiable link between the precursor (4'-methylpropiofenone) and the illicit drug product (4'-methylmethcathinone) for a particular manufacturer and synthetic route of mephedrone.⁸⁹

2.3 Synthetic Cannabinoids

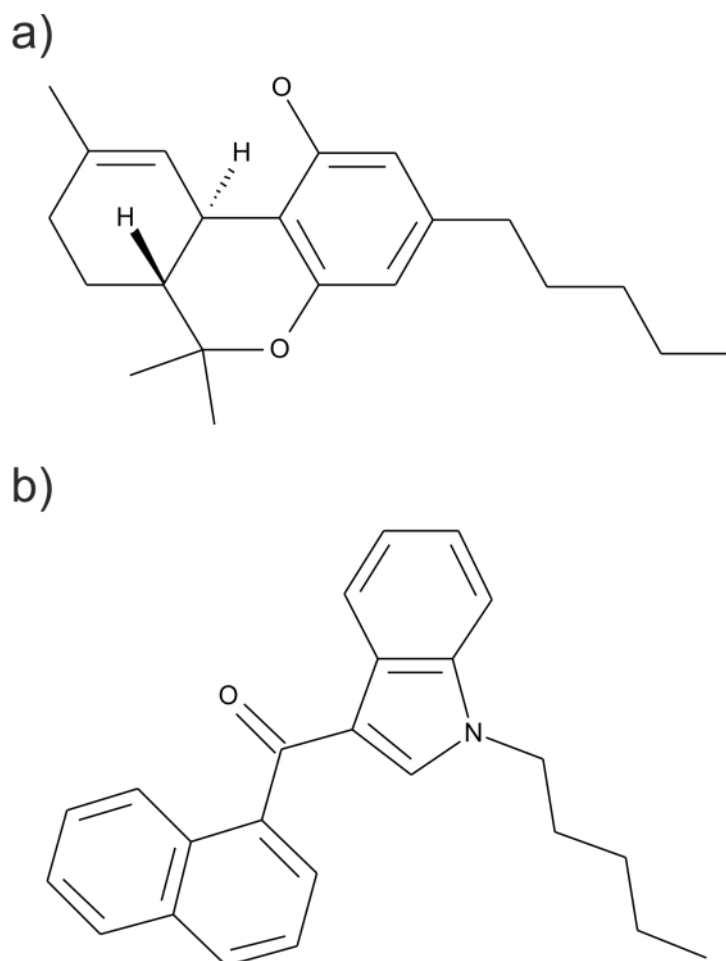
Synthetic cannabinoids emerged as a recreational product *ca.* 2008 in the form of aminoalkylindoles such as JWH-018. They were originally investigated by Professor Huffman⁹⁰ as therapeutic compounds, however they were subsequently abandoned due to the unwanted psychoactive side effects. Despite many classes synthetic cannabinoids becoming controlled under drug legislation, there are still many which remain legal whilst still posing threat to the population. As with synthetic cathinone derivatives, there is often limited to no information on the packaging of the products and the active ingredients present can vary greatly between products of the same name.^{36, 91-94} These compounds were first introduced into products known as 'K2' and 'Spice' with the latter having a market range of: Spice Silver, Spice Gold and Spice Diamond.ⁱ The products, advertised as incense or smoking mixtures, are typically sold consisting of a few grams of finely cut green/brown plant material as to perhaps replicate the appearance of cannabis whilst being infused with the active synthetic cannabinoid component(s). There are instances of retailers selling the active components as research chemicals (similarly to synthetic cathinones) which arrive as a crystalline powder of high purity.⁹⁴

There are various case reports to support the literature and media claims that synthetic cannabinoids have psychoactive effects akin to that of cannabis. Indeed, the components of Spice and related herbal products have been identified as aminoalkylindoles originally synthesised by Huffman and Atwood *et al.* and have demonstrated that JWH-018 is a potent and effective CB₁ receptor agonist.⁹⁵ A comparison of the active ingredient in cannabis and JWH-018 can be observed in Scheme 2-3.

Interesting case reports with regards to the effects of the Spice epidemic include a report by Schneir *et al.*,⁹⁶ who published case studies on two women admitted to a San Diego (USA) emergency department after smoking Spice "Banana Cream Nuke" – disorientated,

ⁱ Ingredients listed on the packaging of products are as follows - Spice Gold: bay bean, blue lotus, Lion's Tail, Indian Warrior, Dwarf Skullcap, Maconha brava, Pink Lotus, Marshmallow, Red Clover, Rose, Siberian motherwort, Vanilla and honey. Spice Gold Spirit: Leonurus, Cardiaca, Pedicularis, Canadensis, Scutellaria, Latero flora, Athaea officinalis, Rosa damascene, Vanilla planifolia. Spice Diamond: Bay bean, Blue lotus, Lion's tail, Indian Warrior, Dwarf Skullcap, Maconha brava, Pink Lotus, Marshmallow, Red Clover, Rose, Siberian motherwort, vanilla, honey, aroma. Note the lack of any real ingredients (chemical) and no mention of any aminoalkylindole (JWH compounds) or cyclohexylphenyls (CP compounds).

feeling unusual and “as if they did not know where they were”.⁹⁶ Another report describes three cases of the effects of Spice⁹⁷, all having a negative urine drug screen whilst



Scheme 2-3 Comparison of a) Tetrahydrocannabinol (THC), the active component in cannabis against b) JWH-018, aminoalkylindole synthetic cannabinoid.

exhibiting agitation, paranoia and tachycardia. Follow up analysis revealed the urine to contain metabolites of JWH-018 and JWH-073⁹⁷. More recent reports also highlight similar observations in adolescents and young adults after intoxication with synthetic cannabinoids.⁹⁸ Vardakou *et al.*⁹⁹ have given an overview of other case reports⁹⁹ and the psychoactive properties of Spice products and “legal highs”.

Laboratory analysis revealed the active components of first generation Spice and related products to be, the previously mentioned, aminoalkylindoles such as JWH-018 and also cyclohexylphenols such as CP-47,497. As their popularity rose through sales in so-called ‘head shops’ as well as on the internet, the substances were legislated as illegal in most

countries worldwide;¹⁰⁰ the range of active synthetic cannabinoid components of first generation Spice products can be observed in Scheme 2-4. *Note:* the aminoalkylindoles (see Scheme 2-4) are given the notation of JWH after the academic who first synthesised these compound, Professor J.W. Huffman.

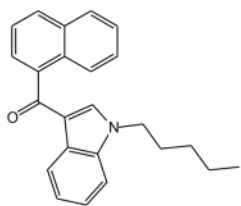
Further confirmation of this came at the end of 2008 when the German company THC Pharma reported JWH-018 was an active ingredient in Spice products.¹⁰¹ Following on from this Auwater *et al.*¹⁰² and Uchiyama *et al.*¹⁰³ identified and characterized the CP 47,497-C8 (see Scheme 2-4) as its isomer – a synthetic by-product in Spice Silver, Gold and Diamond as well as in products named ‘Yuctan Fire’ and ‘Sence’ which is reported to have 5 to 10 times more analgesic potency than tetrahydrocannabinol.¹⁰⁴

An interesting paper from the point of view of the medical staff that have had to deal with the Spice usage patients has a light-hearted title of: *“Spice” girls: Synthetic cannabinoid intoxication.*⁹⁶ The authors noted that a urine drugs-of-abuse immunoassay was negative for amphetamines, barbiturates, benzodiazepines, benzoylecgonine (cocaine metabolite), methadone and opiates, oxycodone, phencyclidine, propoxyphene and tetrahydrocannabinoids. The residue of the patient’s Spice product *“Banana Cream Nuke”* was found to contain the synthetic cannabinoids JWH-018 and JWH-073 (the chemical structure can be seen in Scheme 2-4) through gas chromatography-mass spectrometry (GC-MS) and high performance liquid chromatography with ultraviolet detection (HPLC-UV). The report highlighted the need for drugs-of-abuse screenings to be able to detect the JWH class of compounds, particularly within a clinical setting.

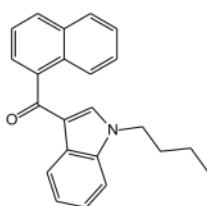
In Germany Lindigkeit *et al.* analysed Spice Gold with a GC-MS method wherein the herbal mixtures were ground and put through a two hour Soxhlet extraction with petroleum ether.³⁶ Analysis revealed the samples contained CP 47,497-C8 and JWH-018 until German health authorities on the 22nd January 2009 prohibited the sale of the active components found in Spice - from this point JWH-018 was absent from Spice,

1) Aminoalkylindoles

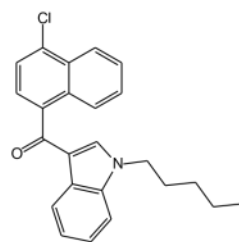
(a) Naphthoylindoles



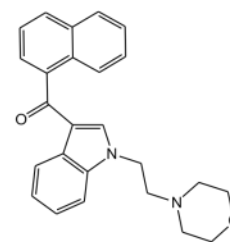
JWH-018



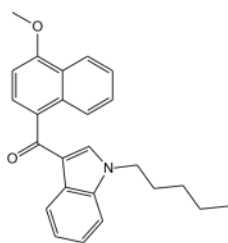
JWH-073



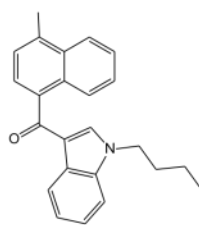
JWH-398



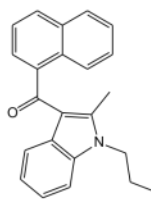
JWH-200



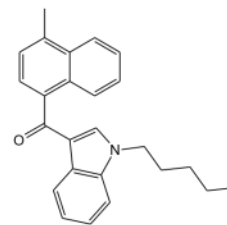
JWH-081



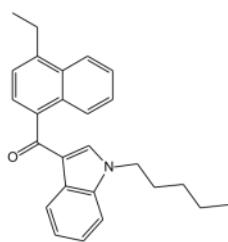
4-Methyl-JWH-073



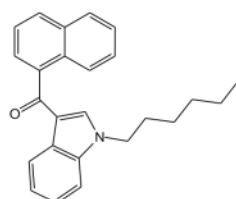
JWH-015



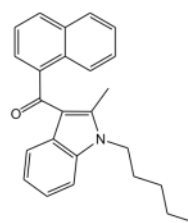
JWH-122



JWH-210

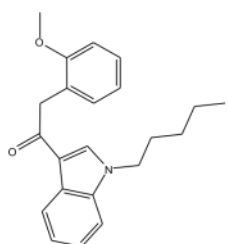


JWH-019

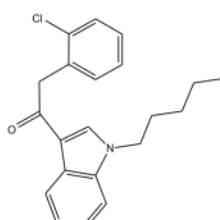


JWH-007

(b) Phenylacetylindoles

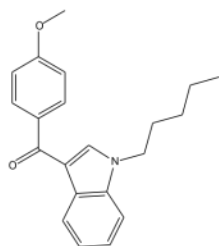


JWH-250

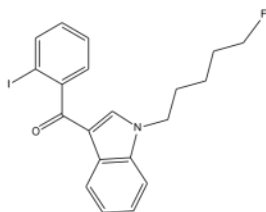


JWH-203

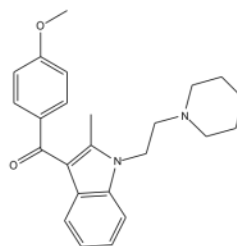
c) Benzoylindoles



RCS-4

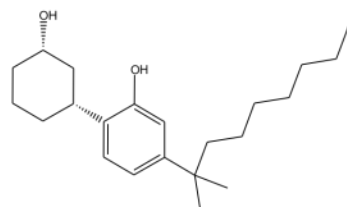


AM-694

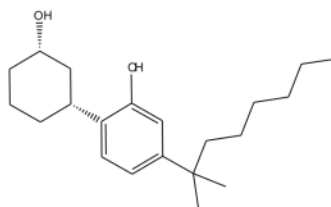


WIN-48,098

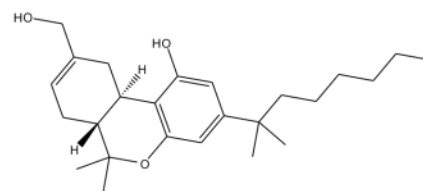
2) Cyclohexylphenoles



CP-47,497-C8



CP-47,497



HU-210

Scheme 2-4 Chemical structures of synthetic cannabinoids found in herbal products such as the Spice range.

however it wasn't long until a new analogue, JWH-073, was found to be contained in Spice products.³⁶ Because the manufacturers of such products can readily change the active components in Spice, a rapid method of detecting prohibited compounds in the complex mixtures is highly sought after.

To this end, Emanuel and co-workers¹⁰¹ reported for the first time the components of Spice "Gold Spirit" using GC-MS (following a simple liquid extraction) alongside the analysis of Spice "Gold" and "Diamond"; at the time the three most popular Spice products used. Results indicated that Spice "Gold" contained CP 47,497-C8 along with ethyl vanillin, α -tocopherol and γ -tocopherol whereas Spice "Diamond" contained caffeine, α -tocopherol, γ -tocopherol, palmitic acid along with CP 47,497-C8 and JWH-018. As for Spice "Gold Spirit", JWH-018 and α -tocopherol were found to be present.¹⁰¹

Other work has of course followed on the analysis of Spice and related herbal products for instance Uchiyama and co-workers⁹² who analysed 46 different herbal products with 44

having synthetic cannabinoids as determined *via* GC-MS and LC-MS. Two major cannabinoids were found; [2-hydroxy-4-(2-methylnonan-2-yl)phenyl]cyclohexan-1-ol (cannabicyclohexanol) and JWH-018 and the analysis of the herbal product (amount of NPS per gram) were found to range from 1.1 to 16.9 mg g⁻¹ and 2.0 to 35.9 mg g⁻¹ respectively.⁹²

In addition to the identification of the chemical components contained within the Spice product range there is a need to understand the effects of the synthetic cannabinoids on the human metabolism. Sobolevsky¹⁰⁵ reported for the first the time, urinary metabolites of JWH-018; clearly highly useful for analysis of patients admitted to emergency departments and for the development of point-of-care tests (see the story of the “*Spice girls*” later). Using LC-MS and GC-MS, two main monohydroxylated metabolites were identified which are almost completely glucuroconjugated with minor metabolites such as *N*-despentyl hydroxy-, carboxy-, dihydroxy-, and reduced di- and trihydroxy-metabolites.¹⁰⁵ It should be noted the parent compound (JWH-018) was reported to not be detected in urine.¹⁰⁵ The authors observed that there are two main metabolites that are valuable for detection of JWH-018 in post-administration urine and LC-MS is a more useful technique as minor metabolites can also be analysed to support analytical findings.¹⁰⁵ Different analytical approaches on Spice and related products have been reported¹⁰⁶⁻¹¹¹ with literature reporting the presence of new cannabimimetic compounds.^{93, 112, 113} Following this pioneering work, there has been a pursuit of studying synthetic cannabinoids in urine.¹¹⁴⁻¹²⁰ Further work by Moran *et al.*¹²¹ has extended the work of Sobolevsky¹⁰⁵ and validated an LC-MS/MS method for the quantitation of human urine metabolites of JWH-018 and JWH-073. The work highlighted 6 metabolites for each molecule with the primary metabolites being distinguishable between JWH-018 and JWH-073. The authors have also extended this using a solid-phase extraction approach.¹²² One criticism of the above work exploring the metabolites in urine is the limited population studies – clearly larger studies will be needed to further understand the pharmacology of synthetic cannabinoids. Other research has been devised to quantify cannabinoids in serum and blood.¹²³⁻¹²⁷

A different strategy has been to analyse cannabinoids in hair to show long term past consumption.¹²⁸ To this end, Hutter *et al.*¹²⁹ reported the hair testing of 22 synthetic cannabinoids in human hair. The methodology involves a simple ultrasonication of the hair sample in ethanol and has a limit of quantification (LOQ) of 0.5 pg mg⁻¹.¹²⁹ Perhaps more

interestingly, synthetic cannabinoids have even been found in the urine of US athletes (although its use to enhance performance is questionable.). Urine samples were collected from 5,956 athletes and analysed via high performance-liquid chromatography-tandem mass spectrometry (HPLC-MS) for the presence of JWH-018, JWH-073 and their metabolites.¹³⁰ In 4.5% of the samples, metabolites of both synthetic cannabinoid compounds were detected; metabolites of JWH-018 and JWH-073 (50%), JWH-018 (49%), and only JWH-073 (1%) were detected in positive samples.

The focus of the research above has focussed on laboratory based instrumentation, rightly so in order to unambiguously quantify NPSs but as highlighted in the case of the “*Spice girls*”, synthetic cannabinoids do not react using traditional THC immunoassay tests. To this end Arnston *et al.*¹³¹ have designed two enzyme linked immunosorbent assays for detection of JWH-018 and JWH-250 in urine. The assay of JWH-018 has significant cross reactivity with several synthetic cannabinoids and their metabolites contrary to the JWH-250 assay which exhibits limited cross-reactivity. To start, assays are calibrated at 5 ng mL⁻¹ with the 5-OH metabolite of JWH-018 and the 4-OH metabolite of JWH-250. To validate the method, 114 and 84 samples of urine for JWH-018 and JWH-250 respectively were used and confirmed by using liquid chromatograph tandem mass spectrometry (LC-MS/MS) testing for metabolites of JWH-018, JWH-019, JWH-073, JWH-250 and AM-2201. Accuracy was deemed to be greater than 98% with 95% sensitivity and specificity for both assays.

Another approach of interest is a presumptive test marketed by “Narcotic Testing Supplies & Equipment Store”.¹³² The test works by inserting a small quantity of a suspected sample into a plastic ampoule containing 25 µL reagent and 150 mg of specially treated absorbing crystals (sodium 36%, potassium iodide 98% and 0.2% ethanol) stirring and comparing the colour of the liquid to a pre-determined colour chart clearly visible from Figure 2-3 however the specificity of such a screening test is questionable.¹³²

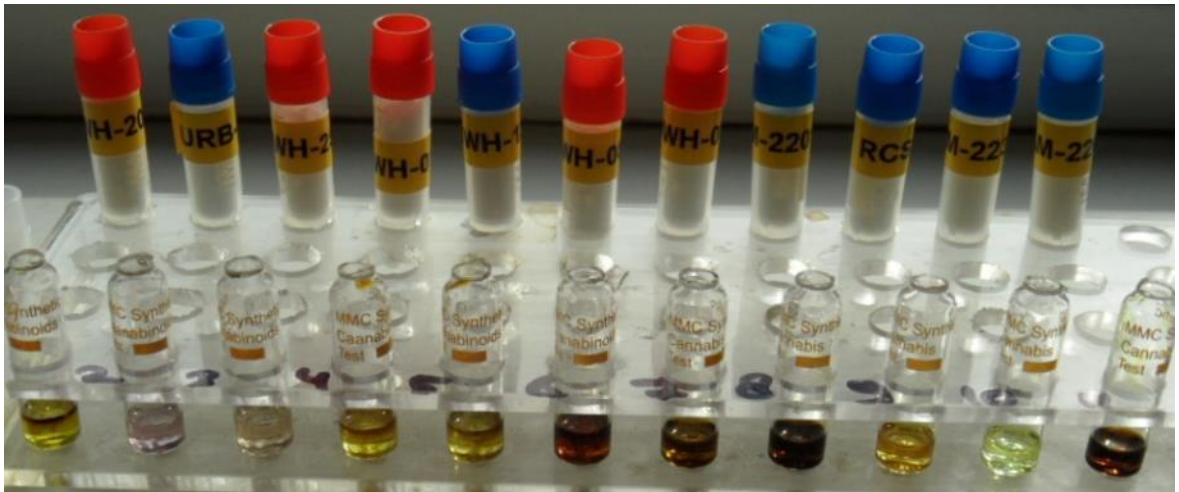


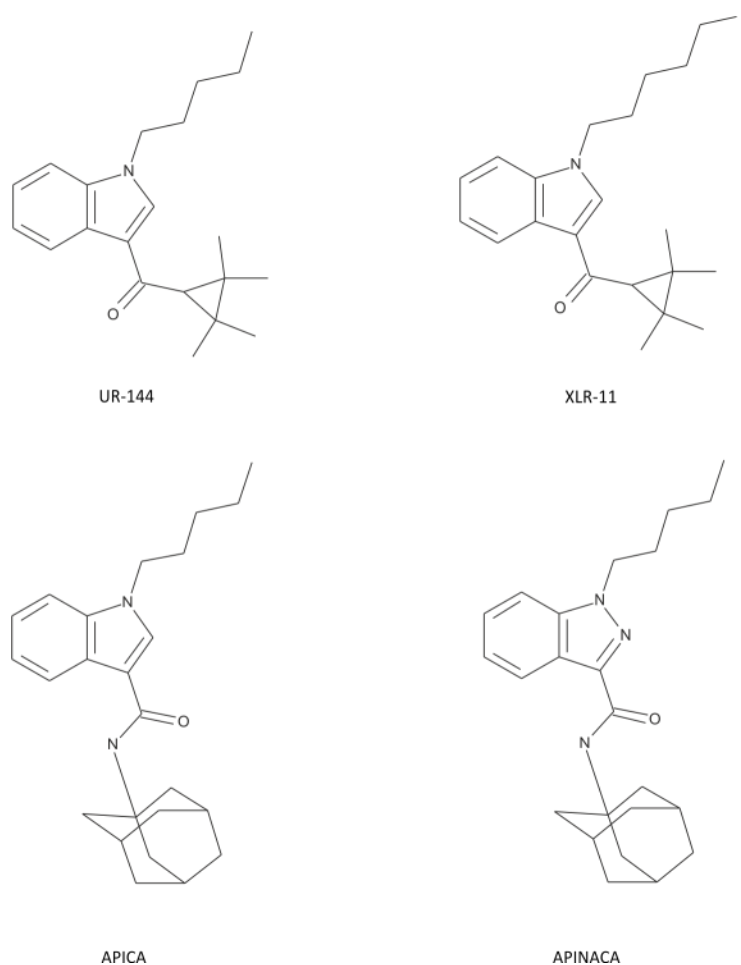
Figure 2-3 Visual representation of synthetic cannabinoid presumptive test.

As components of Spice and related substances become banned, they are replaced with a compound which exhibits similar psychoactive properties yet negating the effectiveness of the newly introduced ban, see the paper: *"Spice: A Never ending story?"* for example.³⁶

As such there is an urgent need for a faster laboratory method; for that reason Emanuel *et al.* reported the use of solid probe mass spectrometry alleviating the need for any sample pre-treatment such as liquid-liquid extraction.¹⁰¹ Since α -tocopherol is always present in the Spice herbs range, the authors demonstrated that once α -tocopherol was subtracted from the obtained spectra, the fragmentation patterns of CP 47,497-C8 and JWH-018 become 'visible'.¹⁰¹ This screening methodology is useful for the rapid analysis of the prohibited substances within the Spice product range (as well as related substances) with a positive response nullifying the need for any pre-treatment step (such as liquid-liquid extraction) allowing a full quantification *via* GC-MS or similar approaches *i.e.* LC-MS. Work from Lesiak *et al.*¹³³ has also attempted to rapidly detect synthetic cannabinoids without the need for sample preparation with the use of direct analysis in real time mass spectrometry (DART-MS)¹³³ being able to screen for AM-2201, JWH-122, JWH-203, JWH-210 and RCS-4.

To highlight the ever moving field of *"legal highs"* with respect to synthetic cannabinoids, in October 2012 new variants were reportedly found where the structures were a modification of compounds from the 3-naphthoylindole series^{36, 91-93, 102, 103, 113, 134-140}

identified from regular seizures made by police in Russia and Belarus.¹³⁴ Shevyrin *et al.* have reported on the analytical characterisation of these new class of synthetic cannabinoids using Gas Chromatography – High Resolution Mass Spectrometry (GC-HRMS), Ultra-High Performance Liquid Chromatography - High Resolution Mass Spectrometry (UHPLC-HRMS), Nuclear magnetic resonance (NMR) and Fourier Transform Infrared Spectroscopy (FT-IR)¹³⁴ providing robust and reliable confirmatory analytical approaches. Reports from South Korea also highlight the ever-changing market detailing the different synthetic cannabinoids which have been identified by their National Forensic Service between 2009 – June 2013.¹⁴¹ The authors note that whilst initially it was largely naphthoylindoles (*e.g.* JWH-018, JWH-073), phenylacetylindoles (*e.g.* JWH-203, JWH-250), benzoylindols (*e.g.* RCS-2, RCS-4) and CP-47,497 derivatives abused; after legislative bans were introduced, gradually over time, the molecules identified became new, typically halogenated, substances such as cyclopropylindoles (*e.g.* UR-144, XLR-11) and adamantylindoles (*e.g.* APICA, APINACA)¹⁴¹ which are represented in Scheme 2-5.



Scheme 2-5 Chemical structures of synthetic cannabinoids discovered after legislative bans were introduced: cyclopropylindoles e.g. UR-144, XLR-11 and adamantylindoles (APICA and APINACA).

Following the influx of new compounds, groups worldwide moved towards their detection. Scheidweiler *et al.*¹⁴² developed and validated a liquid chromatography–tandem mass spectrometric (LC–MS/MS) method for simultaneously quantifying JWH-018, JWH-019, JWH-073, JWH-081, JWH-122, JWH-200, JWH-210, JWH-250, JWH-398, RCS-4, AM-2201, MAM-2201, UR-144, CP 47,497-C7, CP 47,497-C8 and their metabolites, and JWH-203, AM-694, RCS-8, XLR-11 and HU-210 parent compounds in urine.¹⁴² Previously there were no extensive synthetic quantitative methods reported in the literature until this work which presented the novel LC-MS/MS protocol quantifying 20 synthetic cannabinoids and 21 metabolites, and semi-quantifying 12 alkyl-hydroxy-metabolites.¹⁴²

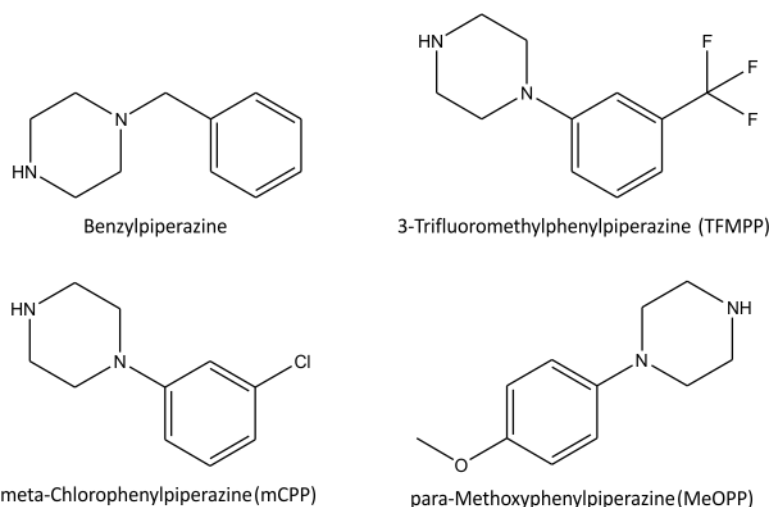
Continuing from this, another approach towards the detection of the new generation of synthetic cannabinoid agonist, Mohr *et al.*¹⁴³ applied Enzyme-Linked Immunosorbent Assay

(ELISA) towards one of the most prevalent synthetic cannabinoids in urine, UR-144, and XLR-11. Once again testing in urine, the method was validated against liquid chromatography-tandem mass spectrometry with 90 positive and negative control samples for UR-144, XLR-11 and its metabolites.

2.4 Miscellaneous

As reported in section 2.1, the novel psychoactive substance epidemic is an ever growing market with a vast array of new materials discovered each year.⁴³ To cover every known substance is beyond the scope of this literary review chapter however; in this section, interesting pieces of research from around the world will be covered.

2.4.1 Piperazines



Scheme 2-6 Benzylpiperazine and other piperazines derivatives which have been historically abused.

N-benzylpiperazine (BZP), the structure of which is shown in Scheme 2-6, is known to be a central nervous system stimulant with its effects reported to be similar to amphetamine in that it also triggers the release of dopamine and norepinephrine whilst inhibiting the uptake of dopamine, norepinephrine and serotonin.¹⁴⁴ Although BZP is structurally similar to amphetamine it is reported to have only one-tenth the potency.¹⁴⁴ Marketed as a 'party pill' before legal restrictions BZP was viewed as a safe alternative to amphetamines such as MDMA.¹⁴⁵ However, recently it has varying degrees of legislative control internationally.¹⁴⁶ Its appearance in "legal high" samples is still reported^{147, 148} nonetheless, after being made illegal the prevalence of its use has declined; for example in New Zealand after being made a prohibited substance in 2008, the use of BZP amongst the general population dropped from 15.3% in 2006 to 3.2% in 2009.¹⁴⁹

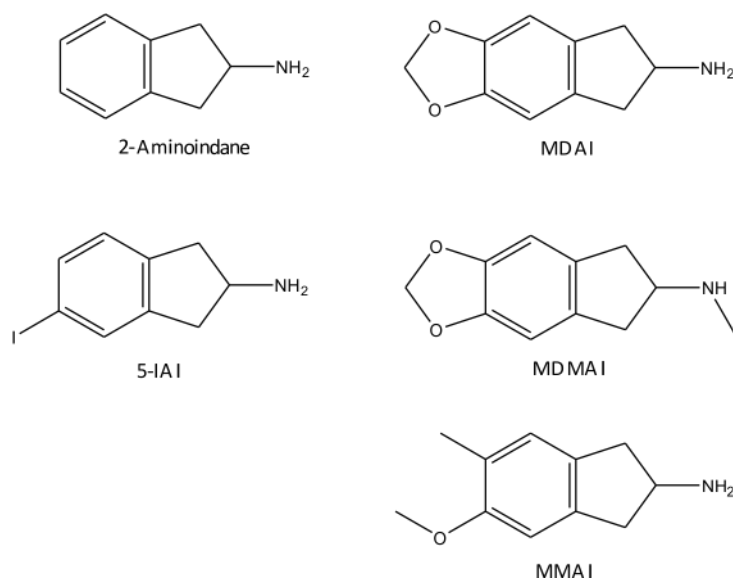
In the UK, the first deaths associated with BZP and 3-TFMPP were three separate fatalities wherein one of either of the drugs were confirmed to be present although not determined to be the direct mechanism of death.¹⁵⁰ Dickson *et al.*¹⁵¹ reported that BZP, 3'-TFMPP and MCPP are present in ecstasy tablets since the former, in some nations, is a legal alternative to MDMA. The authors analysed 251 MDMA positive urine samples using GC-MS *via* a liquid-liquid extraction and pentafluoropropionic anhydride (PFPA) derivatisation as sample pre-treatment to screen for 33 drugs potentially present.¹⁵¹ In 36% of the sample, drugs other than MDMA were found to be present; BZP, 3-TFMPP and MCPP were detected in 15%, 7% and 1% of the samples respectively.¹⁵¹

A wide array of analytical approaches have been reported by many different authors such as LC-MS,^{60, 152} capillary electrophoresis,¹⁵³ HPLC-fluorescence,¹⁵⁴ LC with diode array,^{155, 156} GC-MS¹⁵⁷⁻¹⁵⁹ and chemiluminescence.¹⁶⁰ Arbo and co-workers¹⁶¹ provided a thorough overview of piperazine compounds as drugs of abuse with the full range of analytical techniques and matrices applied, readers are directed to this paper.¹⁶¹

It is clear, something that is generally the case with all “*legal highs*”, confirmatory laboratory based analysis is well developed. Lesser developed, however, are approaches that could be adapted for used in-the-field or within a clinical setting where a near-instantaneous response is required. To this end, currently there are no immunoassays for the detection of piperazines derivatives¹⁶¹ and cross-reactivity of these compounds in fluorescence polarization immunoassay using AxSYM[®], amphetamine/methamphetamine assay has been reported.¹⁶²

Recently Philip *et al.*¹⁶³ have reported on the development and validation of a specific colour test using 1', 2'-naphthoquinone-4-sulphonate (NQS) forming an intense orange-red complex with BZP at room temperature. The authors reported that common cutting agents such as glucose and caffeine did not affect the test. 3-TFMPP, MCPP, pCPP, MeOPP and piperazines produced an orange-red colour change where the apparent brilliance of the BZP-NQS complex made it apparently to be distinguishable from the other colour changes with the potential cross-reactants.

2.4.2 Aminoindanes



Scheme 2-7 Structures of 2-aminoindane and its derivatives, all of which have been found in “legal high” samples.

Aminoindanes are a group of synthetic compounds characterised by the presence of a phenethylamine skeleton, they are currently not controlled globally¹⁶⁴ and have more recently been found to be contained in “legal high” products sold as powders akin to synthetic cathinones.^{165, 166} 2-Aminoindane has a basic ring structure that is similar to amphetamine (and therefore by proxy, substituted cathinones also) that can be chemically modified and the following derivatives (Scheme 2-7); 5', 6'-methylenedioxy-2-aminoindane (MDAI), 5', 6'-methylenedioxy-*N*-methyl-2-aminoindane (MDMAI), 5'-iodo-2-aminoindane (5-IAI), and 5'-methoxy-6'-methyl-2-aminoindane (MMAI) have all reportedly been found in “legal highs”.¹⁶⁵

A number of aminoindane compounds have been thoroughly characterized by Casale and Hays¹⁶⁷ who provided analytical protocols in the form of NMR, MS and Infrared Spectroscopy (IR) for 5-IAI, 4-IAI, their synthetic intermediates and impurities in order to assist forensic analysts.¹⁶⁷ There is other work that reports a LC-MS/MS screening method for 26 analytes,⁷⁰ including MDAI, and such an approach is designed to provide screening, within a clinical toxicology setting, for the potential misuse of “legal highs” via analysis of urine.⁷⁰

Particularly of note, work by Elie and co-workers reports that microcrystalline identification of MDAI, mephedrone and *N*-benzylpiperazine (BZP) is possible.¹⁴⁷ This approach involves dropping 10 μ L of the drug solution with 10 μ L of the reagent solution onto a glass slide; the resulting structures were optically imaged following assisted nucleation (gently swirling a plastic pipette tip in the freshly mixed drop).¹⁴⁷ Scheme 2-7 shows the observed crystal structure which is compared to the crystal structure of illicit drugs. The MDAI free base (Scheme 2-7bi) was found to form flat serrated blades of various dimensions which become irregular with increasing sizes. Smaller crystals are observed to be single blades whereas larger crystals develop two dimensional bunch structures - after drying larger blade crystals are evident. It was noted that crystals grew within 60s following assisted nucleation indicating the potential for a fast presumptive test strategy.¹⁴⁷ The uniqueness of these tests were determined through comparisons of MDAI structure with a range of illicit drugs, indicating that potentially this approach is feasible to identify the MDAI structure in a real sample containing other illicit drugs. To this end the authors¹⁴⁷ purchased “*legal high*” samples and utilised their microcrystalline presumptive test approach which when collaborated with Fourier Transform Infrared Spectroscopy/Gas Chromatography-Mass Spectrometry FTIR/GC-MS.

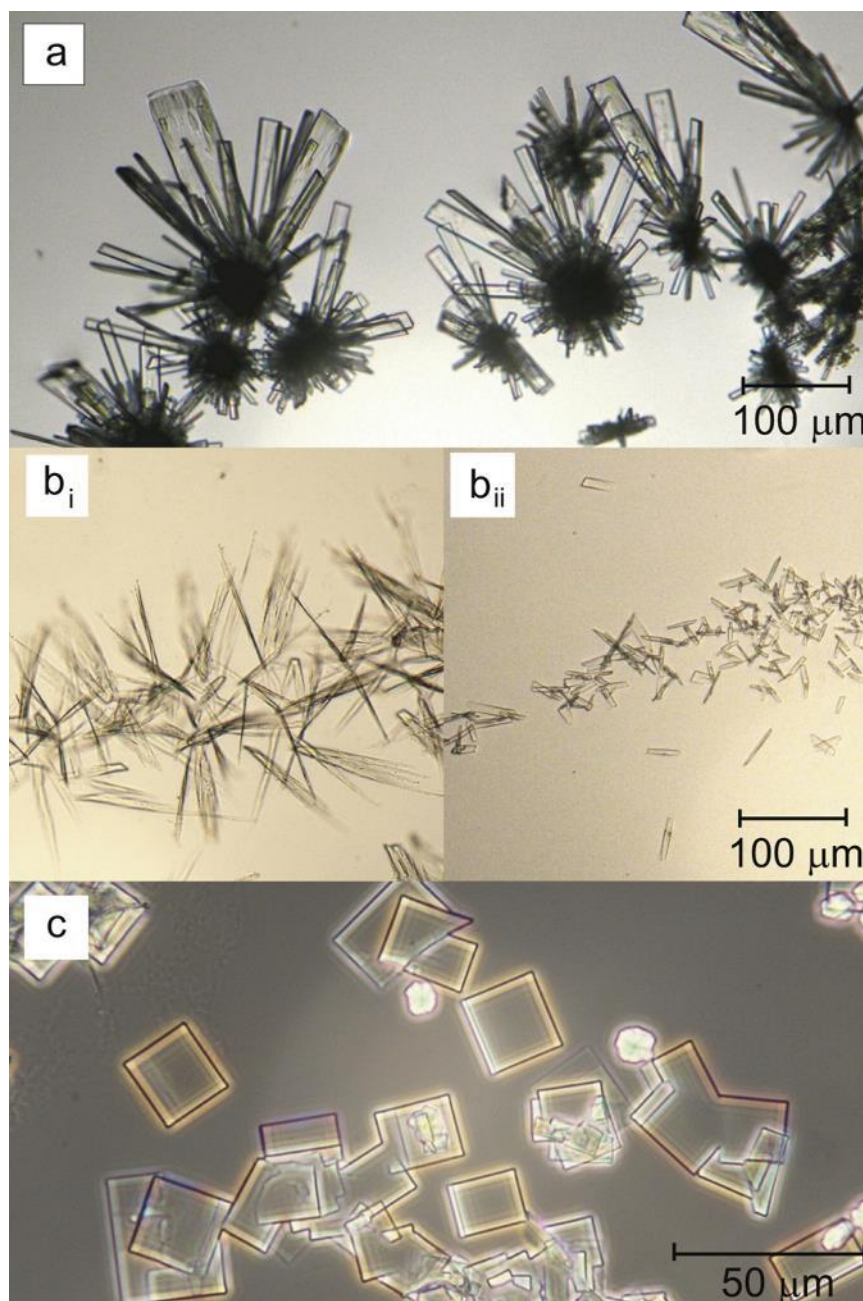


Figure 2-4 Microcrystals formed with mercury chloride and (a) mephedrone (bi) MDAI freebase (bii) MDAI hydrochloride and (c) BZP. Recreated from reference 147.

2.4.3 Salvinorin A (*Salvia Divinorum*)

Salvia divinorum is a hallucinogenic psychoactive herb local to Oaxaca in Central Mexico and for centuries has been used by cultures indigenous to the region.^{168, 169} This rare member of the mint family is also known as ‘magic mint’ and more colloquially: ‘ska Maria’, ‘ska Pastora’, ‘hierba de Maria’, ‘hojas de la Pastora’ all names which pertain to the belief

that *S. divinorum* is the reincarnation of the Virgin Mary.¹⁷⁰ The use of this plant as a psychoactive substance has spread globally, its major constituent – salvinorin A (SA) is a known selective opioid antagonist and to this end emphasis in the literature has been put on detecting SA.¹⁶⁸ A dosage between 200–500 µg of SA has been found to induce profound hallucinations with feelings of physical or mental displacement as well as experiencing extraordinary illusions.¹⁷¹ Recently studies have postured SAs effects involve the endocannabinoid system.¹⁷²

To analyse intact *S. divinorum* leaves for the presence of SA there has been the employing of both thin layer chromatography using desorption electrospray ionization mass spectrometry (TLC-DESI-MS)¹⁷³ and thin layer chromatography teamed with gas chromatography-mass spectrometry (TLC-GC-MS).¹⁷⁴ By utilizing these techniques, the authors of both techniques were able to confirm the presence of salvinorin A in a submitted plant material suspected to be *Salvia divinorum*.^{173, 174}

Pichini and co-workers¹⁷⁵ attempted the detection of Salvinorin A in different biological matrices opposed to the solid leaf matter. Utilising a gas chromatography mass spectrometric protocol, it was applied to detecting SA in plasma, urine, saliva and sweat.¹⁷⁵ Following validation with 17-alpha-methyltestosterone as an internal standard the method was applied to the analysis of urine, saliva and sweat from two consumers after smoking 75 mg plant leaves. Salvinorin A was detected in urine (2.4 and 10.9 ng mL⁻¹) and saliva (11.1 and 25.0 ng mL⁻¹), but not in sweat patches from consumers.¹⁷⁵ The quantification of SA in plasma and cerebrospinal fluid (from a rhesus monkey) has also been attempted and successfully completed using a negative ion liquid chromatography-mass spectrometry atmospheric pressure chemical ionization (LC-MS/APCI).¹⁷⁶ Using the United States Food and Drug Administration (FDA) guidelines the authors of the method concluded the technique had a lower limit of quantification (LLOQ) of 2 ng mL⁻¹ for 0.5 mL of plasma samples over the linear range 2-1000 ng mL⁻¹.¹⁷⁶

2.4.4 Mitragynine (*Kraton*)

Mitragynine is an indole alkaloid derived from the plant *Mitragyna speciosa* which is indigenous to Thailand and other Southeast Asian countries. This is a common “legal high”

and is known commonly as *Kratom* which is also the chemical's Thai name. The leaves of the *M. Speciosa* was historically used as an opium substitute as well as being used traditionally by villages in southern Thailand as a medicine for diarrhoea, muscle pain and hypertension in addition to also being used by agricultural workers and labourers to relieve tiredness and improve efficiency.¹⁷⁷ Its study remains pertinent as reports of a fatality associated with *Kratom* are as recent as 2013.¹⁷⁸

Interestingly, mitragynine is the major constituent of *Kratom* reported to be 66.2% based on the crude base from the young leaves.^{179, 180} Levels of mitragynine in adults plants from Thailand have been reported to be approximately over 60% whereas in Malaysia only over 10%. Payanmtheine and the mitragynine diastereomer speciogynine were the second most abundant alkaloids and the mitragynine diastereomer speciogynine was the third abundant alkaloid in both plants.¹⁸¹

The pharmacology of mitragynine has been extensively studied and has been reported to have analgesic activity on the opioid system.^{177, 182-184} Unlike the case of other NPSs reported in this chapter where they have emerged and analytical techniques have had to be developed/invented for their quantification, mitragynine, due to its historical use analytical methods already exist and are generally applied to facilitate pharmacological studies. To this end, Janchawee¹⁷⁷ reported the first analytical methodology utilising HPLC-UV. A linear range of 0.1 – 10 $\mu\text{g mL}^{-1}$ was reported with a LOD of 0.03 $\mu\text{g mL}^{-1}$ and LOQ of 0.1 $\mu\text{g mL}^{-1}$. Their protocol was applied to determine the pharmacokinetic characteristic of mitragynine in the serum of rats following oral administration.

As the leaves of *Kratom* became sold as “legal highs” in many other countries Kikura-Hanajiri and colleagues¹⁷⁹ reported the detection of mitrogynine and 7-OH-mitragynine (oxidative derivatives of mitragynine)¹⁸⁵ in 13 “legal high” products using liquid chromatography-electrospray ionization- mass spectrometry (LC-ESI-MS). The authors found that 11 of the 13 products were found to contain mitragynine and 7-OH-mitragynine with their content found to range from 1 to 6% and in the latter 0.01 to 0.04%.¹⁷⁹ Other researchers have directed research to study the methods of mitragynine in biological matrices using LC-MS¹⁸⁶⁻¹⁸⁸ and UHPLC-UV.^{189, 190}

From inspection of the literature, it is evident that there are multiple ways for the detection and quantification of *Kratom* ingestion/consumption with detection levels as low as 0.02 $\mu\text{g mL}^{-1}$.¹⁹¹ For example Arndt and co-workers reported a upon a case of a drug and rehabilitation centre reporting an analysis for *Krypton* (another name for *Kratom*) in the urine of a former opiate addicted woman.¹⁹² The immunological drug screenings were performed with test strips and a cloned enzyme donor immunoassay wherein alkaloids and tramadol metabolites were analysed by LC-MS/MS. The immunoassays yielded negative responses for amphetamines, barbituates, benzodiazepines, benzoylecgonine, buprenorphine, ethylgluconoride, methadone, opiates, oxycodone and THC-COOH just as the test strips were negative from tramadol and its metabolites. The LC-MS/MS detected the alkaloids typically found in *Kratom* (mitragynine, speciociliatine, speciogynine, mitraciliatine and paynantheine – detection of these alkaloids served sufficient proof of *Kratom* abuse and after confrontation with data the patient admitted to several infusions of the plant.¹⁹²

2.5 Conclusions and Future Challenges

The work described in this chapter demonstrates the range of new analytical methods and techniques applied to the detection and quantification of NPSs, which have recently emerged on the recreational drugs market. Given the rapidly evolving nature of the recreational drugs market, in terms of the number of new substances being identified (101 new substances, in Europe, in 2014); the ease at which these substances are available through on-line vendors or “*head shops*”; the freely-available information regarding NPS production and/or pharmacology and the lack of globalised drug/precursor control legislation - makes the current analytical, forensic and legal challenges clearly apparent. These issues coupled with the limited availability and range of certified primary reference standards; fully validated, simple and cheap laboratory-based analytical methods and selective and sensitive in-field testing technology highlights the growing gap in knowledge and necessitates economic investment and focused research in this underfunded area.

Future advances can be expected in the following areas: (i) design and development of miniaturised in-field detection systems for NPSs in bulk samples or adulterated products (such as alcoholic drinks); (ii) rapid, non-evasive bioanalytical methods for detection of the principle metabolites of common NPSs; (iii) simple, selective and validated laboratory-based chromatographic methods for the discrimination of new psychoactive substances, their isomers and their principle metabolites in biological matrices and; (iv) impurity profiling and/or source identification of common NPSs. The work within this thesis demonstrates the potential use of electrochemical methods as in-the-field analytical sensors towards NPSs, specifically synthetic cathinones.

Clearly, the “*war on drugs*” is showing no sign of relenting in the near future and the principle challenge facing law enforcement agencies is to be ‘one-step-ahead’ of the clandestine drug manufacturers. By working collectively, analytical chemists, policy makers, law enforcement and forensic practitioners can suitably identify potential classes of molecules that may become the next generation of NPSs and develop advanced methods/technologies for the simultaneous detection/quantification of these substances thereby legislating against potentially dangerous compounds before they pose a serious threat to human health.

The main focus of this research will be the detection of synthetic cathinones, in particular mephedrone. Apparent from the literature review is that there is a distinct lack of in-the-field sensors for this class of analytes largely in part to their only recent emergence. The work contained within this thesis seeks to address this issue by employing electrochemistry with a view to developing a rapid, disposable, accurate, low-cost portable sensor. The benefits of such a method are clear, the ability to analyse samples immediately at the site of the crime improves its forensic integrity whilst even employed as only a rapid screening tool can dramatically reduce time (and therefore costs) in forensic laboratories. The scope of this novel piece of work does not extend towards the analysis of synthetic cathinones in biological media (*e.g.* blood, urine, saliva), moreover, the initial steps taken will be to provide an on-site, low cost (with the use of graphite screen-printed electrodes; SPEs) rapid, easy to use analytical protocol to analyse drug samples for their contents of illicit, harmful, synthetic cathinones. This requires an analytical sensitivity of approximately 6% (w/w),⁵⁹ which should be sufficient to aid law enforcement agencies with on-the-spot drug testing.

The work presented in this chapter is contained within J. P. Smith, O. B. Sutcliffe and C. E. Banks, *Analyst*, 2015, **140**, 4932-4948.

Chapter 3 Experimental Methods

3.1 Chemicals and materials

All chemicals used were of analytical grade and were used as received without any further purification from Sigma-Aldrich (Gillingham, UK). All solutions were prepared with deionised water of resistivity no-less than 18.2 Ω cm. All solutions (unless stated otherwise) were vigorously degassed with nitrogen to remove oxygen prior to analysis. The synthetic cathinone hydrochloride (or hydrobromide) salts, were prepared at the University of Strathclyde prior to the legislative change on 16th April 2010 using the methods outlined below. Four street samples of NRG-2, obtained from independent internet vendors, were received as white crystalline powders in clear zip-lock bags.

3.2 Voltammetric Procedures

Voltammetric measurements were carried out using a Palmsens (Palm Instruments BV, The Netherlands) potentiostat/galvanostat (EmStat) and controlled by PSTrace version 4.4. Experiments were performed using boron doped diamond, glassy carbon and screen-printed graphite macroelectrodes; both the boron doped diamond and glassy carbon electrodes have a 3mm diameter working area along with a platinum wire counter electrode and a Saturated Calomel Electrode (SCE) reference (Radiometer, Copenhagen, Denmark) completing the conventional three electrode electrochemical system. Screen-printed graphite macroelectrodes (denoted as SPEs herein) utilised have a 3 mm diameter working area. Experiments in section 5.1 were performed using two different graphene screen-printed electrodes, denoted GSPE A and GSPE B herein, have a 3 mm and 1 mm diameter working electrode area respectively. All screen-printed electrodes are printed with a carbon counter and silver/silver chloride (Ag/AgCl) reference 'on board' (unless stated otherwise).

For experiments in section 5.1 a 1 pence British coin was used as the working electrode. The 1 pence coin has a different composition depending on the time it was minted; between its inception in 1971 and September 1992 minted coins comprised of bronze (97% copper, 2.5 zinc, 0.5% tin) however post 1992 they have been copper-plated steel. The study herein used coins minted post 1992 in light of the scarcity of coins minted pre-1992. The working electrodes, 1 pence coins, were in to a polytetrafluoroethylene (PTFE) 'housing' unit which comprised of a PTFE cap (with 3.0 mm bore hole leaving a working electrode area of 7.1 mm) and PTFE body allowing easy electrical wiring of the coin;¹⁹³ see Figure 3-1 for a schematic representation of the bespoke electrochemical cell. This cell is required to ensure that a reproducible geometric electrode area is obtained. Prior to analysis the 1 pence coin was sonicated in methanol to provide thorough surface cleaning for 2 mins. A new 1 pence coin was utilised for each experiment with each side utilised. Fe(II) modified graphene SPEs were constructed by suspending Fe(II) into methanol and pipetting aliquots onto a GSPE (A/B) and allowing to dry at 40°C prior to use.

3.3 Electrode Polishing

Experiments performed using boron doped diamond and glassy carbon macroelectrodes required polishing between measurements. A saturated alumina slurry solution was dropped onto precision lapping and polishing cloths (Kemet, UK) and the electrodes were mechanically polished manually in a figure of eight formation as per universal protocol to polish conventional solid electrodes.¹⁹⁴

3.4 Screen-Printing

SPEs were fabricated in-house with appropriate stencil designs using a DEK 248 screen printing machine (DEK, Weymouth, UK). For the fabrication of the screen-printed sensors, firstly, a carbon-graphite ink formulation (Product Code: C2000802P2; Gwent Electronic Materials Ltd, UK) was screen-printed onto a polyester (Autostat, 250 micron thickness) flexible film (denoted throughout as standard-SPE). This layer was cured in a fan oven at 60 degrees for 30 minutes. Next a silver/silver chloride reference electrode was included

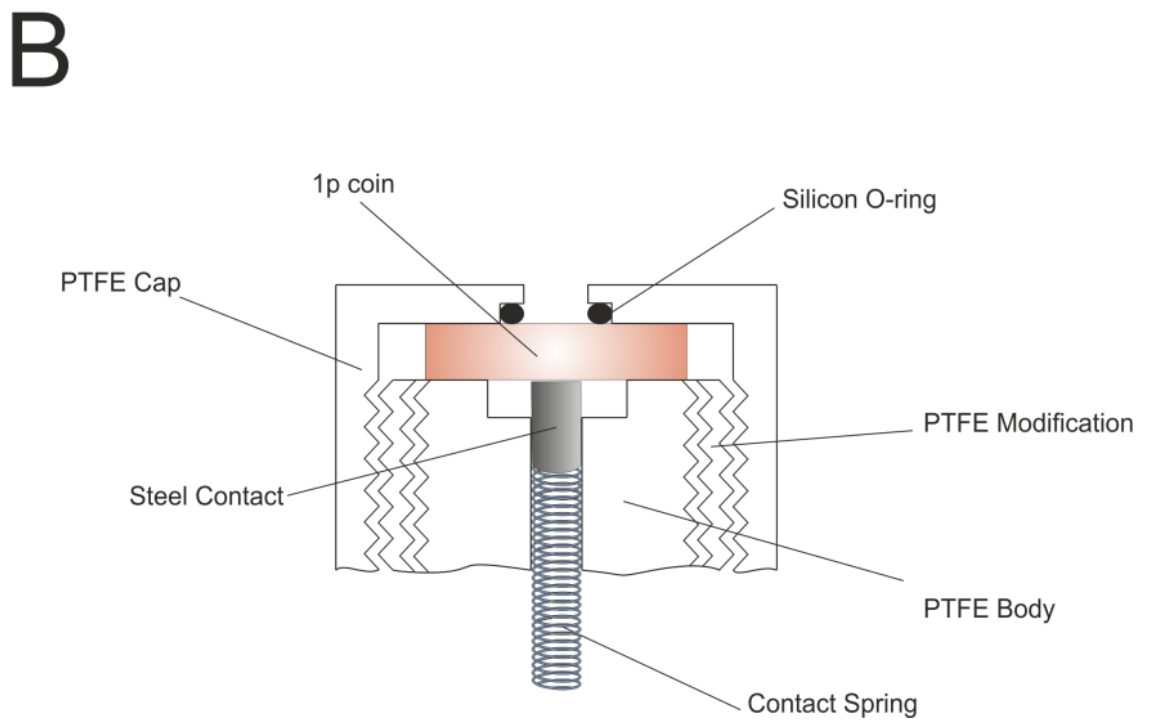
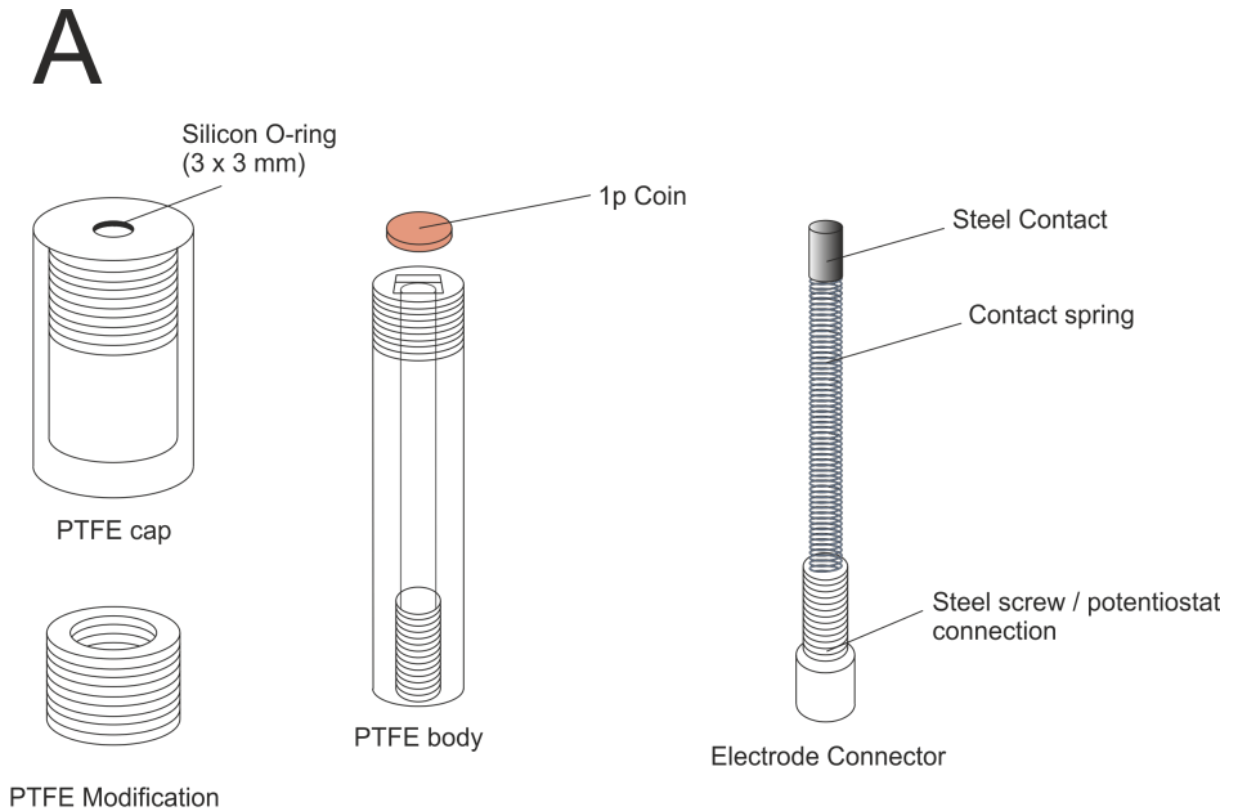


Figure 3-1 A: Schematic diagram of the Regal Electrochemistry experimental cell PTFE 'housing' unit used to hold the 1 pence sensor in place for analysis and accurately defines the working electrode area. B: Cross sectional diagram of assembled PTFE 'housing' unit with a retrofitted 1p-sensor in place which is then inserted into the solution under investigation.

by screen printing Ag/AgCl paste (Product Code: C2040308D2; Gwent Electronic Materials Ltd, UK) onto the polyester substrates. Finally, a dielectric paste (Product Code: D2070423D5; Gwent Electronic Materials Ltd, UK) was then printed onto the polyester substrate to cover the connections. After curing at 60 degrees for 30 minutes the screen-printed electrodes are ready to be used. The reproducibility of the batch of screen-printed sensors were found to correspond to 0.76 % RSD using the $\text{Ru}(\text{NH}_3)^{2+/3+}$ redox probe in 1M KCl.¹² Graphene SPEs (GSPE A/B) created in a similar fashion however using graphene inks: GSPE A (GSPE A; Product Code: HDPlas™ Graphene Ink SC213; Haydale Ltd, UK) and graphene GSPE B (GSPE B; Product Code: Vor-ink S103; Vorbeck Materials Ltd, USA). Note that the graphene used in the fabrication of the GSPE A ink is in the form of graphene nanoplatelets which are produced *via* a split plasma process, resulting in graphene which does not exhibit a basal surface containing structural damage as is the case for wet chemical fabrication approaches.¹⁹⁵ In the case of the GSPE B ink, monolayer graphene produced *via* a chemical exfoliation is used and incorporated into the ink formulation. Shown in Figure 3-2 is the entire GSPE fabricated as described above and a Scanning Electron Microscope (SEM) image of the electrode surface.

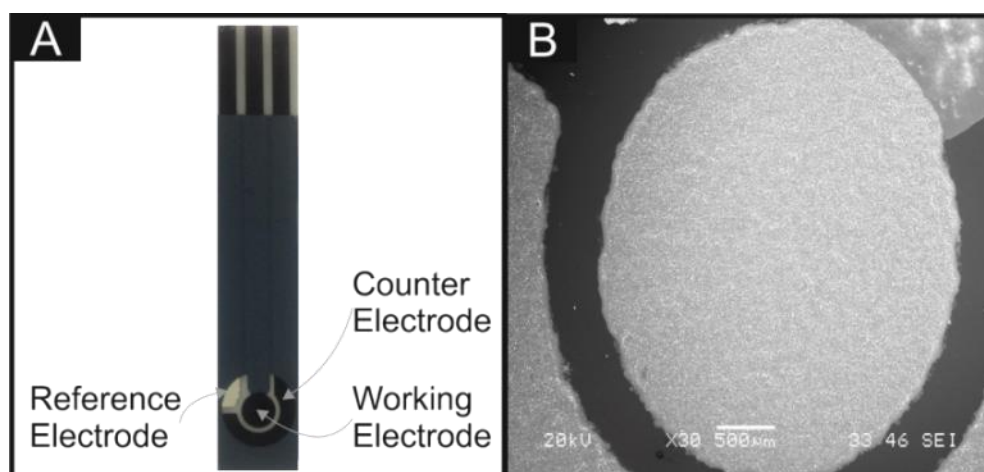


Figure 3-2 A shows an image of the overview GSPE used in this work along with an SEM image (B) of the electrode surface.

3.5 Characterisation

Raman Spectroscopy was performed using a 'Renishaw InVia' spectrometer with a confocal microscope (x50 objective) spectrometer with an argon laser (514.3 nm excitation) at a very low laser power level (0.8 mW) to avoid any heating effects. Spectra were recorded using a 10 s exposure time for 3 accumulations. Note that 5 spectra were recorded and an average representation. X-ray Photoelectron Spectroscopy (XPS) measurements were performed with a Kratos Axis Ultra spectrometer using monochromatic Al K X-rays (1486.6 eV) (independently by CERAM).

For each sample, the aim was to analyse as large an area as possible within the circular region of interest in order to provide an averaged response over the entire graphene domain.

Scanning electron microscope (SEM) images and surface element analysis were obtained with a Zeiss Supra 40vp model equipped with an energy-dispersive X-ray microanalysis package (GenesisEdax).

Chapter 4 Detection of Illicit Compounds

Following review of the literature in Chapter 2, work proceeded to develop an electro-analytical technique for the detection of the prominent class of NPSs – synthetic cathinones. This chapter explores the use of screen-printed technology to address the growing epidemic of NPSs to show proof-of-concept of an on-site detector. Furthermore, screen-printed electrodes are also shown to be sensitive detectors of common ‘date-rape’ drug Rohypnol® (flunitrazepam) which has been associated in drug-facilitated sexual assault for a number of years.

4.1 The electroanalytical sensing of synthetic cathinone-derivatives and their accompanying adulterants in “legal high” products via electrochemical oxidation

The most prominent synthetic cathinone-based “legal highs” abused in the United Kingdom, as mentioned in Chapter 0, are methcathinone and its derivatives; in particular mephedrone. All are structurally related to the natural stimulant, cathinone and possess a pharmacological similarity to the phenethylamine class of psychoactives (e.g. amphetamine and methamphetamine).

Clearly identifiable from a survey of the literature (Chapter 2) is that there are a number of laboratory-based analytical methods for “legal highs” which have been developed and can be used for a confirmatory approach. To date, following thorough research, no established portable hand-held type device that can be used to screen for the presence of the NPS class synthetic cathinones has been identified – therefore the work described herein is both novel, timely and pertinent.

To enable translation from the laboratory into the “field”, screen-printed electrodes are a favourable approach since they provide a low cost, single-shot disposable yet highly reproducible and reliable platform for electrochemical measurement of the target

analyte.^{10-12, 196, 197} The use of electrochemistry with screen-printed electrodes as a tool for the detection and analysis of cathinone-derived designer drugs has not been reported before. However there is one study reporting the electrochemical behaviour of mephedrone using a mercury dropping electrode; Krishnaiah *et al.*¹⁹⁸ reported an analytical range of 2.7×10^{-4} to $1.8 \mu\text{g mL}^{-1}$ with a detection limit of $2.2 \times 10^{-3} \mu\text{g mL}^{-1}$. Whilst yielding favourable analytical responses, a problem arises with the use of the Dropping Mercury Electrode; mercury is widely reported as a harmful chemical and thusly not sanctioned in labs globally;¹⁹⁹⁻²⁰³ additionally the issue of translating the research from the laboratory into the field still needs to be addressed.

Described in the following chapter, for the first time; the electroanalytical sensing of mephedrone (4-MMC) and 4-methylethcathinone (4-MEC) another synthetic cathinone derivative that frequently occurs in “*legal highs*” are reported using both commercially available solid macroelectrodes (boron-doped diamond, glassy carbon) and disposable screen-printed graphite macroelectrodes. Additionally adulterants that are typically found in street samples are electrochemically characterised for their potential interference in the simultaneous sensing of 4-MMC and 4-MEC. All peak currents (or heights), are measured by extrapolating the preceding baseline current, to replicate in-the-field environments a new electrode was used for each scan – as would be the case in forensic investigation.

4.1.1 Direct Electrochemical Oxidation of Methcathinone.

The electrochemical detection of methcathinone in aqueous based buffer solutions at a range of commercially available electrodes was first considered. Figure 4-1 depicts the voltammetric profiles observed at a boron-doped, glassy carbon and screen-printed electrodes (SPEs) in a solution of $500 \mu\text{g mL}^{-1}$ methcathinone in aqueous pH 12 Phosphate-buffered saline (PBS) buffer. It is evident that the electrochemical oxidation of methcathinone is possible and is observed, on electrodes of the same area, to occur at the lowest overpotentials when using SPEs, followed by glassy carbon (GC), and boron-doped diamond (BDD) with the SPE also giving the largest voltammetric peak. This difference is reflected by the greater % global coverage of edge plane – like/sites defects

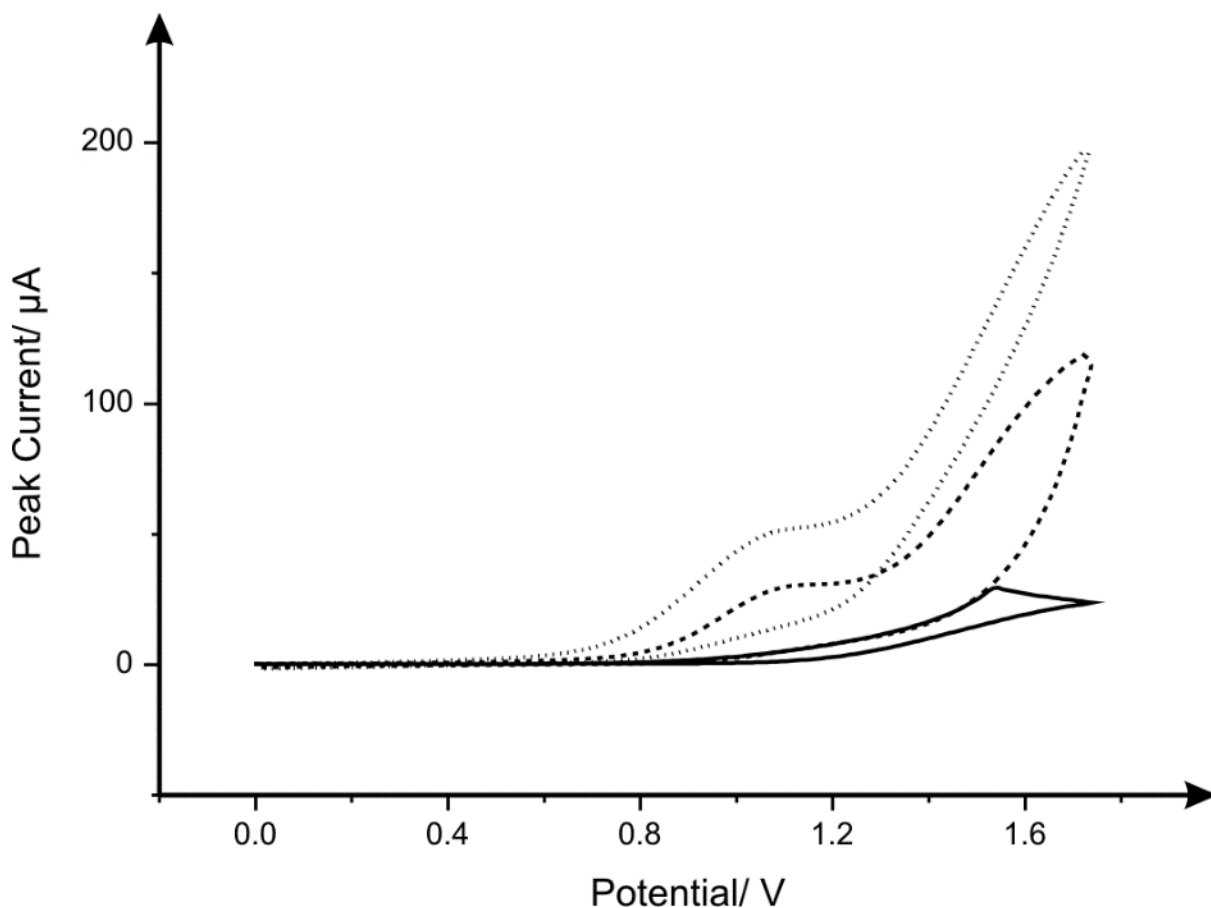


Figure 4-1 Voltammetric profiles observed at a boron-doped (solid line), glassy carbon (dashed line) and SPE (dotted line) electrode in a solution of $500 \mu\text{g mL}^{-1}$ methcathinone in a pH 12 PBS buffer. Scan rate: 100 mV s^{-1} . vs. SCE (BDD, GC) Ag/AgCl (SPE).

residing on the screen-printed graphite electrode over the other electrode surfaces which has been reported before for other target analytes.²⁰⁴

Of interest is the response of the disposable screen-printed graphite electrodes since these allow a portable mass-produced economical sensor to be potentially realised and due to their scales of economy, a single sensor can be used for each voltammetric scan without recourse to electrode polishing as is the case for boron-doped and glassy carbon electrodes; consequently, it is only this electrode platform considered further. A clear comparison of the SPE's response in $500 \mu\text{g mL}^{-1}$ methcathinone is visible in Figure 4-2.

Next, attention was turned to exploring the effect of pH upon the electrochemical signal. A plot of peak potential (E_p) vs. pH, as shown in Figure 4-3, was constructed where a linear range with a gradient of 0.031V is observed ($E/V = -0.031\text{V} + 1.41 E/\text{pH}$

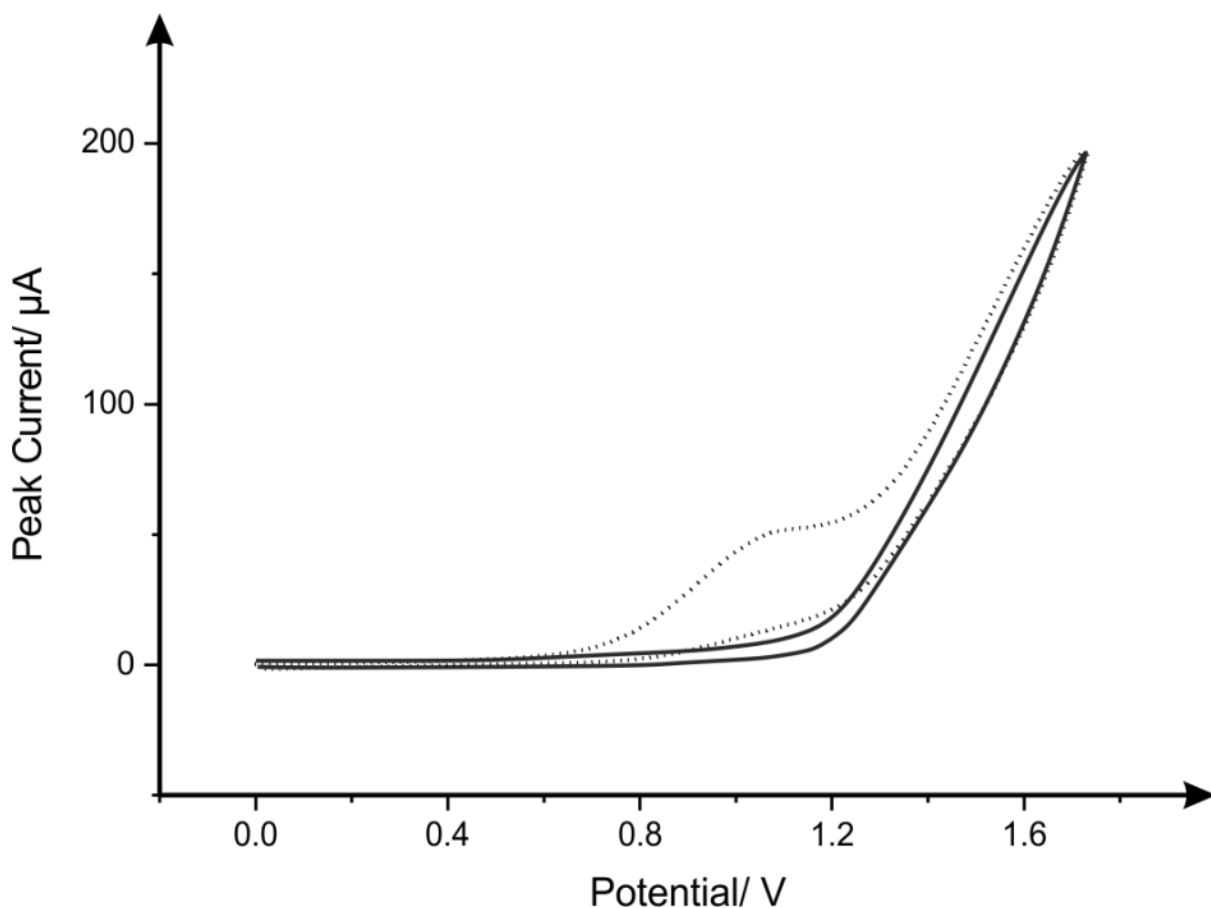


Figure 4-2 Voltammetric profiles observed at a SPEs of blank pH 12 PBS buffer (solid line), and 500 $\mu\text{g mL}^{-1}$ methcathinone (dotted line) in a solution of in a pH 12 PBS buffer. Scan rate: 100 mV s^{-1} . vs. Ag/AgCl.

$R^2 = 0.99$). Such a value is close to that expected for 1 proton and 2 electron process (assuming standard conditions; 30 mV per pH unit at 25 °C) as deduced from

Equation 4-1

$$E_{f,eff}^0 = E_f^0(A/B) - 2.303 \frac{mRT}{nF} pH$$

Below pH 8 the voltammetric peak shifts out of the accessible voltammetric window. Note: the molecule has a reported pK_a value of *ca.* 8²⁰⁵ which offers an explanation. Given the chemical similarity between methcathinone and that of amphetamines, prior work studying amphetamines by Oliveira-Brett *et al.*²⁰⁶ shows similar electrochemical behaviour and it is thought to be the result of the electrochemical oxidation of the secondary amine.²⁰⁶

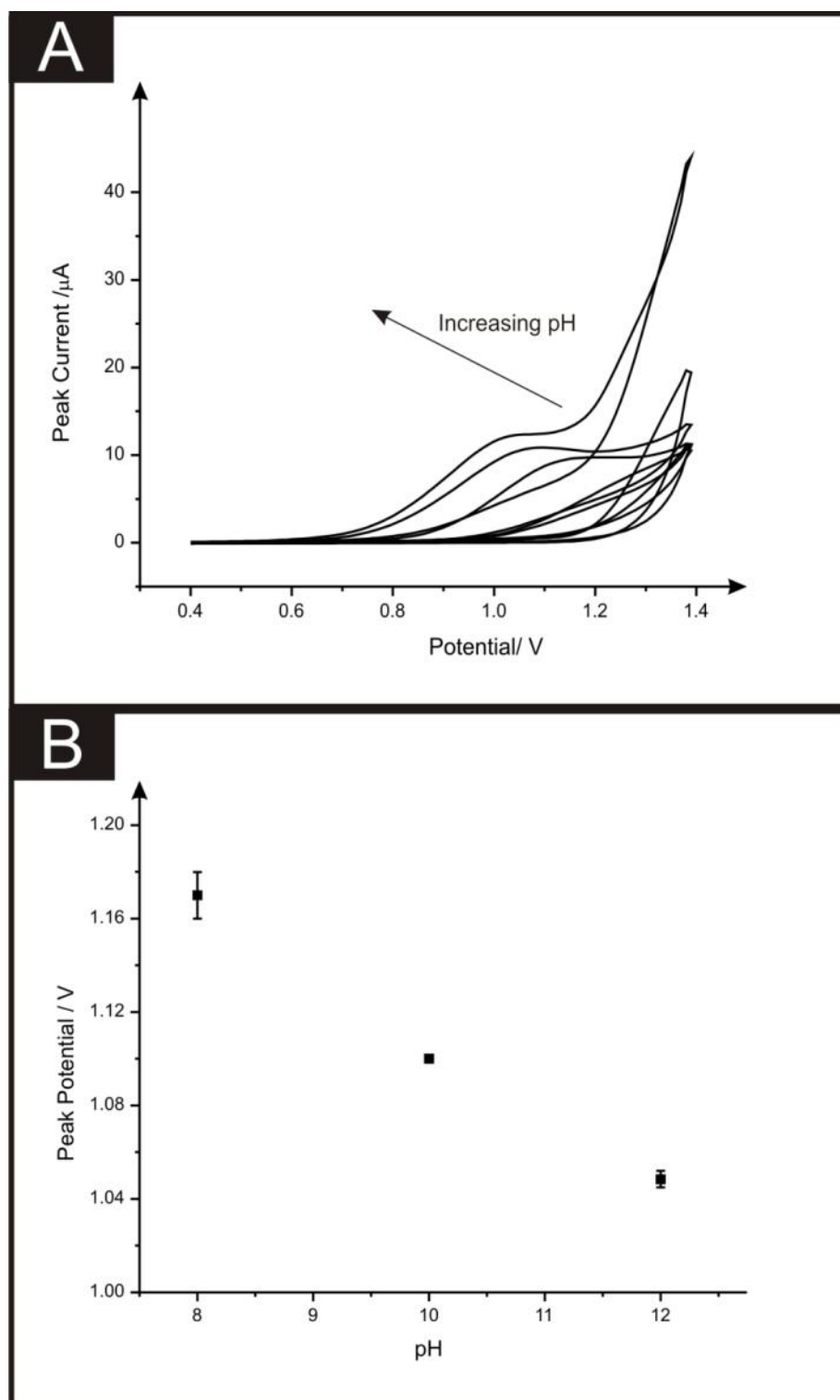


Figure 4-3 A: Cyclic voltammetric responses (A) of methcathinone obtained in phosphate buffer solution at different pHs. B: Plot of peak potential as a function of pH for the electrochemical oxidation of methcathinone Scan rate: 100 mV s^{-1} . vs. Ag/AgCl. The responses shown in (B) represent are an average response (squares) with corresponding error bars ($N = 3$).

Next, the effect of scan rate upon the electrochemical oxidation of methcathinone was explored in a 500 $\mu\text{g mL}^{-1}$, pH 12 solution where a plot of peak height against the square-root of scan rate (Figure 4-4) was found to be linear indicating a diffusional process:

$$(I_p/A = 16.9 \text{ A}(\text{Vs}^{-1})^{-0.5} + 3.61 \text{ A}; R^2 = 0.91);$$

The peak potential is observed to shift to more positive values with increasing scan rate with a linear relation between E_p and \ln scan rate (ν):

$$(E_p(\text{V}) = 0.029 \ln \nu (\text{Vs}^{-1}) + 0.89 ; R^2 = 0.90);$$

For an irreversible electrochemical process, the relationship between E_p and scan rate (ν) is given by Equation 4-2:²⁰⁷

Equation 4-2

$$E_p = E_f^0 - \frac{RT}{\alpha n F} \ln \frac{RTk^o}{\alpha n F} + \frac{RT}{\alpha n F} \ln \nu$$

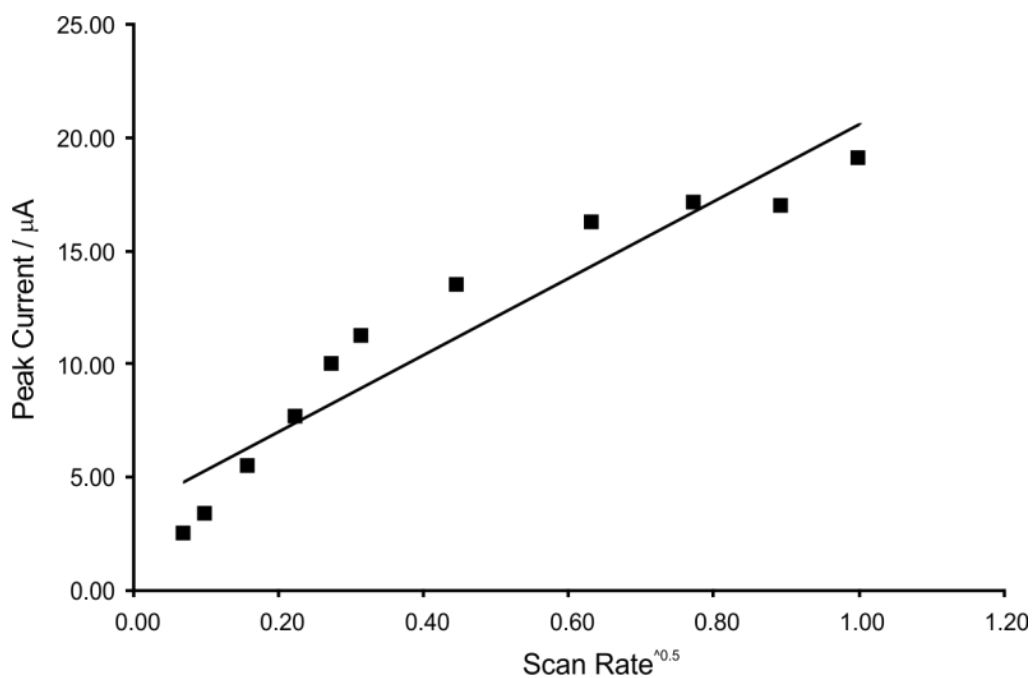


Figure 4-4 Plot of the square root of scan rate against peak current for 500 $\mu\text{g mL}^{-1}$ methcathinone in pH 12 buffer solution.

where E_f^0 is the formal potential, α is the transfer coefficient, n is the number of electrons transferred in the rate determining step, R, T and F have their usual meanings and k^o is the heterogeneous rate constant. From the plot of E_p and $\ln v$ the gradient is found to correspond to 0.0296 where αn is deduced to be 0.87. Assuming α is 0.5, a value of $n = 1.7$, which is close to the value of 2 deduced above with the pH study discussed above.

Next attention was turned towards exploring the analytical performance of the SPEs towards methcathinone. Figure 4-5 shows a typical calibration plot of peak height against

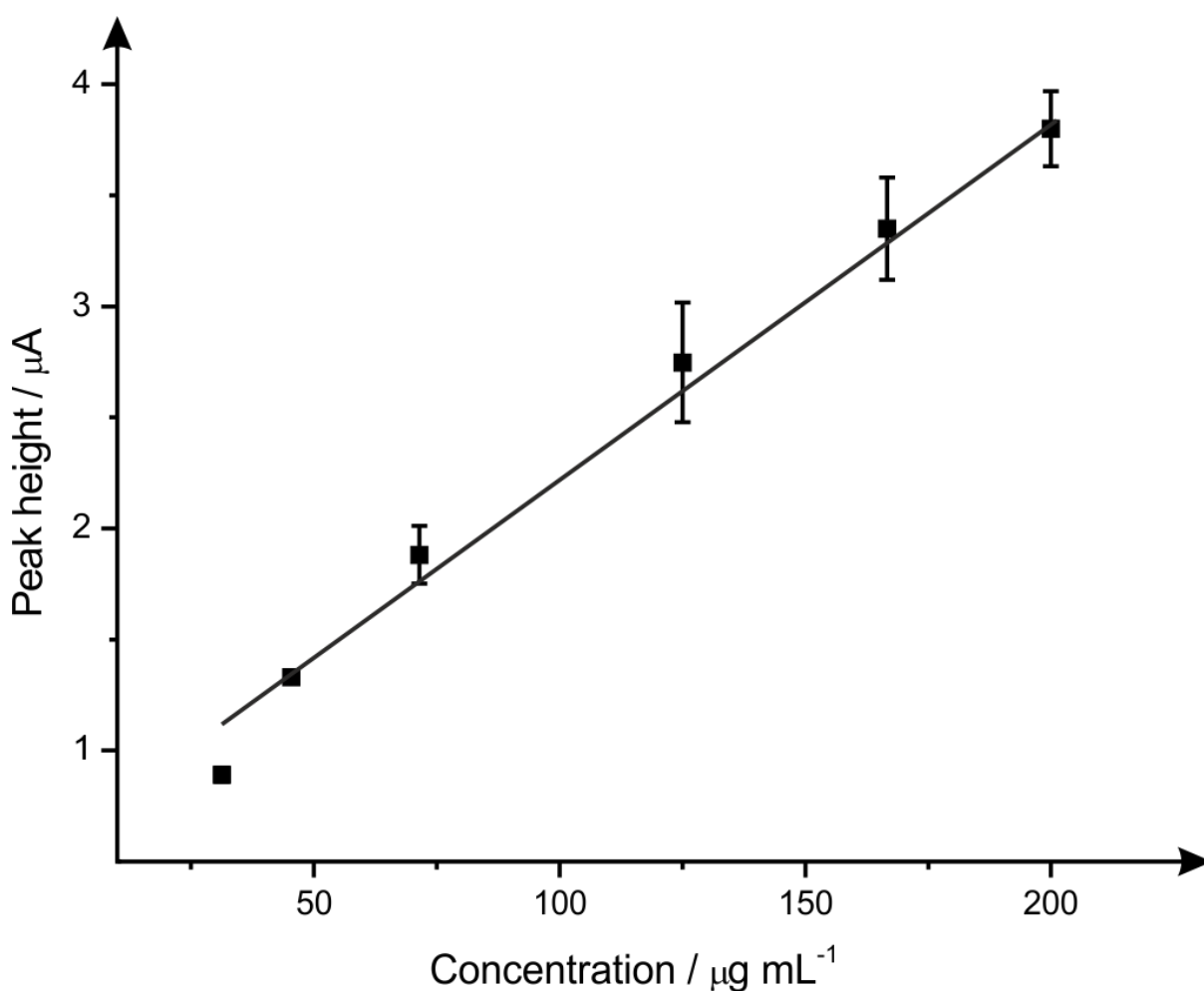


Figure 4-5 A typical calibration plot corresponding to the addition of methcathinone into a pH 12 phosphate buffer solution over the range 31.3 – 200.0 $\mu\text{g mL}^{-1}$ using a new SPE for each addition. The responses shown are an average response (squares) with corresponding error bars ($N = 3$).

methcathinone concentration which exhibits a linear range from 31.2 to 200.0 $\mu\text{g mL}^{-1}$ with a limit of detection (3σ) found to correspond to 24.2 $\mu\text{g mL}^{-1}$:

$$(I_p/A = 0.017A/\mu\text{g mL}^{-1} + 0.57 \text{ A } R^2 = 0.98);$$

Note that this is the first instance of the synthetic cathinone methcathinone being electroanalytically quantified.

4.1.2 Direct Electrochemical Oxidation of Methcathinone Derivatives

Focus was then turned to the synthetic cathinone derivatives that are commonplace in “legal high” samples: 4-MMC and (\pm)-4'-methyl-N-ethylcathinone (4-MEC). Voltammetric profiles for 4-MEC/4-MEC, as shown in Figure 4-6, reveal similar electrochemistry as observed for methcathinone in a pH 12, 500 $\mu\text{g mL}^{-1}$ aqueous buffer solution. A study into the effect of scan rate on the oxidation of both 4-MMC and 4-MEC in 500 $\mu\text{g mL}^{-1}$ pH 12 buffer solution where a plot of peak height against the square-root of scan rate revealed a linear response indicating a diffusional process:

$$(4\text{-MMC } I_p/A = 9.00 \text{ A}(\text{Vs}^{-1})^{-0.5} + 2.00 \text{ A } R^2 = 0.94);$$

$$(4\text{-MEC: } I_p/A = 18.54 \text{ A}(\text{Vs}^{-1})^{-0.5} + 6.11 \text{ A } R^2 = 0.86).$$

The effect of pH was also explored on the voltammetric profiles of both 4-MMC and 4-MEC where it was found that as the pH was decreased from basic conditions, the oxidation peak, similar to that observed in the case of methcathinone, ceased to exist in neutral pH's, however the key difference is that as both solutions become more acidic a new, quasi-reversible wave becomes visible, as shown in Figure 4-7. Note: the exact origin of this new voltammetric profile is currently unknown but it can however provide a useful sensing strategy.

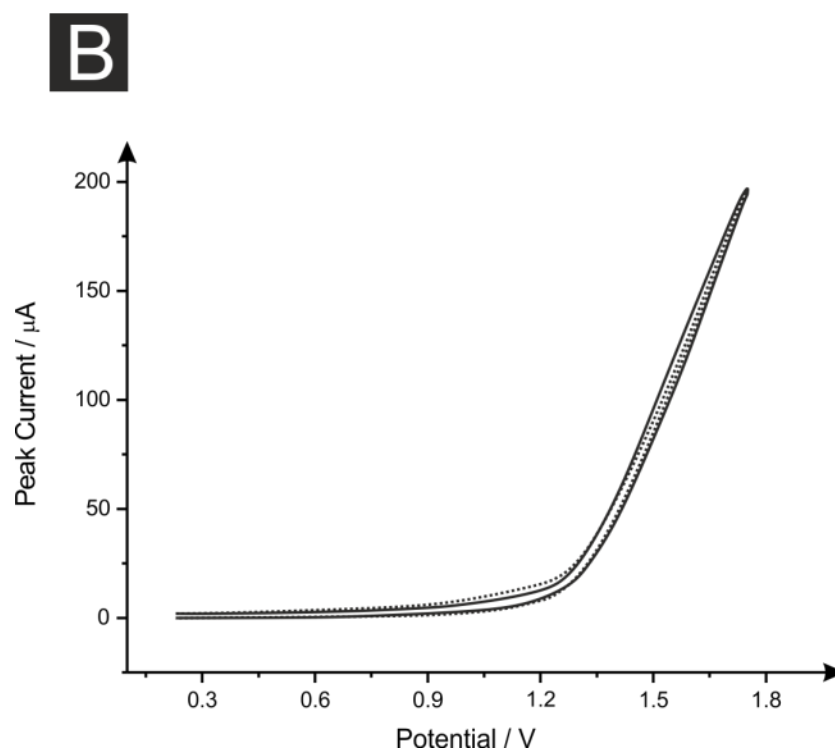
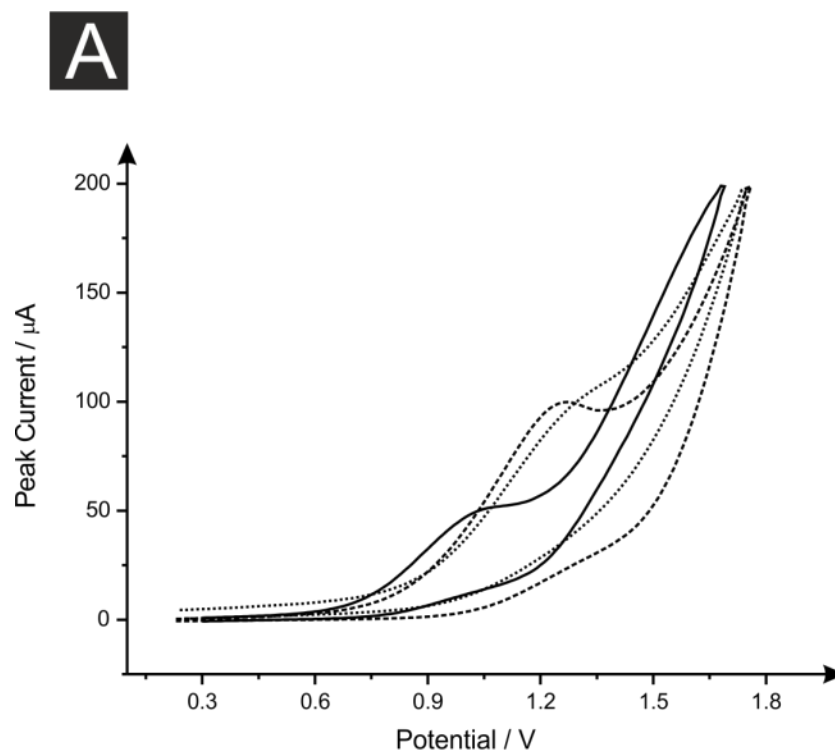


Figure 4-6 A: Voltammetric profiles for both 4-MMC (dotted line) and 4-MEC (dashed line) compared to methcathione (solid line) in a pH 12, $500 \mu\text{g mL}^{-1}$ aqueous buffer solution using SPEs. Scan rate: 100mV s^{-1} , vs. Ag/AgCl. B: *For Reference*, Background Voltammetric profiles for both 4-MMC (solid line) and 4-MEC (dashed line) in pH 12 aqueous buffer solution using SPEs. Scan rate: 100mV s^{-1} , vs. Ag/AgCl.

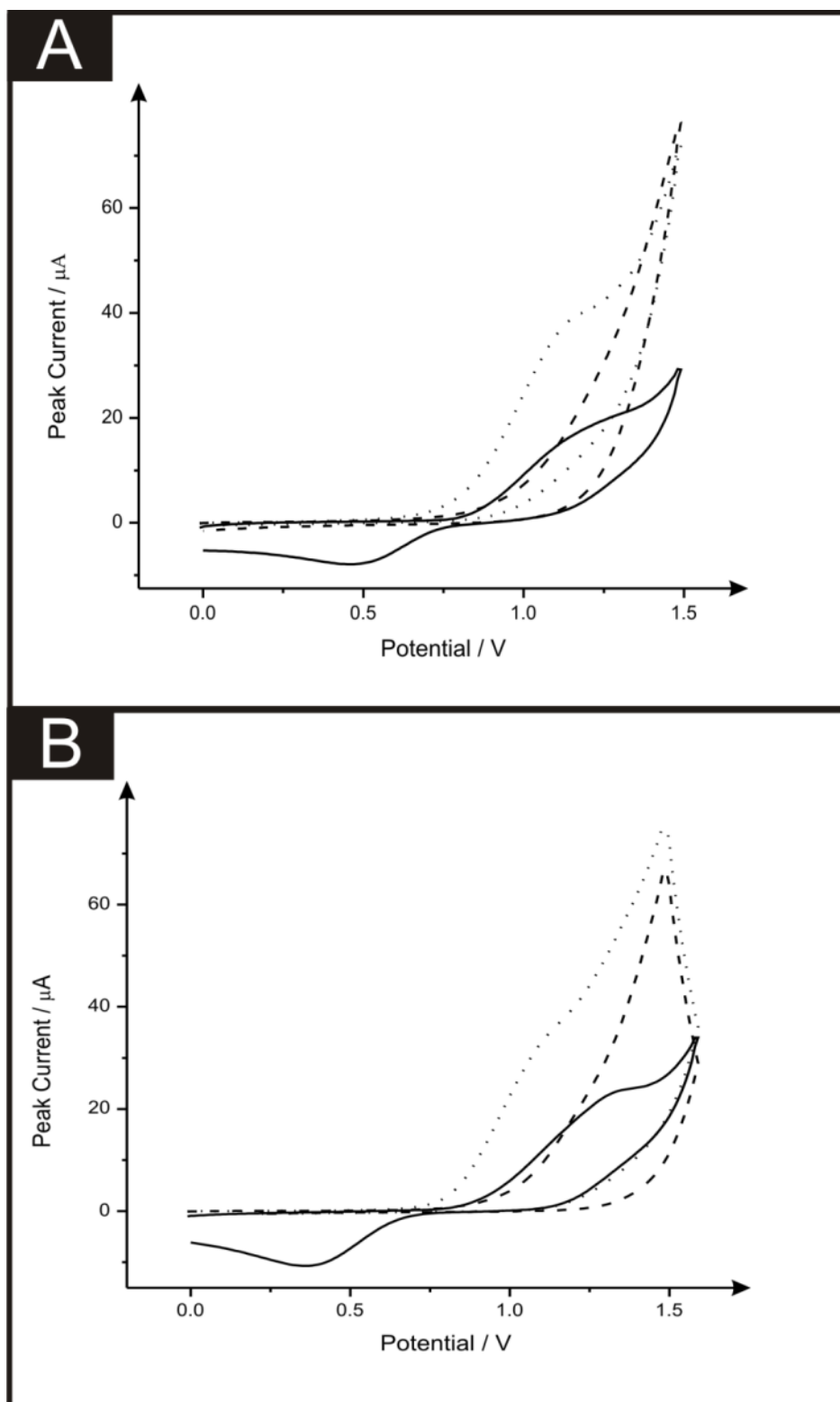


Figure 4-7 A: Cyclic voltammetric responses 4-MMC obtained in phosphate buffer solution at pH 2 (solid line), pH 6 (dashed line) and pH 12 (dotted line). B: Cyclic voltammetric responses of 4-MEC obtained in phosphate buffer solution pH 2 (solid line) pH 6 (dashed line) and pH 12 (dotted line). Scan rate: 100 mV s^{-1} vs. Ag/AgCl.

Taking into consideration the results obtained, which indicate a reaction involving 1 proton and 2 electrons, and earlier research performed,²⁰⁶ a proposed mechanism for the reaction at the electrode surface is observed in Scheme 4-1. The irreversible nature of the voltammetric profile observed may be a result of the lack of H⁺ ions available at pH 12 to allow the reverse of the proposed reaction (Scheme 4-1) at the electrode surface. The introduction of a quasi-reversible wave may be caused, in part, by an increased amount of H⁺ ions available at acidic pHs.

Next the analytical performance of the SPEs in basic conditions (pH 12) were, for the first time, investigated towards the sensing of 4-MMC and 4-MEC where calibration plots (observed in Figure 4-8) of peak height against concentration revealed a linear range from 39.2 to 666.7 $\mu\text{g mL}^{-1}$ for 4-MMC and 95.2 to 1000.0 $\mu\text{g mL}^{-1}$ for 4-MEC with limits of detection (3σ) found to correspond to 13.2 $\mu\text{g mL}^{-1}$ and 36.3 $\mu\text{g mL}^{-1}$ for 4-MMC and 4-MEC respectively.

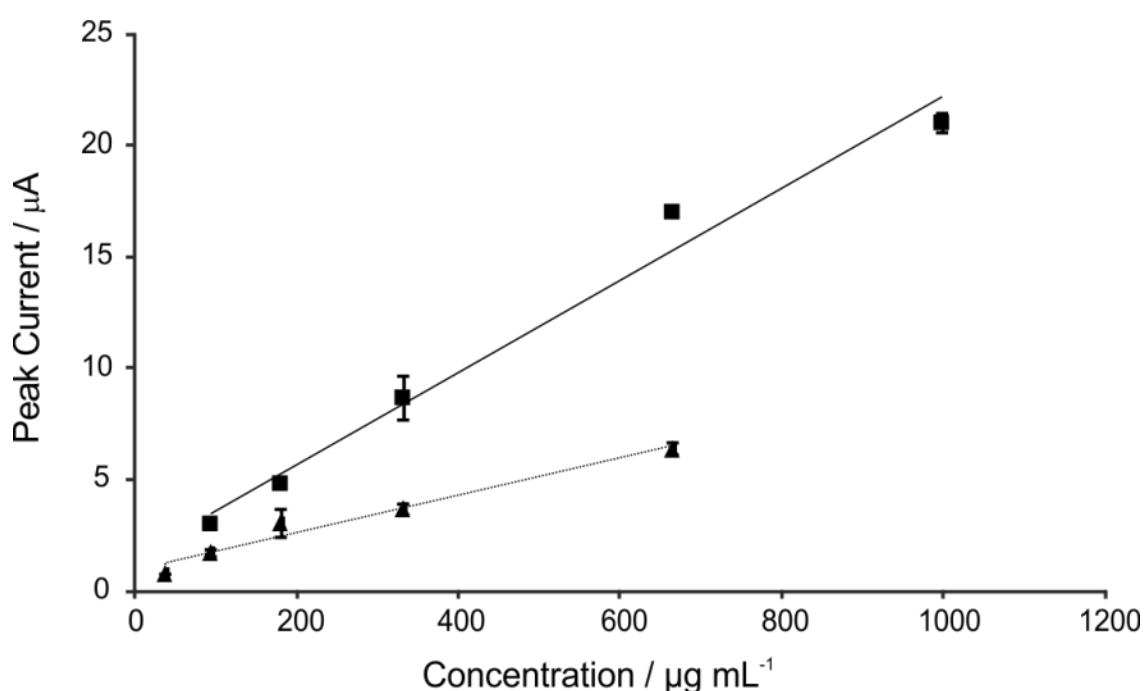
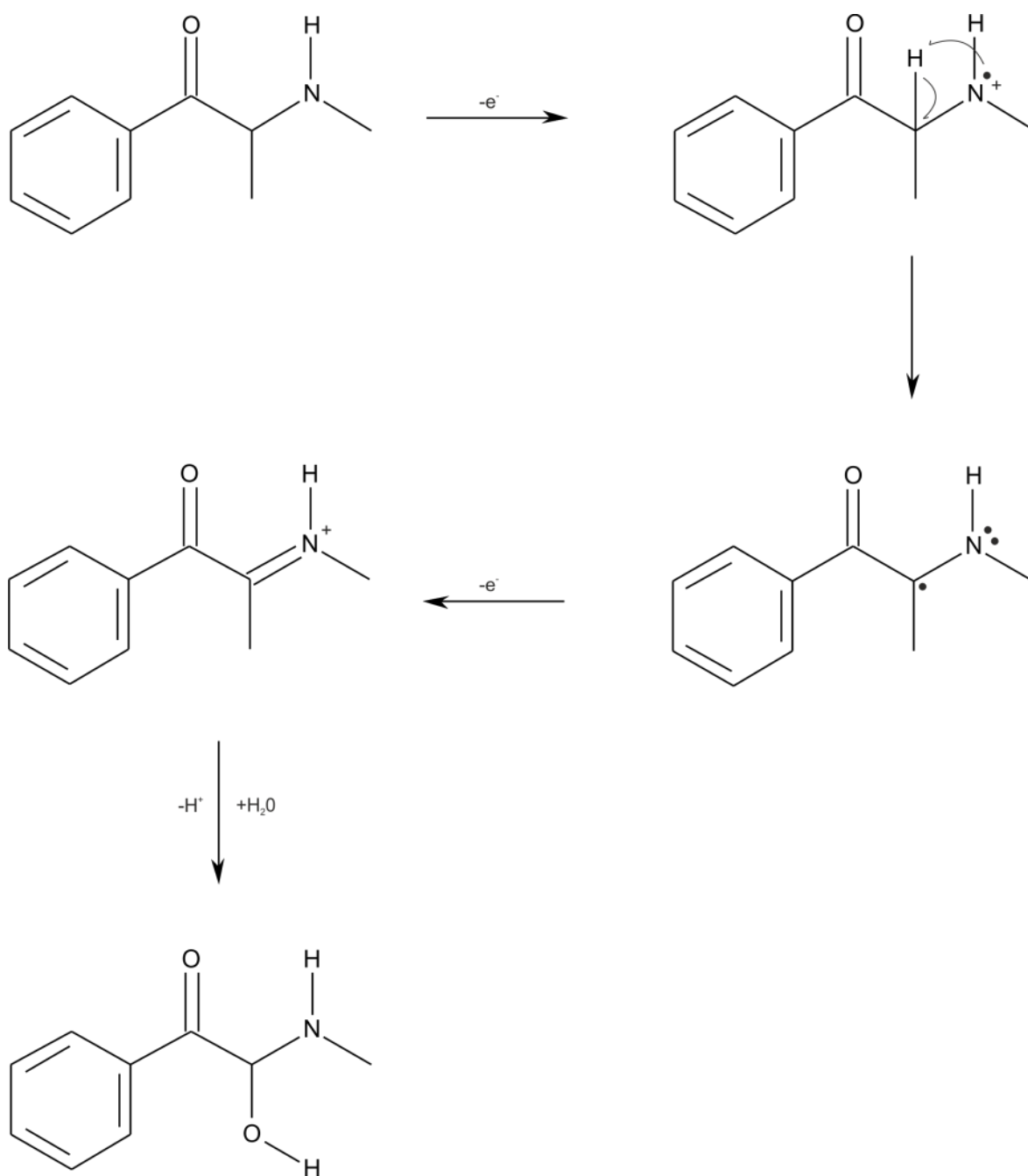


Figure 4-8 Typical calibration plots corresponding to 4-MEC (solid line) over the range 95.2 to 1000.0 $\mu\text{g mL}^{-1}$ and 4-MMC (dotted line) over the range 39.2 to 666.7 $\mu\text{g mL}^{-1}$ into a pH 12 aqueous buffer. The responses shown are an average response with the corresponding error bars ($N = 3$)



Scheme 4-1 Proposed mechanism for the oxidation of methcathinone at the electrode surface.

Given that the pH study of 4-MMC and 4-MEC revealed a redox couple in acidic conditions (one that was not present for methcathinone) the effect of scan rate upon the electrochemical oxidation of both (4-MMC) and (4-MEC) at pH 2 was investigated at $500 \mu\text{g mL}^{-1}$. A plot of the oxidation wave peak height against the square-root of scan rate was found to be linear indicating a diffusional process for both molecules

(4-MMC: $i_p/A = 39.99 \text{ AM}^{-1} + 2.99A \text{ R}^2 = 0.95$);

(4-MEC: $Ip/A = 42.1 \text{ AM}^{-1} + 1.381A$; $R^2 = 0.96$).

The peak potential is observed to shift to more positive values with increasing scan rate with a linear relation between E_p and $\ln v$

(4-MMC: $Ep(V) = 0.045 \ln v \text{ (Vs}^{-1}) + 1.19$; $R^2 = 0.91$);

(4-MEC: $Ep(V) = 0.04 \ln v \text{ (Vs}^{-1}) + 1.17$; $R^2 = 0.85$).

The sensing of 4-MMC and 4-MEC was explored at this pH with a series of additions made into a pH 2 aqueous buffer for both molecules as shown in Figure 4-9, each molecule displayed linearity through the range of 16.1 to 300.0 $\mu\text{g mL}^{-1}$ with limits of detection (3σ) found to correspond to 15.7 $\mu\text{g mL}^{-1}$

($Ip/A = 0.043 \text{ A}/\mu\text{g mL}^{-1} + 0.69A$ $R^2 = 0.99$);

and 16.2 $\mu\text{g mL}^{-1}$ MEC

($Ip/A = 0.044A/\mu\text{g mL}^{-1} + 0.81 \text{ A}$ $R^2 = 0.99$);

for 4-MMC and 4- respectively.

In the majority of legal high samples there are purposely added adulterants contained (to perhaps give each 'legal high' specimen its unique 'high'), popular choices are compounds such as caffeine and benzocaine.⁵⁹ Consequently, an investigation into the electrochemical behaviour (i.e. possible interference) into caffeine and benzocaine was undertaken to see if an electrochemical technique would be a viable option in real street samples containing cathinones and adulterants. As shown in Figure 4-10 the voltammetric profiles of both 500 $\mu\text{g mL}^{-1}$ caffeine and benzocaine in pH 12 can be readily observed. Indicative from inspection and comparison of the observed peak potentials with those of the legal highs is that as a concept, using electrochemistry for the detection of illicit substances in 'legal highs' is not viable. Adulterants added to such samples will most likely interfere (voltammetrically) with the signal response from one of the cathinones due to the overlapping voltammetric profiles.

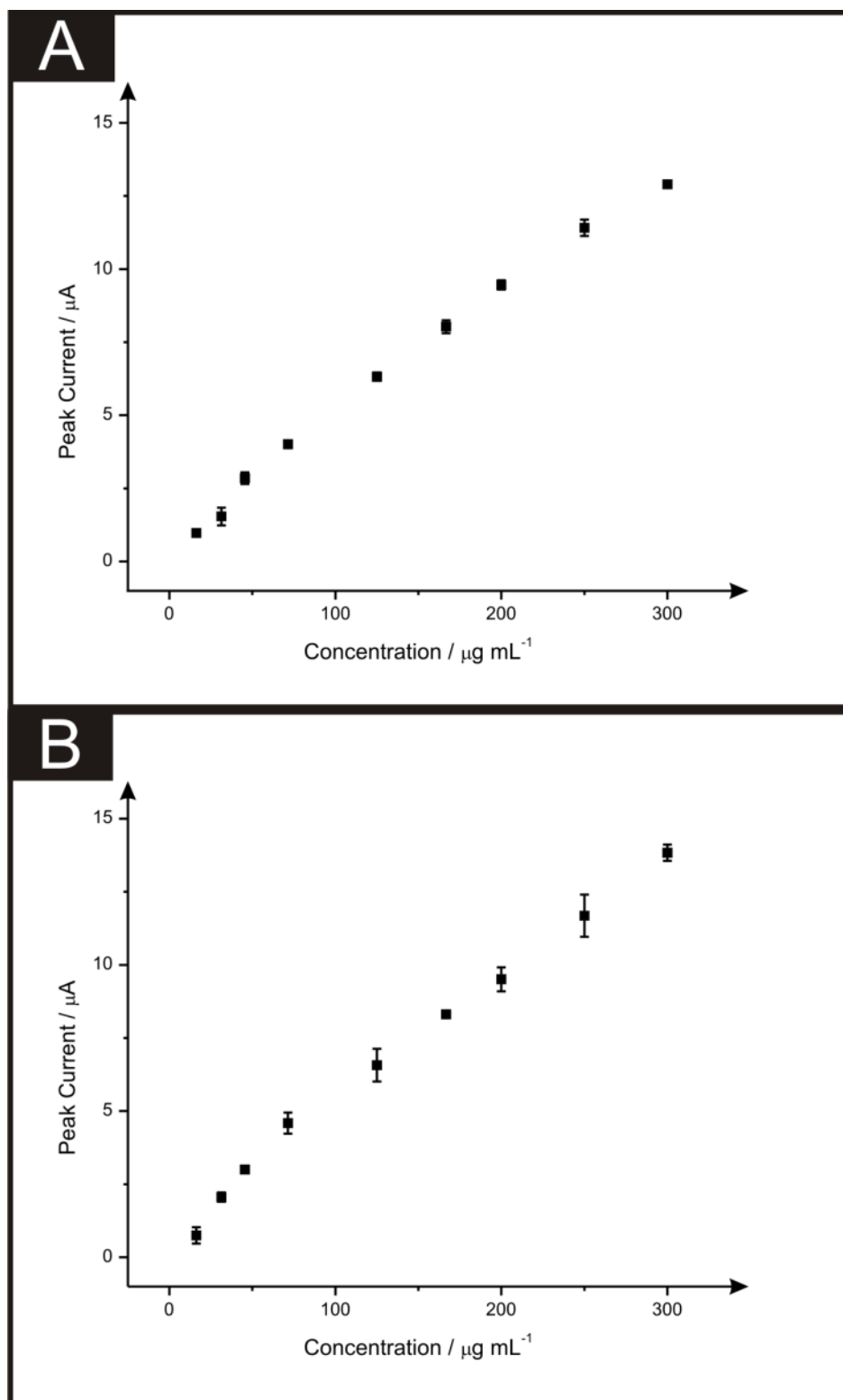


Figure 4-9 Typical calibration plot corresponding to the addition of 4-MEC (A) and 4-MEC (B) into a pH 2 phosphate buffer solution over the range 16.1 – 300 $\mu\text{g mL}^{-1}$ using a new SPE for each addition. The responses shown are an average response (squares) with corresponding error bars ($N = 3$).

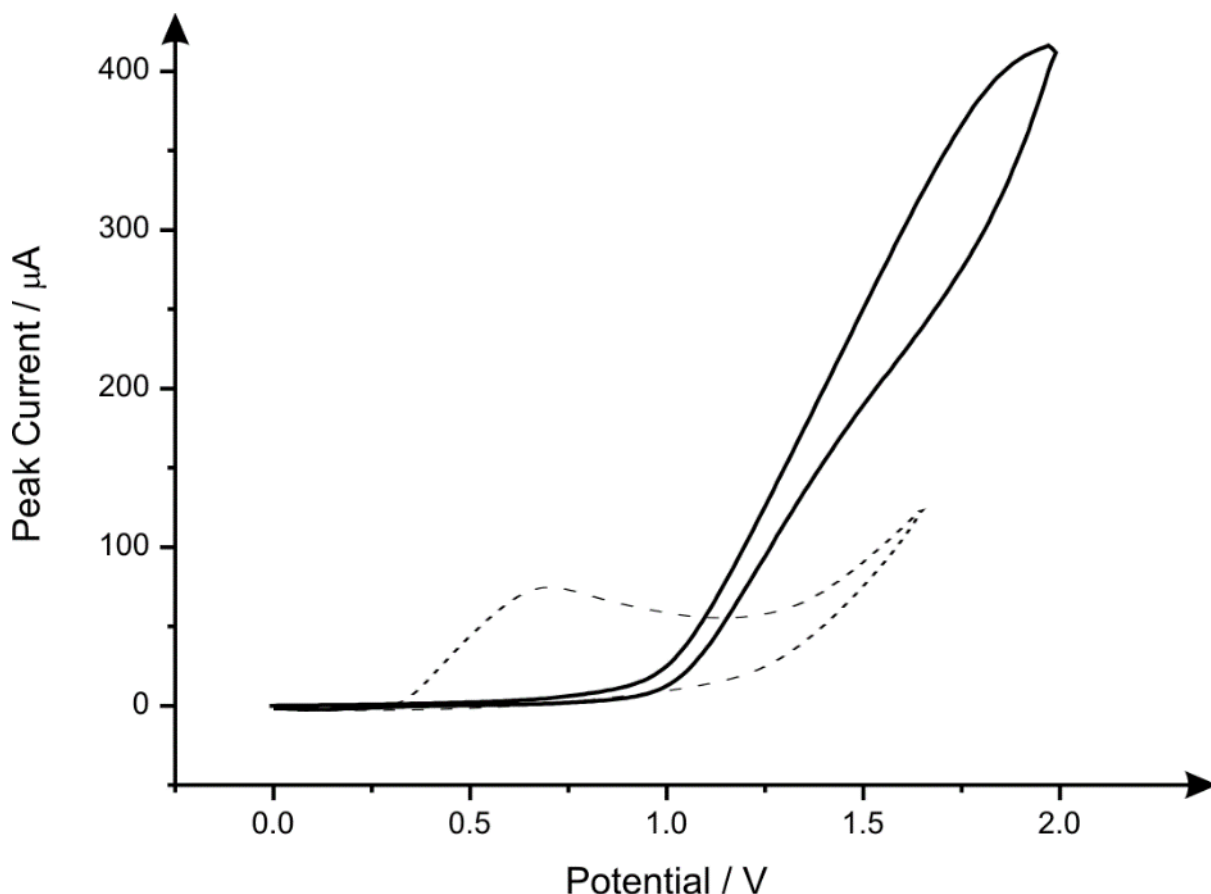


Figure 4-10 Voltammetric profiles of both caffeine (solid line) and benzocaine (dashed line) at pH 12 in $500 \mu\text{g mL}^{-1}$ obtained using SPE. Scan rate: 75mV s^{-1} vs. Ag/AgCl.

With respect to the analytical response for 4-MMC/4-MEC being possible at pH 2 as well as pH 12, attention was turned to the adulterants caffeine and benzocaine to determine whether analyses of mixtures at pH 2 would be a viable option. Voltammetric scans were performed in $500 \mu\text{g mL}^{-1}$ buffer solution on both molecules revealing voltammetric profiles that would again undoubtedly interfere with the responses from 4-MMC and 4-MEC. The cyclic voltammetric responses of all four molecules (4-MMC, 4-MEC, caffeine and benzocaine) at 100mVs^{-1} in $500 \mu\text{g mL}^{-1}$ pH 2 buffer solutions can be observed from inspection of Figure 4-11. Note: the electrochemical oxidation of caffeine at pH 12 and 2, as shown in Figure 4-10 and Figure 4-11 respectively are in good agreement with literature studies using edge plane pyrolytic graphite electrodes that have independently reported that an electrochemically irreversible wave is observed.²⁰⁸ Additionally the voltammetric response of benzocaine is in agreement with literature reports using

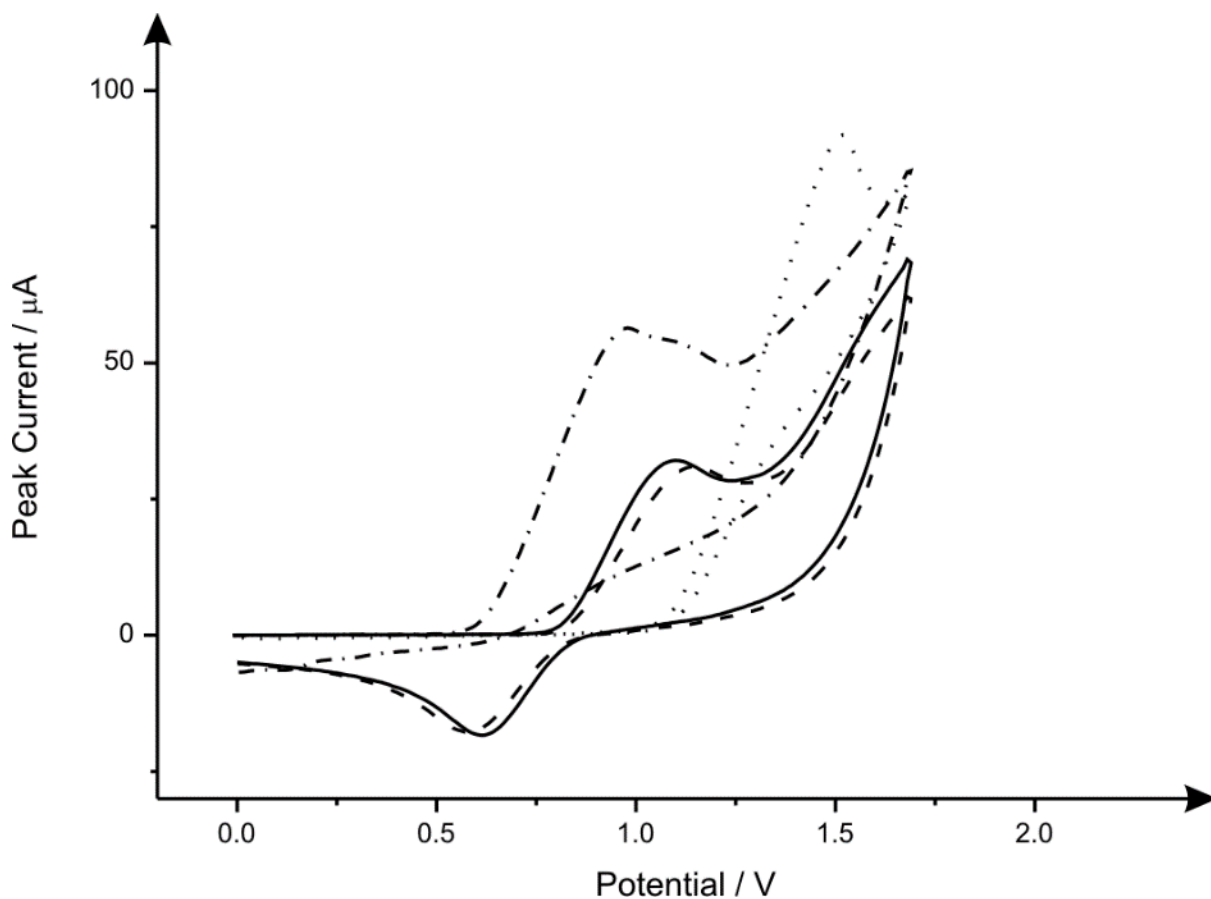


Figure 4-11 Comparison of the voltammetric profiles of 4-MMC (solid line), 4-MEC (dashed line), caffeine (dotted line) and benzocaine (dashed-dotted line) in 500 $\mu\text{g mL}^{-1}$ pH 2 buffer solution. Scan rate: 100mV s^{-1} vs. Ag/AgCl.

graphite electrodes in the pH range studied in this chapter.²⁰⁹ It is noted however, that if analytes were present in the solution together, in both pH 2 and 12, as would be expected when analysing a real sample of legal highs, an overlap of voltammetric waves would occur precluding the use of electrochemistry to be used as the basis of a legal high sensor.

4.2 Forensic Electrochemistry Applied to the Sensing of New Psychoactive Substances: Electroanalytical Sensing of Synthetic Cathinones and Analytical Validation in the Quantification of Seized Street Samples

Section 4.1 reported the first electrochemical method for the sensing of cathinone substitutes, methcathinone, mephedrone (4-MMC) and 4'-methyl-N-ethylcathinone (4-MEC) which were analysed with a scope to provide a potential on-the-spot analytical screening tool with graphite screen-printed electrodes.²⁰⁷ The effect of adulterants that are commonly incorporated into cathinone "legal high" explored and revealed voltammetric profiles that would undoubtedly interfere with the response of substituted cathinones if applied to a real street sample; as such this prior work cannot be easily applied to seized street samples.

In this section, inspired by Krishnaiah *et al.*²¹⁰ as well as other reports that electroanalytical signals have been improved through the use of bismuth modified electrodes (though not yet applied to the sensing of NPSs);²¹¹ the use of *in-situ* formed mercury and bismuth film modified graphite screen-printed electrodes are explored for the first time towards the sensing of the substituted cathinones namely 4-MMC and 4-MEC. While no significant improvements are observed using these film modified electrodes, the *direct* electrochemical reduction is found to be possible for the first time.

A novel electrochemical sensing protocol is proposed utilising disposable graphite screen-printed electrodes and offers a low cost, single-shot disposable yet highly reproducible and reliable sensing platform for a potential portable sensing approach for the detection of NPSs. Adulterants that are typically found in street samples are also electrochemically characterised for their potential interference in the simultaneous sensing of 4-MMC and 4-MEC and found to have no interference. This new electrochemical protocol as a tool is validated in seized street samples which are independently validated with LC-MS and HPLC showing excellent agreement and providing validation that the proposed electroanalytical approach can be used for the quantification of the synthetic cathinone products in seized street samples.

4.2.1 Exploring In-Situ Mercury and Bismuth Film Modified Screen-Printed Electrodes

First considered, in light of the inspiring work by Krishnaiah *et al.*²¹⁰ who reported electrochemical measurements of 4-MMC over the concentration range 2.7×10^{-4} - $1.8 \mu\text{g mL}^{-1}$ with a reported detection limit of $2.2 \times 10^{-3} \mu\text{g mL}^{-1}$ utilising a Dropping Mercury Electrode (DME), an *in-situ* formed mercury surface using Graphite Screen-Printed Electrodes (SPEs) were used in order to try and provide a potential alternative to the DME.

To accomplish this, mercury was formed *in-situ* through the addition of a mercury(II) salt into a pH 4.3 model acetate buffer, as reported previously in the literature.²¹²⁻²¹⁴ In this approach cyclic voltammetry is utilized where the potential is swept cathodically to electrochemically reduce the mercury (II) ions to mercury metal upon the GSPE surface. Figure 4-12 shows the typical electrochemical signatures. The use of *in-situ* formed bismuth modified electrode surfaces were also explored since this has been reported to be a 'green' alternative to mercury.^{215, 216} Similar to that of the *in-situ* formed mercury metallic surface, a bismuth(III) salt was utilised and consequently electrochemically reduced to form bismuth metal on the GSPE surface. As shown in Figure 4-12, the (independent) electrochemical reduction of both metals on GSPE using the aforementioned conditions is visible where the electrochemical deposition of mercury and bismuth metal occur through the application of the cathodic scan with stripping potentials at $\sim +0.1$ V and ~ -0.3 V (vs. *Ag/AgCl*) respectively, which is in agreement with current literature.²¹⁶

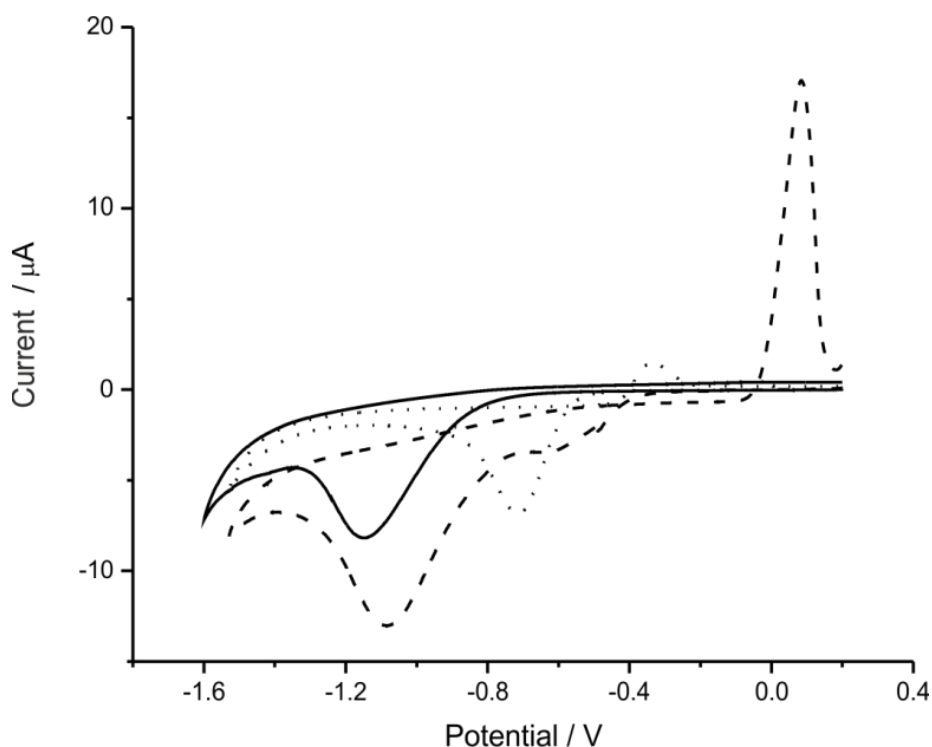


Figure 4-12 Cyclic voltammetric background responses in the absence (solid) and presence of mercury (II) (dashed line) and bismuth (III) (dotted line) recorded in an pH 4.3 acetate buffer using SPEs. The voltammetric scan is ran cathodically inducing the electrochemical deposition of mercury and bismuth metals (separately), visible as anodic peakss at $\sim +0.1$ V (vs. *Ag/AgCl*) and ~ -0.3 V (vs. *Ag/AgCl*) respectively. Scan rate: 50 mV s^{-1} (vs. *Ag/AgCl*).

The *in-situ* formed mercury and bismuth metal modified SPEs were tested towards the electrochemical detection of the “legal high” constituent 4-MMC. 4-MMC is able to be electrochemically reduced directly in pH 4.3 acetate buffer solution exhibiting a wave at $\approx -1.4\text{V}$, (vs. *Ag/AgCl*). Figure 4-13 shows the voltammetric profiles of each as well as a typical calibration plot with additions of 4-MMC made over the range $100 - 400 \mu\text{g mL}^{-1}$. In all cases there was a reduction peak $\approx -1.4\text{V}$ however, the difference in peak heights was marginal. The limit of detection (3σ) was determined to correspond to $28.61 \mu\text{g mL}^{-1}$

(4-MMC: $Ip/A = -0.06A/\mu\text{g mL}^{-1} - 6.89A$; $R^2 = 0.99$; $N = 6$);

$15.22 \mu\text{g mL}^{-1}$,

(Bismuth: $Ip/A = -0.07 \text{ A}/\mu\text{g mL}^{-1} - 1.95A$; $R^2 = 0.99$; $N = 6$);

And $38.45 \mu\text{g mL}^{-1}$,

(Mercury: $Ip/A = 0.05 \text{ A}/\mu\text{g mL}^{-1} - 7.031A$; $R^2 = 0.99$; $N = 6$);

For 4-MMC, 4-MMC with the *in-situ* formed bismuth film and 4-MMC with the *in-situ* formed mercury film respectively. It is indicative from this study that the *in-situ* mercury and bismuth film modified SPEs do not improve the electrochemical signal with respect to the sensing of 4-MMC. To demonstrate this further, a clear depiction of the reduction of 4-MMC on unmodified SPs is observed in Figure 4-14. Note the occurrence of a peak at ≈ 1.0 V in Figure 4-13/Figure 4-14 (and subsequent scans), as of yet the cause of this peak is indiscernible and requires further research to its cause.

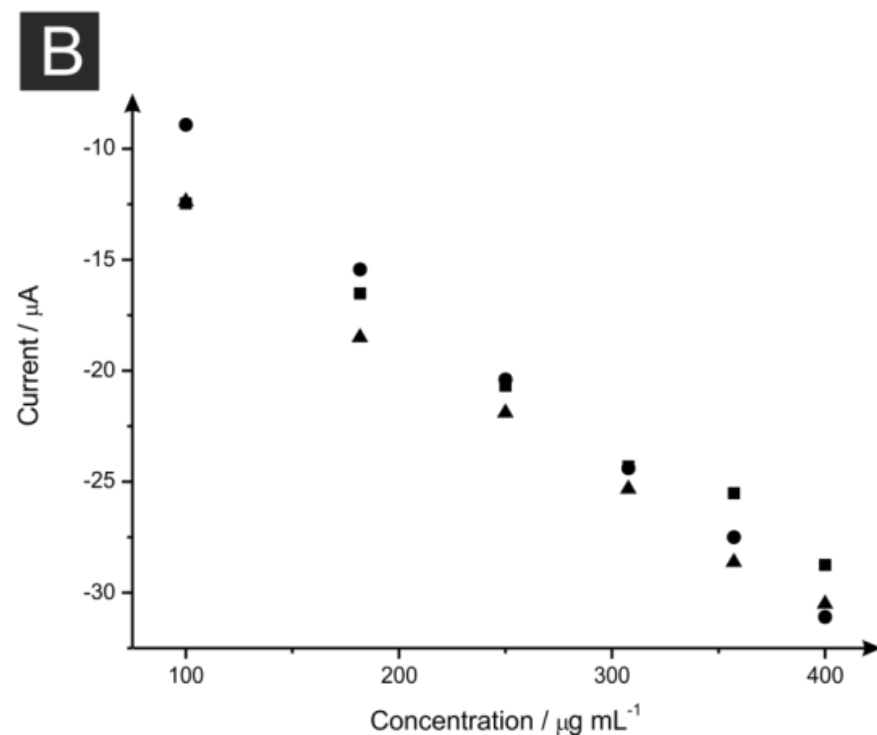
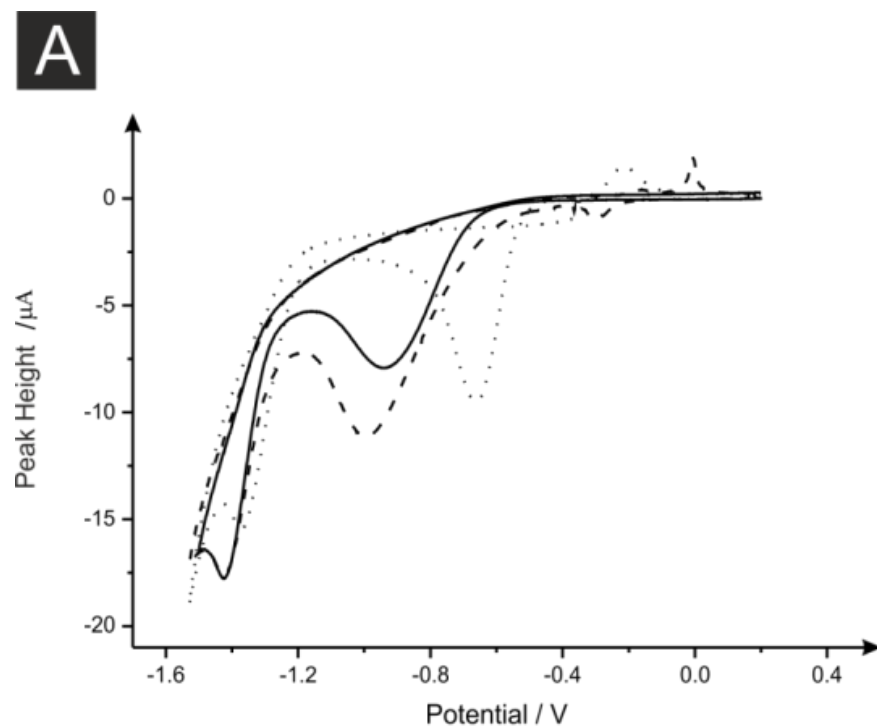


Figure 4-13 A: Voltammetric responses of acetate buffer in the presence of 4-MMC (solid line) using the *in-situ* formed mercury(II) (dashed line) and bismuth(III) film modified SPEs (dotted line) recorded in a pH 4.3 acetate buffer. Scan rate: 50 mV s⁻¹ (vs. Ag/AgCl) B: Typical calibration resulting from the analysis of the voltammetric signatures obtained in (A) in the form of a plot of peak height against 4-MMC concentration using SPEs in a pH 4.3 acetate buffer (triangles) and with the *in-situ* film formed mercury (squares) and bismuth (circles) over a linear range of 100 - 400 $\mu\text{g mL}^{-1}$. Note: a new SPE was utilised with each scan/addition. Scan rate: 50 mV s⁻¹ (vs. Ag/AgCl).

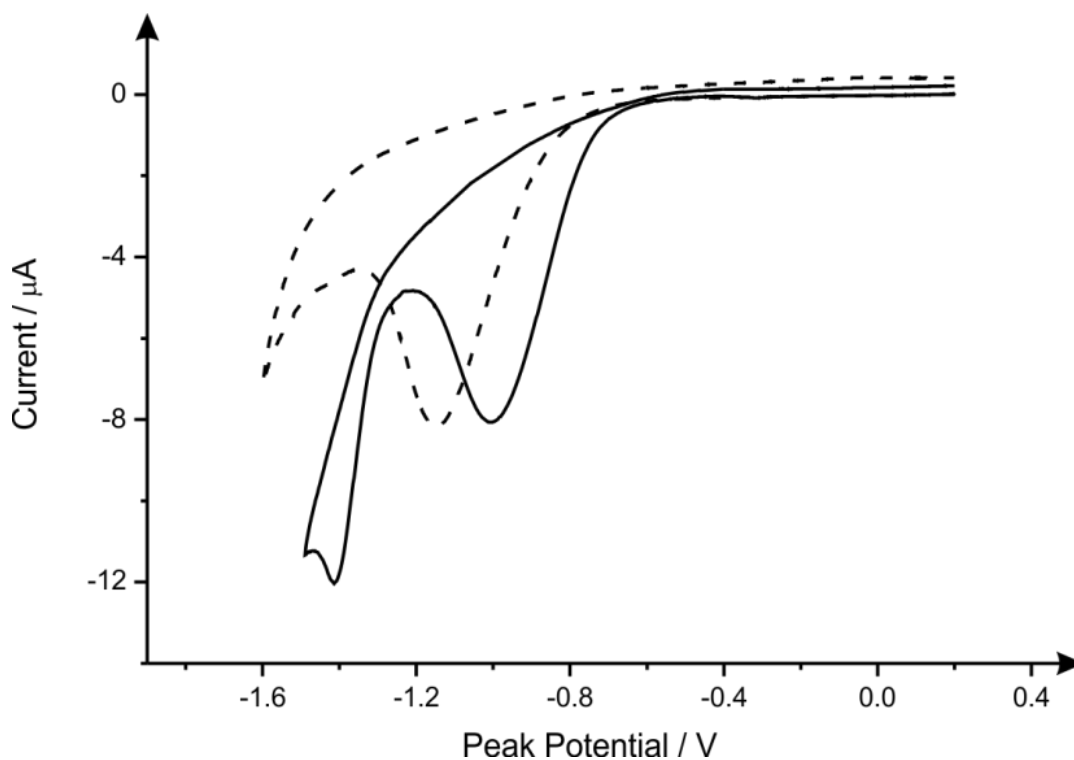


Figure 4-14 Typical cyclic voltammetric profiles recorded using SPEs in the presence (dashed line) and the absence (solid line) of $47.62 \mu\text{g mL}^{-1}$ 4-MMC. Experimental conditions: pH 4.3 Acetate buffer; Scan rate: 50 mV s^{-1} (vs. Ag/AgCl).

4.2.2 Direct electrochemical reduction of NPs 4-MMC and 4-MEC

Attention was now solely turned to improving the electrochemical performance of 4-MMC where the electrochemical reduction of 4-MMC in acetate buffer solutions was explored with a range of commercially available carbon based electrodes. Evident from the voltammetric profiles, as depicted in Figure 4-15, comparable electrochemical reduction overpotentials are observed using glassy carbon and SPEs. A more intense voltammetric peak is achieved with the GSPEs while no wave is visible for boron-doped diamond in the proposed scan range and is likely outside the accessible voltammetric window.

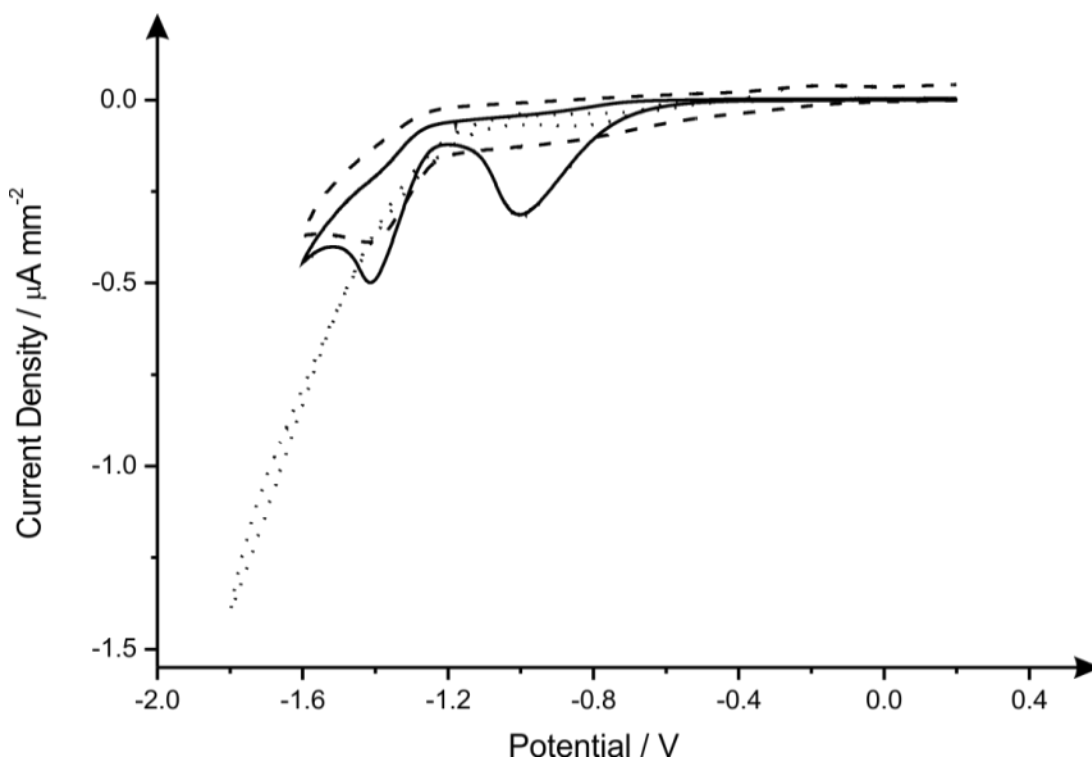


Figure 4-15 Cyclic voltammetric profiles recorded using a boron-doped (dotted), glassy carbon (dashed line) and SPEs (solid line) in $90.91 \mu\text{g mL}^{-1}$ 4-MMC, pH 4.3 acetate buffer. Scan rate: 50 mV s^{-1} (vs. Ag/AgCl).

Attention was turned to exploring the effect of the electrochemical reduction signal as a function of pH over the range of 2 - 12 where the reduction peak is observed to shift to more negative potentials with increasing pH. The reduction peak at pHs greater than 6, whilst having larger peak currents, have large overpotentials which is not desirable and pHs lower than 4 the peak current is low in intensity justifying the use of pH 4.3 acetate buffer solution for optimum sensing conditions. A plot of peak potential E_p/V vs. pH was constructed where a gradient of 0.033V was observed

$$(E_p/\text{V} = -0.033\text{V} - 1.30 \text{ E/p } R^2 = 0.87).$$

This value is indicative of an electrochemical process involving double the number of electrons over that of the protons (30 mV per pH unit at 25°C) as described from Equation 4-3. Where E_f^0 is the formal potential, n/m are the number of electrons/protons transferred in the rate determining step respectively, R the ideal gas constant, T temperature in Kelvin and F the Faraday constant.

Equation 4-3

$$E_{f,eff}^0 = E_f^0(A/B) - 2.303 \frac{mRT}{nF} pH$$

While the exact electrochemical mechanism is unknown, the electrochemical process likely involves 1 proton and 2 electrons. Future work will be focused to elucidate this however in light of the aforementioned results it can be said that it is unlikely to be a reduction of the carbonyl group present on mephedrone (Scheme 2-1 for reference) to a hydroxyl group which would involve 2 protons and 2 electrons. A lack of supporting research into the reduction of synthetic cathinones means at present nothing further can be proffered.

The analytical response of the promised sensing methodology was re-explored; *note* earlier the solutions comprised metal salts for the *in-situ* formation of the mercury and bismuth film modified electrode. To this end the analytical performance of 4-MMC using SPEs in model pH 4.3 acetate buffer solution was explored with additions made over the linear range 0.00 – 200.00 $\mu\text{g mL}^{-1}$ (Figure 4-16)

($Ip/A = -0.11 \text{ A}/\mu\text{g mL}^{-1} - 6.82\text{A}$; $R^2 = 0.95$; $N=10$).

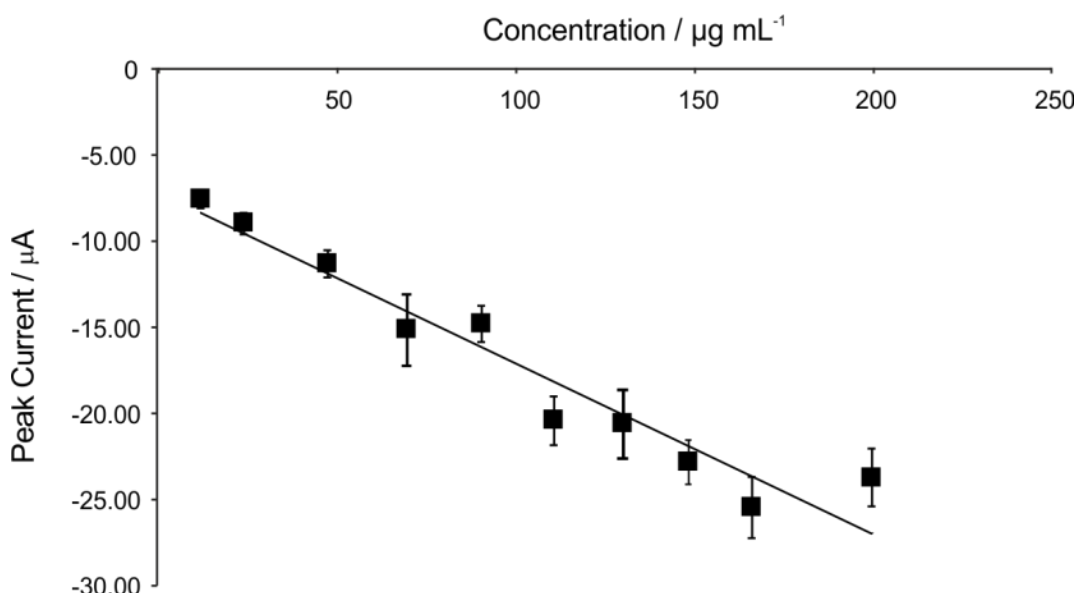


Figure 4-16 A calibration plot corresponding to the addition of 4-MMC into a model pH 4.3 acetate buffer solution over the concentration range 0.00 – 200.00 $\mu\text{g mL}^{-1}$ using a *new* SPE upon each addition. Also included are error bars ($N = 3$).

The limit of detection (3σ) was found to correspond to $11.80 \mu\text{g mL}^{-1}$ when compared to the value reported earlier of $28.61 \mu\text{g mL}^{-1}$ using SPEs.

Now attention was turned to another substituted cathinone commonly found in street samples - 4-MEC. The effect of the electrochemical reduction signal of 4-MEC as a function of pH over the range of 2 - 12 was investigated. As with 4-MMC, the reduction peak for 4-MEC ($\sim -1.4 \text{ V}$) is observed to shift to more negative potentials with increasing pH. A plot of $E_p / (\text{V})$ pH has a gradient of 0.029 mV again indicating a 1 proton and 2 electron process (according to Equation 4-3). Similarly the peak potential decreased with increasing scan rate with the plot of peak height against the square-root of scan rate was linear ($i_p/A = 108.6 \text{ A}(\text{V s}^{-1})^{-0.5} - 0.55 \text{ A}$; $R^2 = 0.98$) and therefore, again, a diffusional process. Additions of 4-MEC into pH 4.3 acetate buffer using SPEs, the corresponding calibration plot demonstrated a linear response (Figure 4-17)

($i_p/A = -0.07 \text{ A}/\mu\text{g mL}^{-1} - 10.04 \text{ A}$; $R^2 = 0.93$; $N=10$)

over the linear range $0.00 - 200.00 \mu\text{g mL}^{-1}$, the limit of detection (3σ) was found to correspond to $11.60 \mu\text{g mL}^{-1}$.

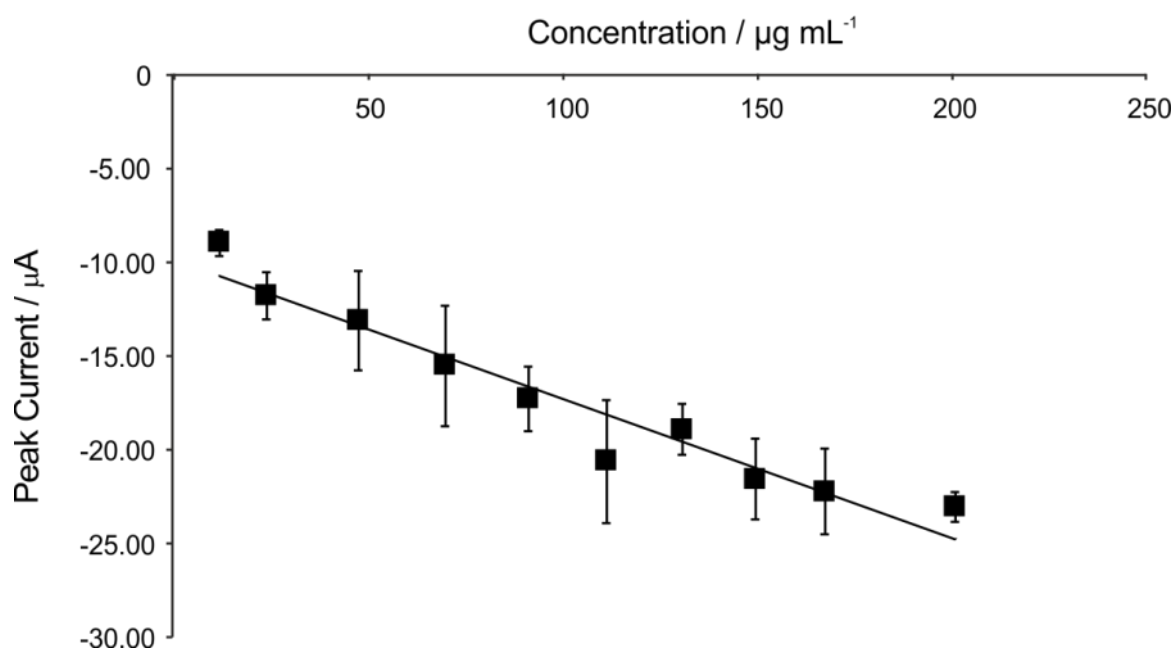


Figure 4-17 A calibration plot corresponding to the addition of 4-MEC into a model pH 4.3 acetate buffer solution over the concentration range $0.00 - 200.00 \mu\text{g mL}^{-1}$ using a *new* SPE upon each addition. Also included are error bars ($N = 3$).

A comparison of the typical responses of both 4-MMC and 4-MEC is observed in Figure 4-18, readily apparent is the similarity of the signals; with both peaks occurring at ≈ -1.5 V. Further work, such as adding a rapid microfluidic separation pre-treatment could be a potential solution to a more resolved signal, however for the use as an in-the-field on-site rapid qualification method this is more than apt.

Typically, street samples containing cathinones are 'cut' with adulterants such as caffeine and benzocaine. With this in mind, both caffeine and benzocaine's effect on the response in pH 4.3 acetate buffer was tested. *Note:* Benzocaine will not dissolve in pH 4.3 acetate buffer and requires 20% methanol to dissolve. Visible from Figure 4-19 is the adulterants' effect on the electrochemical response; caffeine shows little interference around the reduction overpotential for the substituted cathinones (~ 1.45 V vs. *Ag/AgCl*) however benzocaine has a considerable effect on the entire voltammetric waveform. Considering methanol is required to dissolve benzocaine, by simply dissolving samples into aqueous buffer solution without alcohol serves as a simple pre-treatment as the benzocaine is

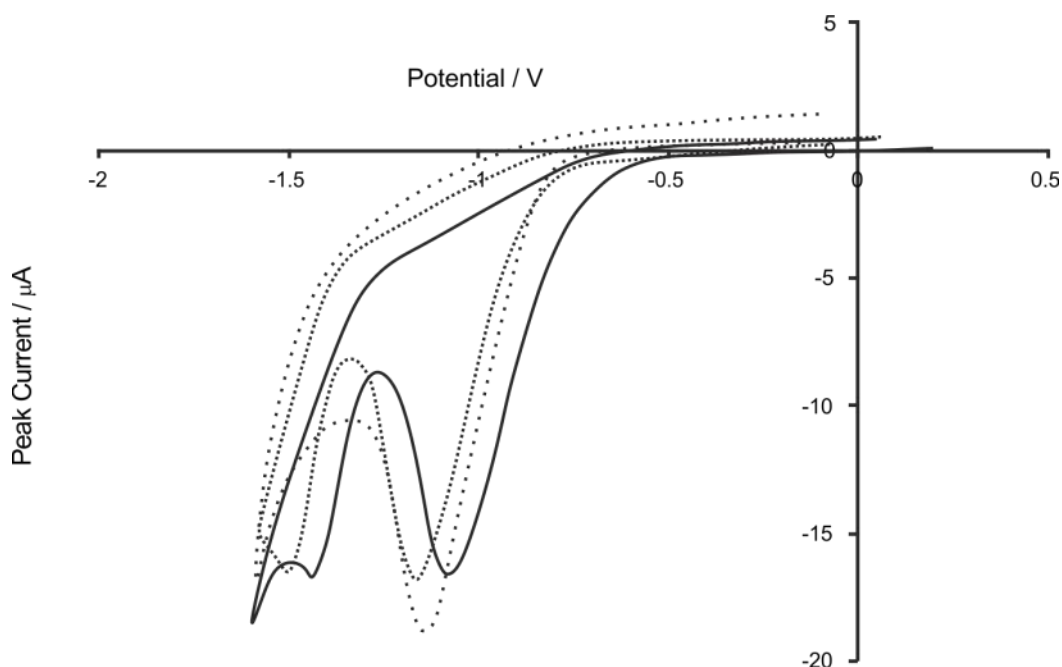


Figure 4-18 Cyclic voltammetric profiles recorded using an SPE in the absence (dashed) and presence of $90.91 \mu\text{g mL}^{-1}$ 4-MMC (solid) and $90.91 \mu\text{g mL}^{-1}$ 4-MEC (dotted line), pH 4.3 acetate buffer. Scan rate: 50 mV s^{-1} (vs. *Ag/AgCl*).

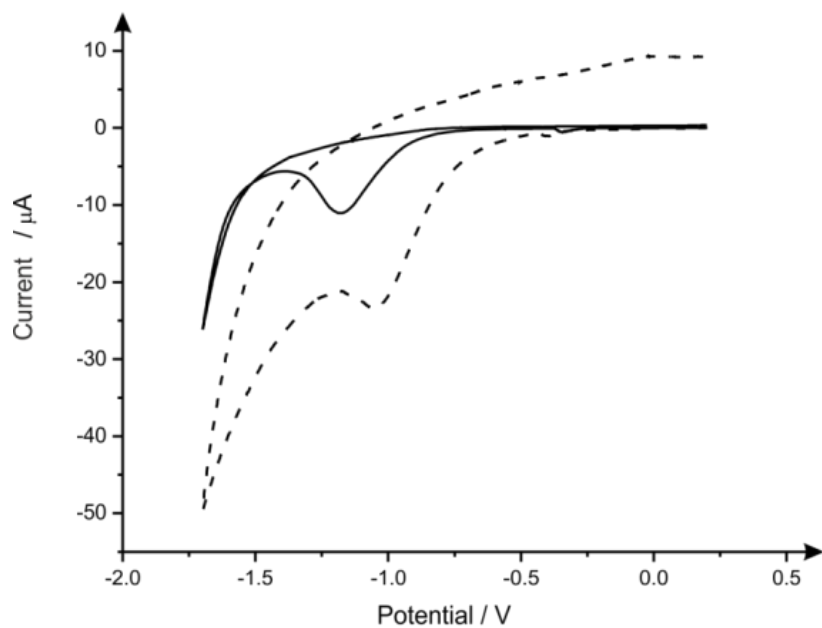
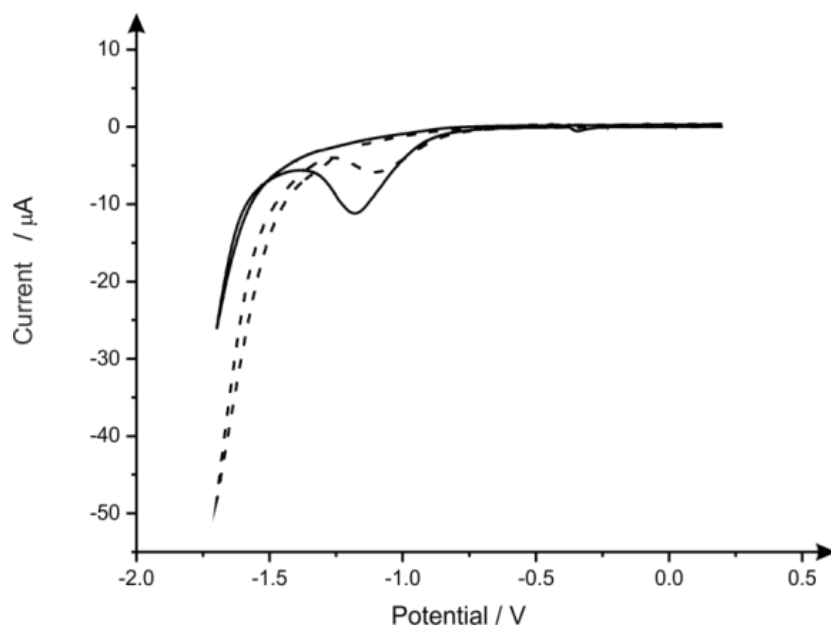
A**B**

Figure 4-19 Effect of common adulterants on the electrochemical response of pH 4.3 acetate buffer using SPEs. A: With (dashed line) and without (solid line) the presence of 1000 $\mu\text{g mL}^{-1}$ benzocaine. B: With (dashed line) and without (solid line) the presence of 1000 $\mu\text{g mL}^{-1}$ caffeine. Scan rate: 50 mV s^{-1} .

insoluble and can just be filtered off and the remaining constituents can be electroanalytically analysed; this becomes evident when applied into the sensing of NPSs in real samples (see below).

The limits of detection reported herein are an improvement on the values reported in our earlier work²⁰⁷ (13.2 $\mu\text{g mL}^{-1}$ for 4MMC and 36.3 $\mu\text{g mL}^{-1}$ for 4MEC) and are sufficient for use in-the-field as opposed to the lower as the values reported by Krishnaiah *et al.* which utilises a DME that is not suitable for use in-the-field and banned in many countries (see above).

4.2.3 HPLC and LC-MS analysis of seized street samples

Khreit *et al.* have reported the utilisation of HPLC and LC-MS techniques for the analysis of NRG-2 products.⁵⁹ The validated HPLC method (which can detect 4-MMC, 4-MEC and 4-MBC) at levels of 0.02 $\mu\text{g mL}^{-1}$) was expanded and re-validated to screen for these compounds in the presence of 4-FMC, MDPV, caffeine and benzocaine based on new intelligence received from law enforcement agencies.

A gradient elution programme was employed, to ensure both optimal detection of the analytes and a rapid analysis time. The five cathinone derivatives eluted at 4.9 (4-FMC), 6.6 (4-MMC), 7.2 (4-MEC), 8.4 (MDPV) and 10.8 (4-MBC) min respectively, with a slight peak tailing (asymmetry factor; $A_s \sim 1.2\text{--}1.7$) observed in each case.⁵⁹ Calibration standards were prepared and the strongly UV-absorbing components (4-FMC, 4-MMC, 4-MEC, 4-MBC, caffeine and benzocaine) demonstrated a linear response ($R^2 = 0.999 - 1$) over a 0.5 – 10.0 $\mu\text{g mL}^{-1}$ range with excellent repeatability (RSD = 0.014 – 0.799%; $N = 6$). The limits of detection for these components were determined as being in the range 0.03 - 0.25 $\mu\text{g mL}^{-1}$.⁵⁹ The method was also suitable for the detection and quantification of MDPV which exhibited a weaker UV response. MDPV demonstrated a linear response ($R^2 = 0.999$) over a 2.0 – 40.0 $\mu\text{g mL}^{-1}$ range with exceptional repeatability (RSD = 0.026 – 0.325%; $N = 6$) and the limit of detection was determined to be 0.12 $\mu\text{g mL}^{-1}$. The UV-inactive analytes (sucrose, mannitol and lactose) were shown not to interfere with the seven target analytes.⁵⁹ The limits of quantification were determined to be 0.36 (4-FMC), 0.14 (4-MMC), 0.09 (4-MEC),

0.36 (MDPV) and 0.41 $\mu\text{g mL}^{-1}$ (4-MBC) respectively, which is comparable to the previously reported method.⁵⁹

The four NRG-2 samples obtained from Internet vendors (January 2013) were all purported to be >99% pure and to contain 1 g of NRG-2. The samples were arbitrarily labelled NRG-2-A, NRG-2-B, NRG-2-C and NRG-2-D. Preliminary LC–MS analysis indicated that all four samples contained two components:

NRG-2-A: $t_R = 4.48$ min [minor], $m/z = 178.1$ [M+H]⁺; $t_R = 6.47$ min [major], $m/z = 166.2$ [M+H]⁺;

NRG-2-B: $t_R = 2.57$ min [minor], $m/z = 195.1$ [M+H]⁺; $t_R = 6.47$ min [major], $m/z = 166.2$ [M+H]⁺;

NRG-2-C: $t_R = 2.57$ min [major], $m/z = 195.1$ [M+H]⁺; $t_R = 5.34$ min [minor], $m/z = 192.2$ [M+H]⁺;

NRG-2-D: $t_R = 2.57$ min [major], $m/z = 195.1$ [M+H]⁺; $t_R = 4.48$ min [minor], $m/z = 178.1$ [M+H]⁺.

4.2.4 Application of the proposed electroanalytical protocol

With substantial evidence supporting an electroanalytical approach for detecting various substituted cathinones in street samples, the viability of the proposed protocol was tested. The “street” samples were re-analysed using the validated HPLC method at a concentration of 5 $\mu\text{g mL}^{-1}$. The results (Table 4-1) confirmed that all the samples only contained two components:

NRG-2-A: [minor, 4-MMC, 6.95% w/w, %RSD = 0.01%, $N = 3$] and [major, benzocaine, 93.87% w/w, %RSD = 0.01%, $N = 3$];

NRG-2-B: [minor, caffeine, 34.21% w/w, %RSD = 0.07%, $N = 3$] and [major, benzocaine, 68.77% w/w, %RSD = 0.06%, $N = 3$];

NRG-2-C: [major, caffeine, 76.03% w/w, %RSD = 0.05%, $N = 3$] and [minor, 4-MEC, 19.16% w/w, %RSD = 0.36%, $N = 3$];

NRG-2-D: [major, caffeine, 87.99% w/w, %RSD = 0.08%, $N = 3$] and [minor, 4-MMC, 11.15% w/w, %RSD = 0.07%, $N = 3$]).

The results of both LC-MS and HPLC analysis are shown in Table 4-1.

The effect of O_2 on the electrochemical signal was also explored (as it would be present in a real street sample). It was discovered that whilst having a detrimental effect on the limit of detection (3σ) (4-MMC: $13.2 \mu\text{g mL}^{-1}$ without degassing, $50.86 \mu\text{g mL}^{-1}$ when saturated with pure O_2) it is more than adequate for quantifying the synthetic cathinone constituent of the street sample. The effect of O_2 on a number of the scans is observed in Figure 4-20.

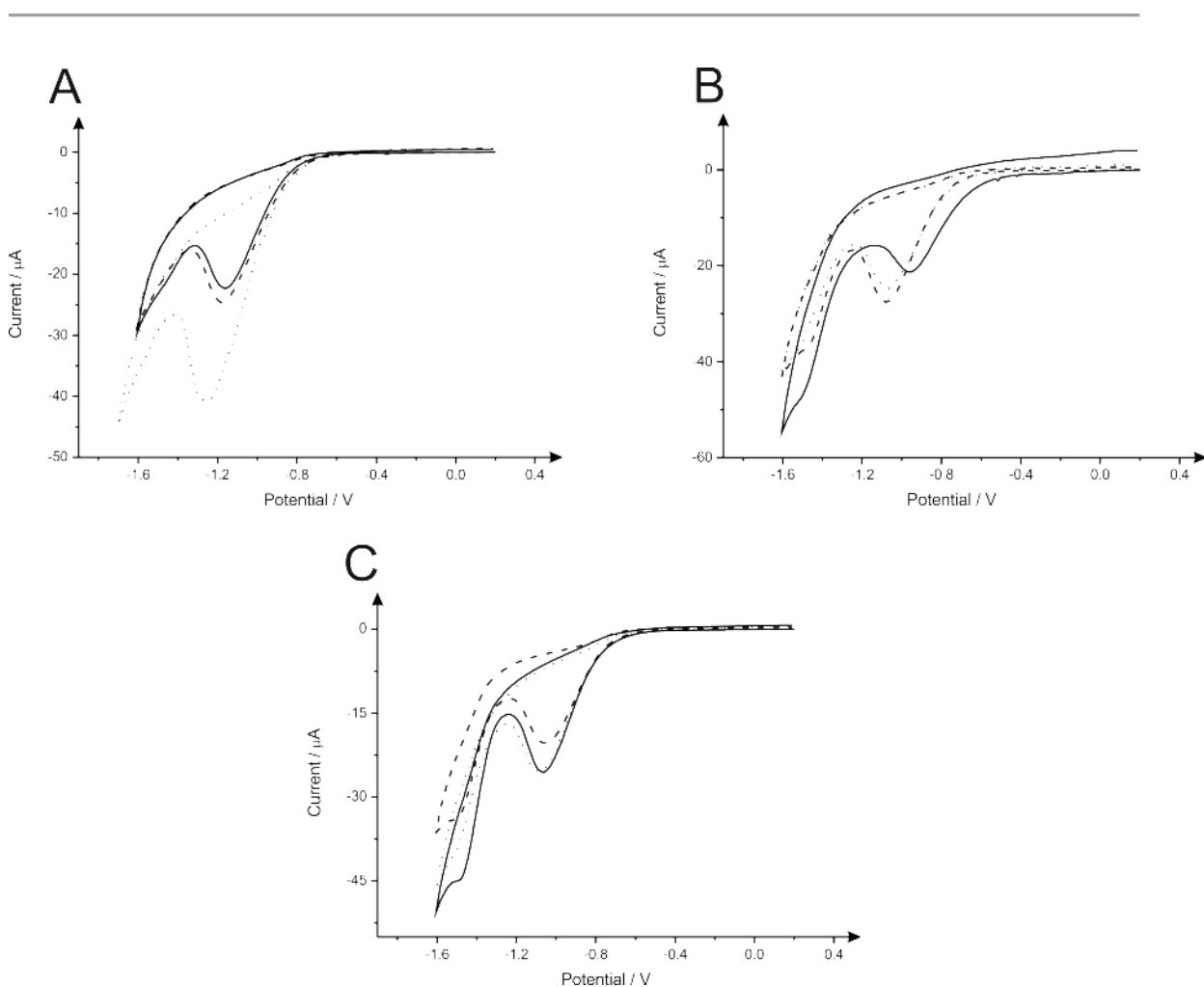


Figure 4-20 Cyclic voltammetric profiles recorded using SPEs in the presence of A: $12.35 \mu\text{g mL}^{-1}$ B: $148.94 \mu\text{g mL}^{-1}$ C: $200.00 \mu\text{g mL}^{-1}$ 4-MMC following being degassed with N_2 (solid line), un-changed (dashed) and saturated with O_2 (dotted). Scan rate: 50 mV s^{-1} (vs. Ag/AgCl).

Table 4-1 LC-MS and HPLC analysis of the purchased NRG-2 "street" samples.

Sample	LC-MS Analysis ($n = 3$)	HPLC Analysis ($n = 3$)	Notes
NRG-2-A	$t_R = 4.48$ min [minor], $m/z = 178.1$ [M+H] ⁺ ; $t_R = 6.47$ min [major], $m/z = 166.2$ [M+H] ⁺	$t_R = 6.6$ min [minor, 6.95% w/w, %RSD = 0.01%] and $t_R = 10.1$ min [major, 93.87% w/w, %RSD = 0.01%]	Sample contains benzocaine (93.87% w/w) and 4-MMC (6.95% w/w)
NRG-2-B	$t_R = 2.57$ min [minor], $m/z = 195.1$ [M+H] ⁺ ; $t_R = 6.47$ min [major], $m/z = 166.2$ [M+H] ⁺	$t_R = 5.2$ min [minor, 34.21% w/w, %RSD = 0.07%] and $t_R = 10.1$ min [major, 68.77% w/w, %RSD = 0.06%]	Sample contains caffeine (34.21% w/w) and benzocaine (68.77% w/w)
NRG-2-C	$t_R = 2.57$ min [major], $m/z = 195.1$ [M+H] ⁺ ; $t_R = 5.34$ min [minor], $m/z = 192.2$ [M+H] ⁺	$t_R = 5.2$ min [major, 76.03% w/w, %RSD = 0.05%] and $t_R = 7.2$ min [minor, 19.16% w/w, %RSD = 0.36%]	Sample contains caffeine (76.03% w/w) and 4-MEC (19.16% w/w)
NRG-2-D	$t_R = 2.57$ min [major], $m/z = 195.1$ [M+H] ⁺ ; $t_R = 4.48$ min [minor], $m/z = 178.1$ [M+H] ⁺	$t_R = 4.2$ min [major, 87.99% w/w, %RSD = 0.08%] and $t_R = 6.6$ min [minor, 11.15% w/w, %RSD = 0.07%]	Sample contains caffeine (87.99% w/w) and 4-MMC (11.15% w/w)

Unlike the NRG-2 samples that were analysed by Khreit *et al.*, three NRG-2 samples principally contained only benzocaine (NRG-2-A, 93.87% w/w) or caffeine (NRG-2-C and NRG-2-D, 76 – 88% w/w) in combination with small quantities (<20% w/w) of two controlled cathinones [4-MEC and/or 4-MMC]; whilst a single sample (NRG-2-B) only contains benzocaine and caffeine. These observations, however, are in agreement with the information reported by Brandt *et al.*³ who noted that many of these second-generation “legal high” products contained increased levels of commonly used diluents and adulterants.

A known amount of the street sample(s) was dissolved into pH 4.3 acetate buffer after which the electrochemical protocol was applied. In terms of NRG-2-B, the sample was filtered prior to testing (see below). Electrochemical interrogation of the samples revealed responses of samples NRG-2-A, -C and -D showed reduction peaks observed at $\approx -1.4\text{V}$ (vs. *Ag/AgCl*) which is attributed to the respective cathinones in each of the samples showing promise of a quantitative electroanalytical method for cathinones in street samples. Sample NRG-2-B showed the interference caused by benzocaine, which can be avoided if the sample is dissolved into solely aqueous buffer and no methanol is used. Example cyclic voltammograms of NRG-2-B (caffeine 34.21% w/w, benzocaine 68.77% w/w) and NRG-2-D (caffeine 76.03% w/w, 4-MEC 19.16% w/w) are visible in Figure 4-21.

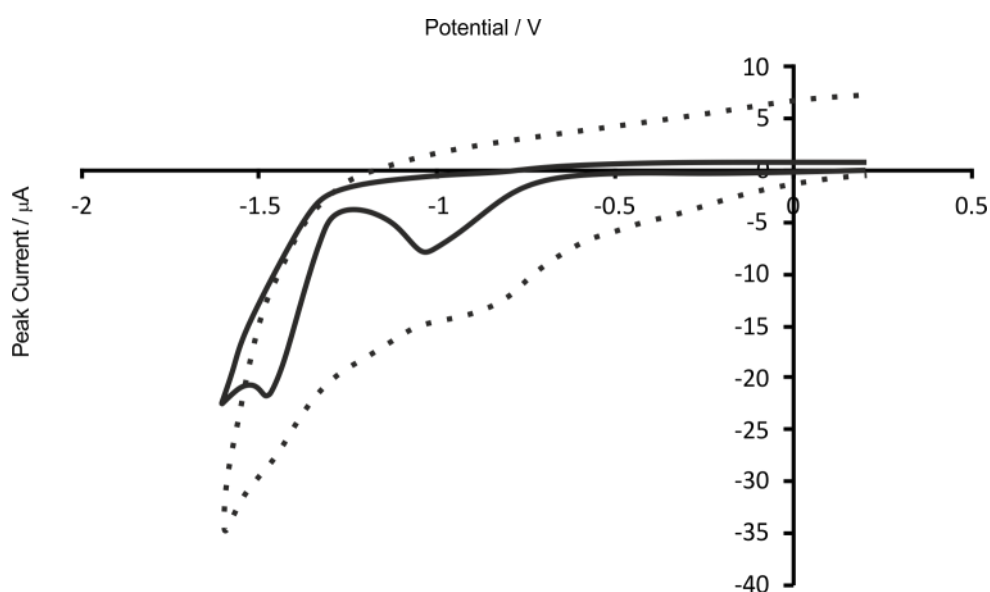


Figure 4-21 Typical cyclic voltammetric profiles of 1 mg mL⁻¹ NRG-2-B (caffeine 34.21% w/w, benzocaine 68.77% w/w) in pH 4.3 acetate buffer + 20% methanol (to dissolve benzocaine) and 1 mg mL⁻¹ NRG-2-D (caffeine 76.03% w/w, 4-MEC 19.16% w/w) in pH 4.3 acetate buffer. Scan rate: 50 mV s⁻¹ (vs. Ag/AgCl).

The benzocaine (insoluble in aqueous buffer), as previously mentioned, can be simply filtered off as a simple, fast, pre-treatment step. Following from this, the standard addition method was utilized in an attempt to quantify the amount of synthetic cathinone in obtained street samples using the proposed electrochemical protocol and is compared to HPLC. Table 4-2 overviews a comparison between quantification of serial street sample analysis via HPLC and the electrochemical technique proposed in this thesis (omitting NRG-2-B as it contains no synthetic cathinone product) where excellent agreement between the two analytical approaches is evident. Apparent from Table 4-2 and an unpaired student *t*-test the difference between the two approaches for the quantification of synthetic cathinone products 4-MMC and 4-MEC in seized street samples is considered to be not statistically significant (in agreement with 95% confidence limits).

A comparison of this method, compared to others in the literature for the analytical detection of 4-MMC (the more prevalent of the two) is featured in Table 4-3. Whilst the limits of detection (3σ) are greater than other methods, the benefits of this electrochemical protocol as a forensic approach are still readily apparent: rapid test time, cost effectiveness, safety, ease of use and portability whilst still providing adequate sensitivity for samples found in the field (Table 4-2) justify its utility.

To summarise there is no electrochemical report of the quantification of synthetic cathinones using graphite based electrochemical substrates that has been *successfully validated* in seized street samples with independent validation provided with HPLC and LC-MS demonstrating excellent agreement between our proposed electroanalytical protocol and that of “gold standard” laboratory based equipment. There is only one other electrochemical report using mercury based electrodes²¹⁰ which was not applied to seized street samples and since mercury is banned in many countries, it is very unlikely to be adopted either as a laboratory tool or in-the-field sensor.

Table 4-2 Direct comparison between quantification data collected from HPLC and the new proposed electrochemical protocol proposed for the analytical quantification of synthetic cathinones composition in a selection of seized street samples.

	HPLC / % w/w		Electrochemical / % w/w	
	4-MMC	4-MEC	4-MMC	4-MEC
NRG-2-A	6.95(±0.013)	-	8.03(±0.013)	-
NRG-2-C	-	19.16(±0.36)	-	18.75(±0.017)
NRG-2-D	11.15(±0.073)	-	11.32(±0.012)	-

Table 4-3 Comparison of the analytical methods for the detection of 4-MMC, emphasis added to the method presented in this thesis.

Analytical Method	Linear Range	Limit of Detection	Matrix	Reference
Gas chromatography–mass spectrometry with electron ionisation (GC–MS-EI)	-	0.2 mg L ⁻¹	Blood	57
High performance liquid chromatography (HPLC)	0.5–10 µg mL ⁻¹	0.1 µg mL ⁻¹	Mobile phase	58
Liquid chromatography-tandem mass spectrometry (LC-MS/MS)	-	2 ng mL ⁻¹	Mobile phase	66
Liquid chromatography-electrospray tandem mass spectrometry (LC-ESIMS/MS)	10-250 mg L ⁻¹	0.5-3 mg L ⁻¹	Blood	67
Surface enhanced Raman scattering (SERS)	0.1 – 100 µg mL ⁻¹	1.6 µg mL ⁻¹	Aqueous	87
Microcrystalline identification	0.1 - 10 g L ⁻¹	3 g L ⁻¹	Aqueous	147

Analytical Method	Linear Range	Limit of Detection	Matrix	Reference
Liquid chromatography-tandem mass spectrometry (LC-MS/MS)	5–100 µg/mg	2.5 µg/mg	Hair	217
High-performance liquid chromatography-diode array detection (HPLC-DAD)	25-2400 ng mL ⁻¹	40 ng mL ⁻¹	Urine	75
Differential pulse voltammetry – (electrochemical reduction of target analyte using mercury)	2.65 × 10 ⁻⁴ - 1.77 µg mL ⁻¹	2.21 × 10 ⁻³ µg mL ⁻¹ ¹	Aqueous buffer	198
This Method	0.00 – 200 µg mL⁻¹	11.80 µg mL⁻¹	Aqueous Buffer	-

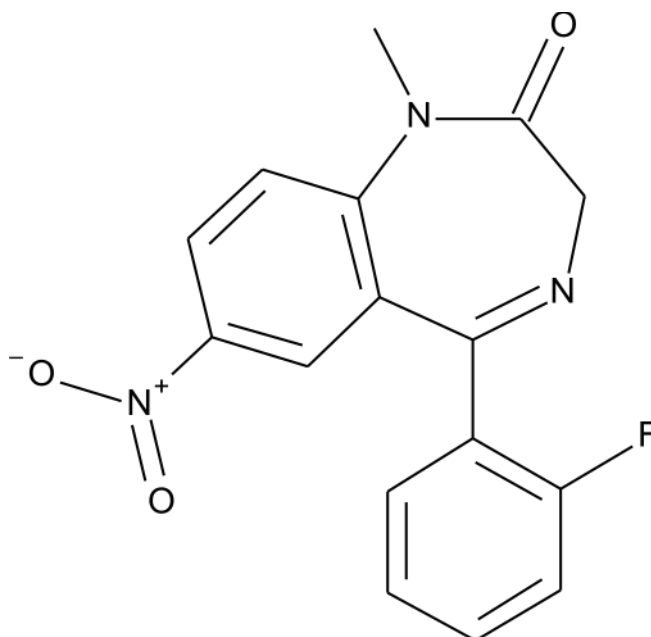
4.3 The electroanalytical sensing of Rohypnol® (Flunitrazepam) using Screen-Printed Graphite Electrodes without Recourse for Electrode or Sample Pre-treatment

Flunitrazepam, a benzodiazepine known better by the trade name Rohypnol® is a medicinal drug originally used as a potent sedative for the treatment of insomnia and is reported to be 10 times more potent than Valium (diazepam).^{218, 219} Due to these attributes, Rohypnol® is associated with “drug-facilitated sexual assault”.²²⁰⁻²²⁴ Rohypnol® when dissolved into solutions is colourless, odourless and tasteless.²²⁴ In a typical scenario, Rohypnol® is placed into alcoholic beverages of unsuspecting victims where the consumption of Rohypnol® and ethanol result in clinical manifestations of drowsiness, impaired psychomotor activity and anterograde amnesia.^{224, 225} Rohypnol® is usually spiked into alcoholic drinks above the recommended pharmacological dose of 0.5 - 1.0 mg in adults,²²⁶ with mild impairment coming around 2 mg, whilst with doses above 5 mg result in strong sedation and amnesia.²¹⁸ The effects of Rohypnol® are reported to greatly increase in combination with alcohol²¹⁸ with concentrations of 25 µg mL⁻¹ considered to be the minimum dosage to produce effects most often associated with cases involving drug facilitated sexual assaults.²²⁷

The clinical manifestations of Rohypnol® generally begin half an hour following ingestion and peak after approximately two hours. The following day the effects of the drug may be felt and include drowsiness, light-headedness, confusion and ataxia.²²⁸ The low dosage and high biotransformation of the drug makes its analysis very problematic since it is so rapidly metabolised and excreted from the body.²²⁶ Due to these unique effects of Rohypnol®, also known as ‘roofie’, it has been immortalised within the media, namely in the film ‘The Hangover’.

In this section the electrochemical response of disposable screen-printed graphite macroelectrodes for the sensing of Rohypnol® in aqueous solution (buffers) is explored as

well as in two well-known coloured commercial drinks: Coca Cola™ and the alcopop WKD. The structure of Rohypnol® (Flunitrazepam) is observed in Scheme 4-2.



Scheme 4-2 Chemical structure of Rohypnol® (Flunitrazepam)

4.3.1 Electrochemical Behaviour of Rohypnol®

First explored is the cyclic voltammetric behaviour of Rohypnol® in aqueous buffer solutions. Figure 4-22 depicts a typical voltammetric response obtained in pH 6 phosphate buffer using a screen-printed graphite electrode (SPE) in the absence and in the presence of Rohypnol®.

Inspection of the resultant cyclic voltammograms reveals the presence of three reduction peaks observed at -0.9 V, -1.3 V and -0.3 V respectively in order of potential cycling and a single oxidation peak at -0.2 V in addition to the reduction peak noted within the blank phosphate buffer solution at a potential of -1.1 V. This is in excellent agreement with previous literature where such electrochemical behaviour has been reported at different electrode materials including carbon fibre veil²²⁹ and glassy carbon electrodes.²³⁰

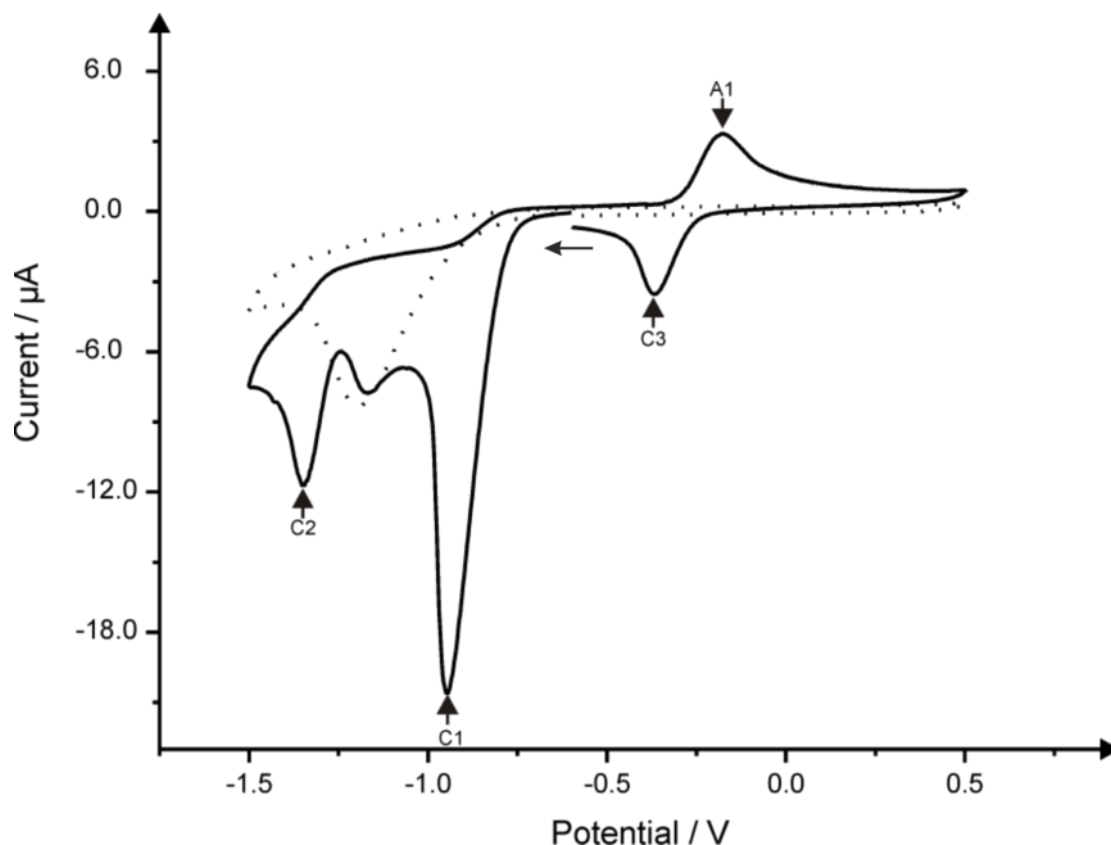


Figure 4-22 Cyclic voltammetric responses obtained in pH 6 phosphate buffer solution in the absence (dotted line) and presence (solid line) of $50 \mu\text{g mL}^{-1}$ Rohypnol[®] using a SPE. Scan rate: 100 mV s^{-1} .

It was found that the peak labelled A1 only appears once the cathodic scan to $\sim -1.5 \text{ V}$ has been performed and additionally the appearance of C3 is only evident once A1 has been achieved. The effect of the pH on the voltammetric response of the A1/C3 couple was explored as a function of pH over the range pH of 2 to 10.3 where the peak potential (E_p) of the A1/C3 couple was observed to shift to more negative potentials with increasing pH with a plot of peak potential against pH (Figure 4-23A) exhibiting a linear relationship

$$(E_p / \text{V} = -0.064 \text{ V/pH} + 0.269 \text{ V}; R^2 = 0.99);$$

with a gradient of 64.0 mV/pH indicating an equal proton and electron transfer.

From what is known in the literature on the chemistry of Rohypnol[®],²³¹ it is likely that the peak labelled C1 results from the $4e^-$, $4H^+$ reduction of the 7-nitro group to hydroxylamine

with an associated loss of water as described by

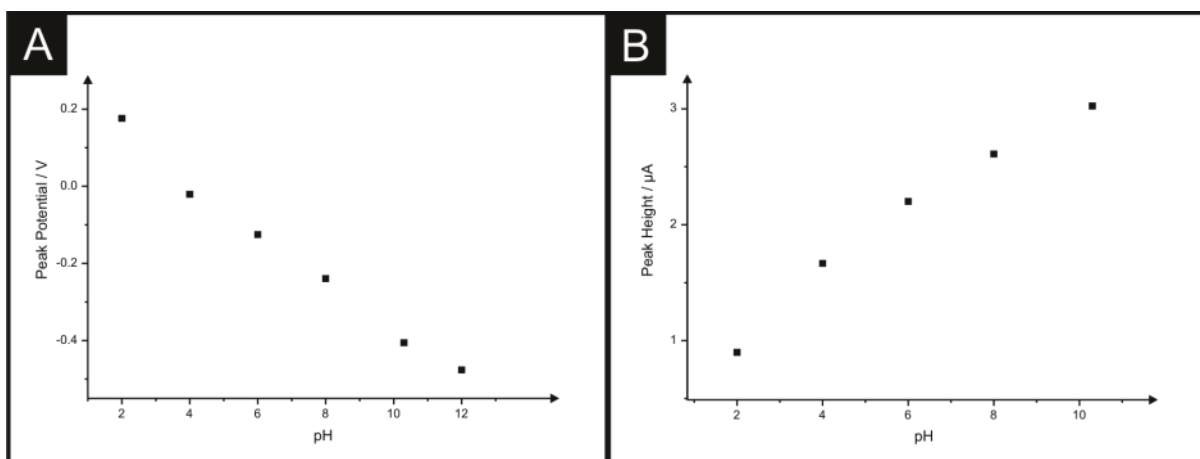


Figure 4-23 A: A plot of peak potential, E_P (A1), as a function of pH for the electrochemical oxidation of $125 \mu\text{g mL}^{-1}$ Rohypnol[®] using a SPE and the. Scan rate: 100 mV s^{-1} . B: A plot of peak height, I_P (A1), as a function of pH for the electrochemical oxidation of $125 \mu\text{g mL}^{-1}$ Rohypnol[®] using a SPE and the. Scan rate: 100 mV s^{-1} .

Equation 4-4.

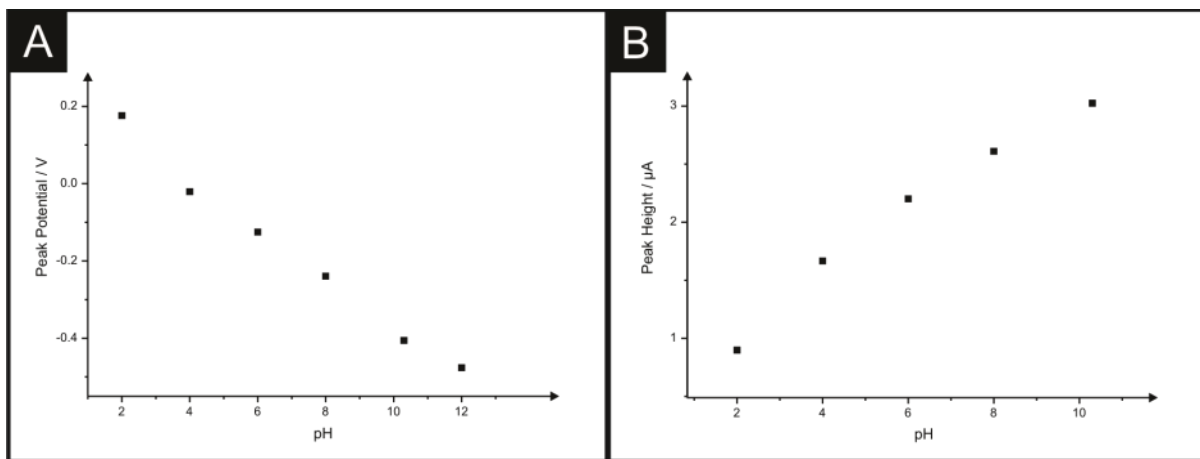
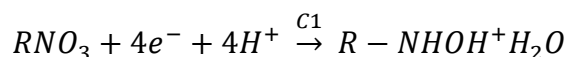


Figure 4-23 A: A plot of peak potential, E_P (A1), as a function of pH for the electrochemical oxidation of $125 \mu\text{g mL}^{-1}$ Rohypnol[®] using a SPE and the. Scan rate: 100 mV s^{-1} . B: A plot of peak height, I_P (A1), as a function of pH for the electrochemical oxidation of $125 \mu\text{g mL}^{-1}$ Rohypnol[®] using a SPE and the. Scan rate: 100 mV s^{-1} .

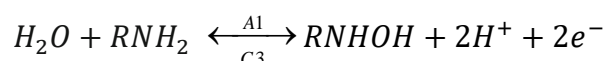
Equation 4-4



Equation 4-5



Equation 4-6



As is seen in Figure 4-22, the peak labelled C2 likely results from the $2e^-$, $2H^+$ reduction of the formed hydroxylamine group as described by Equation 4-5 to the analogous amine. On the return voltammetric positive scan an oxidation peak (A1) is observed, likely resulting from the oxidation of the amine to the hydroxylamine which is reduced (C3) to the amine, as described by Equation 4-6. The hydroxylamine as formed *via* Equation 4-5 now is likely adsorbed on the surface of the SPE which might explain the observation of different potentials ($E_{C3} \neq E_{C2}$), where E_{C3} demands a lower activation energy since hydroxylamine is adsorbed on the surface and at lower overpotential compared to C2 (Equation 4-6). This is all further confirmed with the 7-amino analogue cyclic voltammogram (Figure 4-24), which lacks a $-NO_2$ moiety, and hence no reduction waves are observed but however, the A1/C3 redox couple is still observed, likely corresponding to the electrochemical process described in Equation 4-6.

7-aminoflunitrazepam is a pharmacologically-active metabolite of Rohypnol® and as an *in-vitro* degradation product, is useful for confirmation of Rohypnol® ingestion. Consequently, in postmortem specimens, the Rohypnol® may have been entirely metabolised over time to 7-aminoflunitrazepam making this a critical analyte in such instances.²³²⁻²³⁴ When concentrating on the utilisation of Rohypnol® for the spiking of drinks and the consequential confirmation of such activities using a drink sample, the monitoring of the metabolite 7-aminoflunitrazepam is devoid of purpose and as such has not been further investigated within the study at hand.

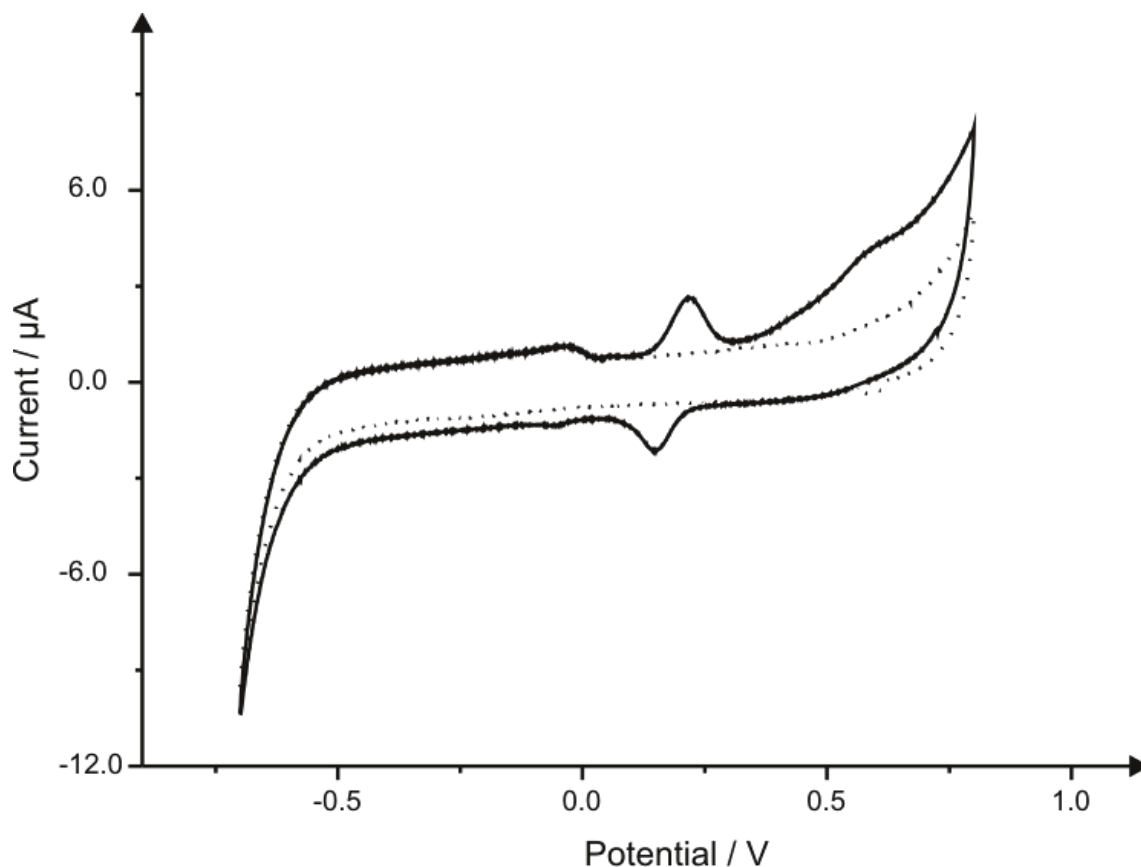


Figure 4-24 Cyclic voltammetric responses obtained in pH 6 phosphate buffer solution in the absence (dotted line) and presence (solid line) of $0.3 \mu\text{g/mL}$ 7-aminoflunitrazepam using a SPE. Scan rate: 100 mV s^{-1}

Figure 4-23B also depicts the voltammetric peak height recorded at a fixed concentration of $125 \mu\text{g mL}^{-1}$ over the pH range studied. Evidently, upon increasing the pH an increase in the voltammetric peak observed (A1) occurs, suggesting that more favourable voltammetric responses would be attained at higher pHs. Although this would appear to be contrary to the speculated mechanism, at such low concentrations the availability of protons may not present an hindrance to the reaction. Crucially however, such high pHs are not generally relevant with the sensing of analytes in beverage samples as is intended in this purpose, with such samples tending to be more acidic in nature.

From an analytical perspective, the peaks labelled A1/C3 are the optimal choice since these occur at facile voltammetric potentials close to $+0.0 \text{ V}$, where the possibility from interferences, such as O_2 , is greatly reduced when applied to real samples. Consequently, the reversible peak (A1/C3) is used as the analytical signal, the precluding reduction of C1 and C2 is still performed however not shown for simplicity. The electroanalytical method

was explored further through additions of Rohypnol® in a pH 2 phosphate buffer using the SPEs; Figure 4-25 depicts the observed response. The solution pH of 2 was chosen herein for analytical measurements due to the intended application of the sensor into the monitoring of Rohypnol® in beverages which are often acidic in nature (see later). Additionally, as a result of this transition in pH to a more acidic value the recorded voltammetric peaks: C1, 2, 3 and A1 shift to more electrochemically facile potentials of – 0.56 V, - 1.0 V, + 0.03 V and + 0.13 V respectively.

As is depicted in Figure 4-25A the oxidation peak observed at $\sim + 0.13$ V increases in magnitude upon the addition of Rohypnol®. The corresponding calibration plot (Figure 4-25B) demonstrates the linear response observed

$$(I/\mu A = 3.79 \times 10^{-2} \mu A/\mu g \text{ mL}^{-1} + 1.78 \times 10^{-1} \mu A, R^2 = 0.99);$$

Over the analytical range studied ($1 - 95.24 \mu\text{g mL}^{-1}$). It is critical to note that although as described within the Experimental Section (Chapter 3) all solutions were degassed prior to analysis, further studies determined with matching calibration plots were obtained with or *without* prior degassing; this is a critical parameter as the intended application envisages that a sample of the potentially adulterated drink beverage is

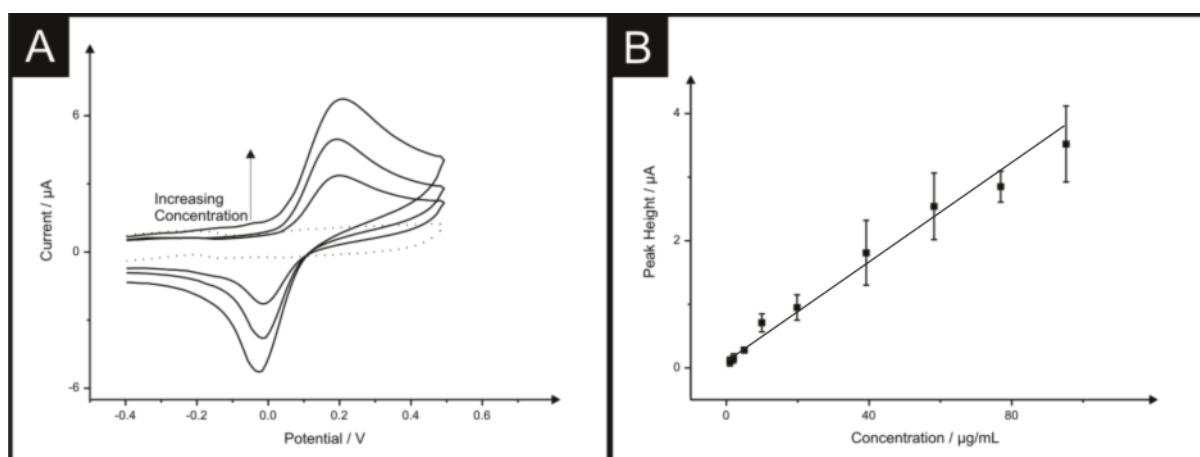


Figure 4-25 Cyclic voltammetric responses obtained in pH 6 phosphate buffer solution in the absence (dotted line) of Rohypnol® and in the presence (solid line) of Rohypnol® ranging from $1 \mu\text{g mL}^{-1}$ to $95.2 \mu\text{g mL}^{-1}$ (39.2 , 76.9 and $95.2 \mu\text{g mL}^{-1}$ depicted) using a *new* SPE upon each addition. Scan rate: 100 mV s^{-1} B: Typical corresponding calibration plot with error bars ($N = 3$).

Simply put onto the electrode (or the electrode is dipped into the suspected beverage) with the voltammetric measurement run allowing the screening of beverages to be readily

achieved. The limit of detection (3σ) for Rohypnol® utilising the SPE was determined to correspond to $0.47 \mu\text{g mL}^{-1}$. While other techniques may offer improved limits of quantification and detection, our results are well within the dosage range from minimal clinical effects to those found in drug-facilitated crime cases whilst offering exceptionally rapid testing times in addition to the possibility of on-site determination through the coupling of electrochemical techniques with disposable screen-printed sensors.

4.3.2 Application of the Proposed Electroanalytical Protocol

Following confirmation that successful cyclic voltammetric determination of Rohypnol® was possible using the SPE under ideal conditions utilising a standard pH 2 phosphate buffer, the viability of the analytical protocol was tested towards detection within analytically relevant media. First attention was turned to exploring the analytical sensing of Rohypnol® in Coca Cola™; closely related to its determination in Pepsi Max as reported by Honeychurch and co-workers, though in this instance in addition to complex analytical procedures including the use of liquid chromatography with dual electrode detection, extensive sample preparation was essential prior to analysis of beverage-based samples such as pH modification for example.²²⁹ Under the same conditions detailed section 4.3.1 (degassed, new electrode per scan, 100 mV s^{-1}), additions were made into the Coca Cola™ solution over the concentration range of 1 to $245.6 \mu\text{g mL}^{-1}$ measured using the SPEs. This concentration range of Rohypnol® was selected which, whilst not encompassing ultra-low concentrations as demonstrated to be possible utilising some analytical techniques, does cover those relevant to the intended application for the sensing of Rohypnol® in beverages where concentrations of $25 \mu\text{g mL}^{-1}$ is considered the minimum dosage to produce effects most often associated with cases involving drug facilitated sexual assaults using Rohypnol®.²²⁷ Note, during measurement a new SPE was utilised upon each addition of Rohypnol®. As is shown in Figure 4-26, the calibration plot resulting from the addition of Rohypnol® is linear over the entire concentration range

$$(I/\mu\text{A} = 4.49 \times 10^{-2} \mu\text{A}/\mu\text{g mL}^{-1} - 3.25 \times 10^{-1} \mu\text{A}, R^2 = 0.97).$$

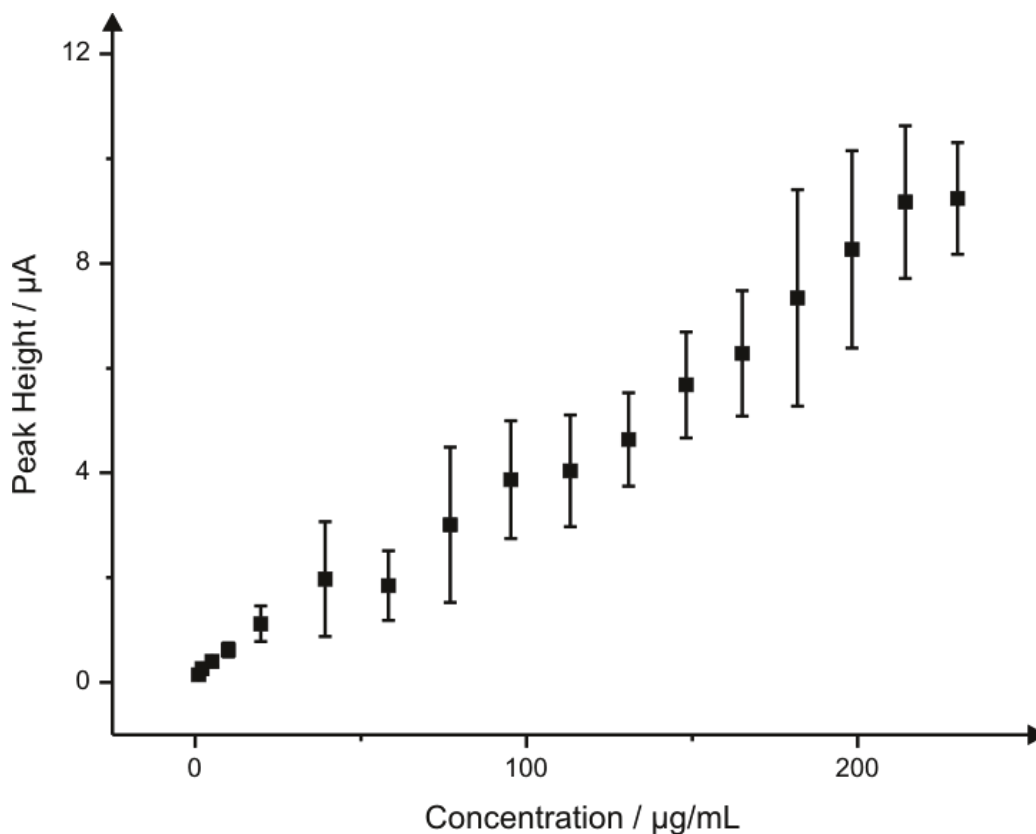


Figure 4-26 A calibration plot corresponding to the addition of Rohypnol[®] into an unmodified Coca Cola[™] solution over the concentration range 1 – 245.6 $\mu\text{g mL}^{-1}$ using a *new* SPE upon each addition. Also included are error bars ($N = 3$).

Note that the reproducibility of the proposed analytical methodology is shown in the form of the average response and standard deviation over the analytical range studied. Due to the electrochemical mechanism involving an adsorbed electrochemically generated species, the %RSD are somewhat higher than would usually be expected and in-fact the batch is highly reproducible as found using a common outer-sphere redox probe. However, the analytical protocol is still useful as we envisage that these sensors would be used on-site where a suspected adulterated beverage would be screened. Returning to the observed analytical response, a limit of detection (3σ) of $1.09 \mu\text{g mL}^{-1}$ was determined for the monitoring of Rohypnol[®] in Coca Cola[™]. Critically the Coca Cola[™] solution utilised was not modified in any way prior to use thus highlighting the truly useful nature of the analytical protocol when utilised for real-world applications.

In comparison with other analytical protocols (summarised in reported for the sensing of Rohypnol[®] in drinks the limit of detection offered by the electroanalytical method utilising

SPEs was found to be competitive. Chen *et al.*²¹⁸ report the detection of Rohypnol® in alcoholic beverages using Desorption Electrospray Ionization-Mass Spectrometry providing a limit of quantification of 3 µg mL⁻¹. Additionally, fluorescence Spectroscopy was reported to allow for a limit of detection of ~1.0 µg mL⁻¹ within a colourless alcoholic beverage, which was determined to equate to approximately one-fourth a Rohypnol tablet in 250 mL spirit.²³⁵ Evidently such a limit of detection is comparable to that obtained when utilising the SPE, however unlike fluorescence techniques, the electrochemical methodology does not suffer from colour interference and as such can be applied into coloured drinks as demonstrated herein. It is important to note that as reported by Honeychurch *et al.*²²⁹ lower limits of detection of 20 ng mL⁻¹ of Rohypnol® in a similar caffeine based drink (Pepsi Max™) is possible through utilisation of Liquid Chromatography with dial electrode detection, though as such a protocol title would suggest such methods are not portable and also much more time consuming than that reported herein.²²⁹

Finally, after successful determination of Rohypnol® within an unmodified soft drink (Coca Cola™) we turn to exploring the voltammetric response of the Rohypnol® in a sample alcoholic beverage: WKD. WKD is a brand of alcopop which is sold and heavily marketed in the United Kingdom with the slogan 'Have you got a WKD side?' (Have you got a wicked side?), and also in many countries in mainland Europe. Furthermore AC Nielsen, a leading information and measurement company providing market research and insights into customer behaviour ranked it as the number-one UK ready-to-drink brand in 2006.²³⁶ A linear response is observed ($I/\mu A = 5.69 \times 10^{-2} \mu A/\mu g mL^{-1} - 7.83 \times 10^{-1} \mu A$, R² = 0.96) over the large concentration range of 1 to 245.61 µg mL⁻¹ studied with only minor deviations from linearity being observed (Figure 4-27). A limit of detection (3σ) of 2.03 µg mL⁻¹ was determined for the monitoring of Rohypnol® in WKD. Critically, as was the case with the Coca Cola™ solution, no prior preparation or modification of the test solution was required.

Analytical Method	Analytical Linear Range	Limit of Detection	Matrix	Reference
Gas chromatography – Mass spectrometry (GC-MS)	-	0.1 pg/mL	Oral saliva	237
Liquid chromatography – Atmospheric pressure chemical ionization mass spectrometry	1 – 500 µg/L	0.2 ng/mL	Human serum	238
HPLC – UV Vis	-	1 ng/mL	Human serum	239
Fluorescence spectroscopy	0 – 5 mg/L	1 ng/mL	Beverage	235

Analytical Method	Analytical Linear Range	Limit of Detection	Matrix	Reference
High pressure liquid chromatography – Multi wave	0.01 – 5 mg/L	5 ng/mL	Human serum	240
High pressure liquid chromatography – Dual electrode detection	0 – 1 mg/L	20 ng/mL	Beverage	229
This work	1 – 95.24 µg/mL	0.47 µg/mL	Buffer, Beverage	
Desorption electrospray ionization - Mass spectrometry	3 – 20 µg/mL	3 µg/mL	Beverage	218
Gas chromatography – Electron capture	25 – 300 ng/mL	1mg/mL	Human serum	241

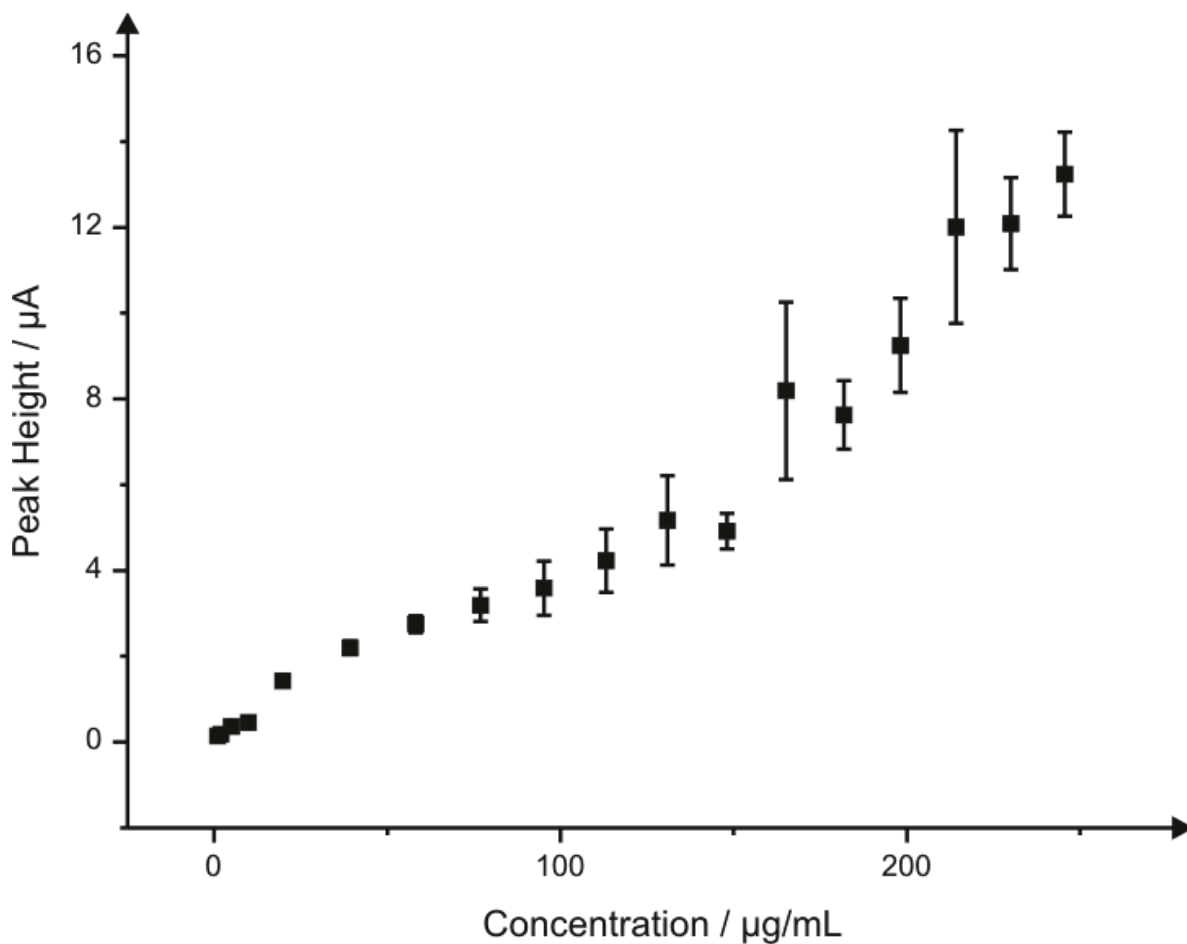


Figure 4-27 A calibration plot corresponding to the addition of Rohypnol® into an unmodified WKD alcopop solution over the concentration range 1 – 245.6 $\mu\text{g mL}^{-1}$ using a *new* SPE upon each addition. Also included are error bars ($N = 3$).

The successful application of the SPE sensor for the determination of Rohypnol® into unmodified soft and alcoholic drinks, particularly those which may result in unsuccessful colour change warnings due to their already coloured nature, holds great promise and potential for the application of the protocol into the determination of such drug contamination in the field offering a truly novel, rapid and portable analytical protocol thanks to the combination of both screen printing and electrochemical technology.

Work featured in this chapter has featured in a number of articles: J. P. Smith, J. P. Metters, C. Irving, O. B. Sutcliffe and C. E. Banks, *Analyst*, 2014, **139**, 389-400., J. P. Smith, J. P. Metters, O. I. G. Khreit, O. B. Sutcliffe and C. E. Banks, *Anal. Chem.*, 2014, **86**, 9985-9992. and

J. P. Smith, J. P. Metters, D. K. Kampouris, C. Lledo-Fernandez, O. B. Sutcliffe and C. E. Banks, *Analyst*, 2013, **138**, 6185-6191. The next chapter takes the concept of *Forensic Electrochemistry* further by exploring other materials which can be utilised as portable sensors in-the-field in a forensic environment.

Chapter 5 Exploration of New Materials for Electrochemical Detection

Following the success of graphene based screen-printed electrodes in Chapter 4, new materials were explored to appraise their utility as an electro-analytical sensor in a hope to yield improved sensitivity and selectivity towards drugs of abuse. The following chapter evaluates the 2d material graphene as a screen-printed electrode material whilst also showing proof-of-concept with the use of British currency (GBP) as an electrode material.

5.1 Exploring Graphene as an Alternative Screen-Printed Electrode Material

Graphene is being widely explored in a plethora of technical applications due to its reported beneficial properties. One promising application is an electrode substrate for sensing applications, energy storage and generation.^{242, 243}

In terms of employing graphene as an electrode material, a major experimental obstacle is the electrical ‘wiring’ of the graphene to allow it to be utilised efficiently as an electrode substrate. The widely adopted approach is to drop-cast aliquots of a graphene suspension onto an electrode surface, such that one immobilises graphene and effectively averages the total response over that of the graphene domains.^{244, 245} However, careful modification is required in order that the underlying electrode surface is not exposed which can potentially influence and dominate the observed electrochemistry. Additionally, in some cases a graphene “coffee-ring” effect can leave concentrated zones of graphene at the edges of the electrode surface in addition to areas where there is little or no graphene coverage.²⁴⁵ The result of this is uneven graphene distribution effectively leaving areas of both fast (multilayer graphene) and slow (single layer graphene) electron transfer^{246, 247} and thus an electrochemically heterogeneous surface. Furthermore it has been demonstrated that different impurities, resulting from the way the graphene was produced, such as

surfactants, carbonaceous substances and metallic impurities can influence the electrochemical performance.^{245, 247} With graphene prepared from synthetic or natural graphite, there are impurities due to the presence of impurities in the starting graphite.^{62, 248} Alternatively techniques such as using permanganate to treat graphite during graphene preparation introduces the impurity MnO^{195} or redox active impurities can be introduced by un-scrolling carbon nanotubes (essentially rolled up graphene).²⁴⁹ Lastly, there is also Chemical vapour deposition (CVD) grown graphene which contains electroactive impurities,²⁵⁰ all of these various impurities are giving rise to false claims of electrocatalysis due to graphene.^{62, 243, 248, 251}

There are numerous approaches to overcome the limitations identified above whilst allowing for graphene to be implemented from the laboratory into-the-field; electrode fabrication *via* inkjet printing²⁵² and screen-printing²⁵³ have been developed to potentially facilitate the mass-production of graphene electrodes which are cost-effective and exhibit electrochemically reproducible responses. In the latter case it has recently been reported, for the first time, the fabrication of true graphene screen-printed electrodes (SPEs) utilising two different commercially prepared 'graphene' inks which have long screen ink 'lifetimes' (>3 hours). The work demonstrated a proof-of-concept for the mass-production of graphene sensing platforms.²⁵³ In this section, it is shown that the electrochemical response of graphene SPEs can be dominated by metallic impurities rather than the graphene itself; such work is of importance so that false claims of electro-catalysis due to graphene are inferred with respect to graphene/graphene SPEs.

Two different graphene inks (denoted GSPE A and GSPE B) were utilised and fabricated as described in Chapter 3 and have been characterised in a prior publication.²⁵³ In brief, electrochemical characterisation with the $\text{Ru}(\text{NH}_3)_6^{3+/2+}$ redox probe revealed values of $3.68 \times 10^{-3} \text{ cm s}^{-1}$ and $1.94 \times 10^{-3} \text{ cm s}^{-1}$ respectively for the GSPE A and B electrodes. Raman analysis indicates that in the case of the GSPE A electrodes, there are characteristic bands observed at 1580 cm^{-1} which is typical of graphite, which is also associated with a band at 1355 cm^{-1} that is characteristic of graphitic defects typically observed in commercially available graphite samples with a small peak present at 2700 cm^{-1} .^{254, 255} The GSPE B electrode exhibits a large characteristic graphene band at 2710 cm^{-1} the intensity of which is lower than the characteristic graphite peak at 1580 cm^{-1} but does not exhibit the

characteristics expected for graphite. This is attributed to few layer graphene, likely corresponding to 6 – 8 layers. While graphene is used in the fabrication of the ink formation, it is likely that the graphene accumulates/stacks in the ink forming few-layer graphene rather than true monolayer graphene. Such observations have been observed in the fabrication of graphene paste electrodes.²⁵⁶

First considered is the voltammetric signature arising from the electrochemical oxidation of hydrazine (an analyte shown to be sensitive to metallic impurities) in a pH 7 PBS at the GSPE A and GSPE B electrodes, (pH 7 chosen in line with prior publications, the background responses of PBS pH 7 can be seen in Figure 5-1A). Note that previous work using carbon nanotubes, contain metal-catalyst impurities that can dominate the response,²⁵⁷⁻²⁵⁹ which has been extended to the case of graphene.^{62, 260} Figure 1B compares the electrochemical oxidation of hydrazine at the GSPE A, GSPE B, and GSPE surfaces where oxidation peaks are evident at + 1.1, + 0.2, and + 0.8 V (vs. *Ag/AgCl*). The signal observed at + 0.8 V using the GSPE is in good agreement with edge plane pyrolytic graphite and glassy carbon electrodes.²⁴⁸ It is readily apparent that the GSPE B gives rise to a electrocatalytic voltammetric response at + 0.2V, with an associated peak at $\sim + 1.1$ V, at a lesser magnitude than that former; clearly the GSPE B has a heterogeneous surface. Such a response of observing a larger voltammetric signal using the GSPE B at a lower overpotential compared to the GSPE A and GSPE electrode substrates would be deemed in the literature to exhibit an electro-catalytic response towards hydrazine. Note that this electro-catalysis observed at the GSPE B is intermittent in that in some instances the electrochemical activity towards hydrazine is observed upon the first scan while using other electrodes potential cycling (>3) is needed to “activate” the electrode surface. As well as hydrazine, glucose and oxygen were explored to see if a similar electro-catalytic response was observed, but no meaningful/conclusive evidence was observed.

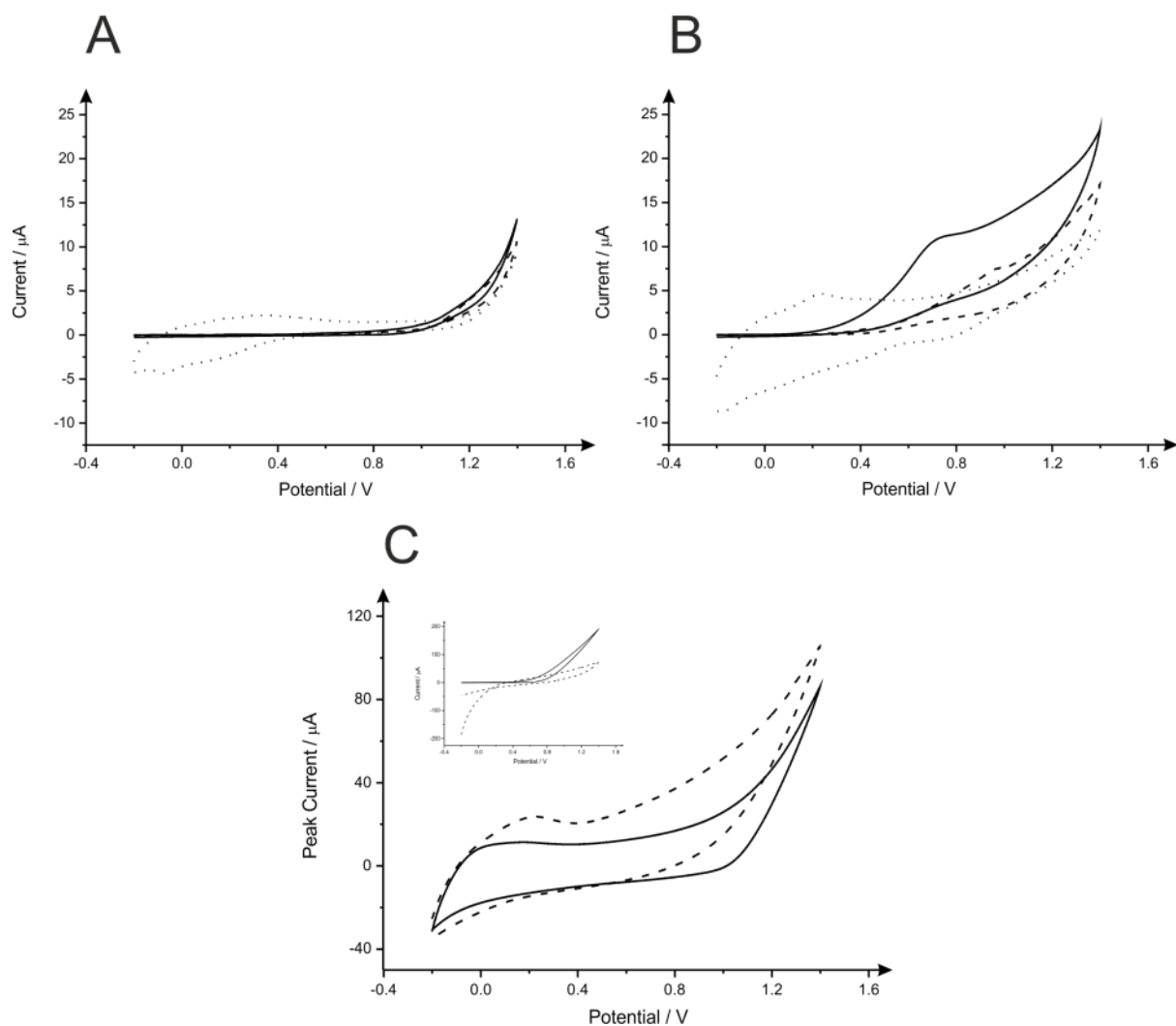


Figure 5-1 A: The cyclic voltammetric responses in PBS pH 7 for GSPE (solid line), GSPE A (dashed line), and GSPE B (dotted line). Scan rate 50 mV s^{-1} (vs. Ag/AgCl). B: The electrochemical oxidation of 10 mM hydrazine at the GSPE (solid line), GSPE A (dashed line), and GSPE B (dotted line) where oxidation peaks are evident at +0.8, +1.1, and +0.2 (vs. Ag/AgCl) respectively. Scan rate 50 mV s^{-1} . C: Observed electrochemical response for Fe(II) modified GSPE in the absence (solid line) and presence (dashed line) of 10 mM hydrazine. Scan rate 50 mV s^{-1} (vs. Ag/AgCl). Inset: Voltammetric profiles of Mn(II) (solid line) and Fe(III) (dashed line) modified GSPE in the presence of 10 mM hydrazine. Scan rate 50 mV s^{-1} (vs. Ag/AgCl).

Inspection of the XPS analysis, as presented in Table 5-1, of the fabricated GSPE electrodes reveals that the GSPE B contains iron and manganese, which are both absent in the GSPE A and other electrodes whilst both having the potential to be involved in the electrocatalysis of hydrazine (other constituents contained within are unlikely to be the cause *i.e.* sulfur, bromine silicon). This could potentially explain the origin of the electro-catalytic signal offered at the GSPE B electrode (Figure 5-1B).

Table 5-1 De-convolution of the functional group percentages *via* XPS for the fabricated graphene electrodes, presented as % totals.²⁵³

Element	GSPE A	Element	GSPE B
Carbon	87.6	Carbon	86.8
C-H	3.4	C-C:C-H	64.8
C-C	48.6	C-O	8.7
CH ₂ -CHCl	14.3	Tail 1	7.4
CHCl	14.3	Tail 2	5.9
Tail 1	4.7	Total	86.8
Tail 2	2.4		
Total	87.7		
Chlorine	9.3		
Oxygen (organic)	2.94	Oxygen	11.97
		O=C	0.63
		O-C-C	10.34
		O-C-O	1
		Total	11.97
Silicon	0.06	Silicon	0.16
Sulfur	0.08	Iron	0.3
		Manganese	0.08
		Sulfur, S-	0.21
		Sulfur, SO _x	0.39
		Bromine	0.09

To further comprehend this, Fe(II) modified SPE (see Chapter 3 for more details) were explored towards the electrochemical sensing of hydrazine. As shown in Figure 5-1B, a large voltammetric response is observed at $\sim + 0.2V$ at the Fe(II) modified SPEs which is in excellent agreement with the response observed at the GSPE B electrode (Figure 5-1B) suggesting the observed oxidative peak in the latter case is due to the metallic impurity within the ink/graphene screen-printed electrode. We note that Fe (III) and Mn(II) was also investigated however no similar voltammetric responses were observed (voltammetric profiles visible in Figure 5-1C inset), the presence of Fe on the surface of GSPE B was

mapped out using Scanning Electron Microscope - Energy-dispersive X-ray (SEM-EDX) and is visible in Figure 5-2.

Such a response with the Fe(II) modified SPEs (Figure 5-1C) confirms that the observed voltammetry in figure 1B at the GSPE B is due to metallic impurities. Last, both GSPE A and GSPE B were tested towards the electrochemical detection of hydrazine. In the case of the former, since no metallic species dominate the response, the voltammetric peak at $\sim + 1.1$ V was used while in the case of the latter, the voltammetric peaks at both $+ 0.2$ V (corresponding to the metallic impurities) and $+ 1.1$ V were utilised. Additions of hydrazine were made into a pH 7 PBS where it was found in the case of the metallic impurity catalysed signal, additions of hydrazine were found to not be reproducible or quantitative, indicating that the amount of metallic impurity varies across the electrode batch and is not evenly distributed, as expected, within the graphene ink used to fabrication the electrodes. Calibration plots (Figure 5-3) were able to be constructed for both the GSPE A and GPSE B electrode with a linear range from 400 to 3900 μM . The limit of detection (3σ) was determined to correspond to 280 μM

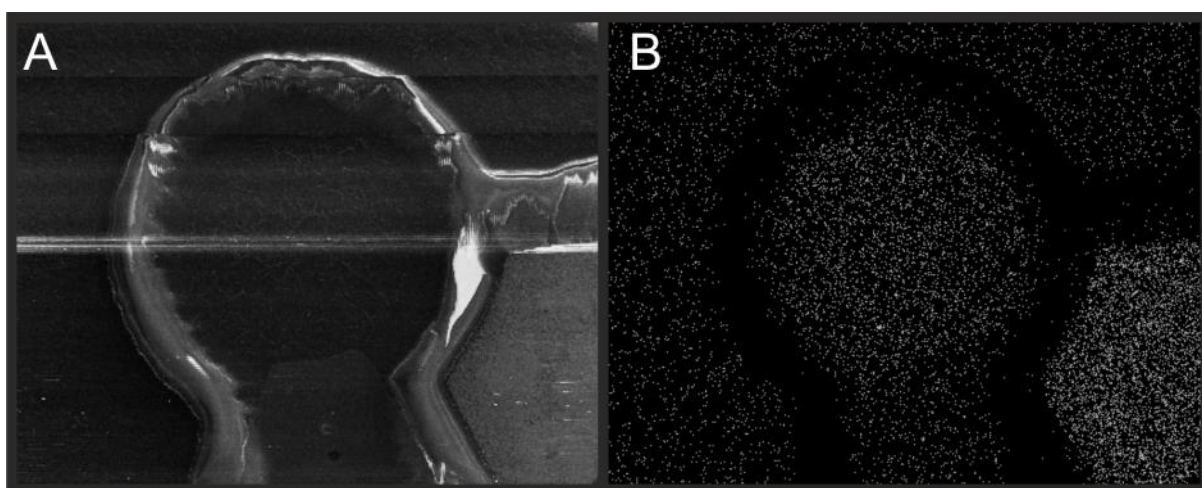


Figure 5-2 A: SEM Image of the GSPE B surface at $\times 200 \mu\text{m}$ B: The SEM-EDX “map” of the iron impurities present on the GSPE B surface; relative intensities of iron present is represented by brightness of the dot at $\times 200 \mu\text{m}$.

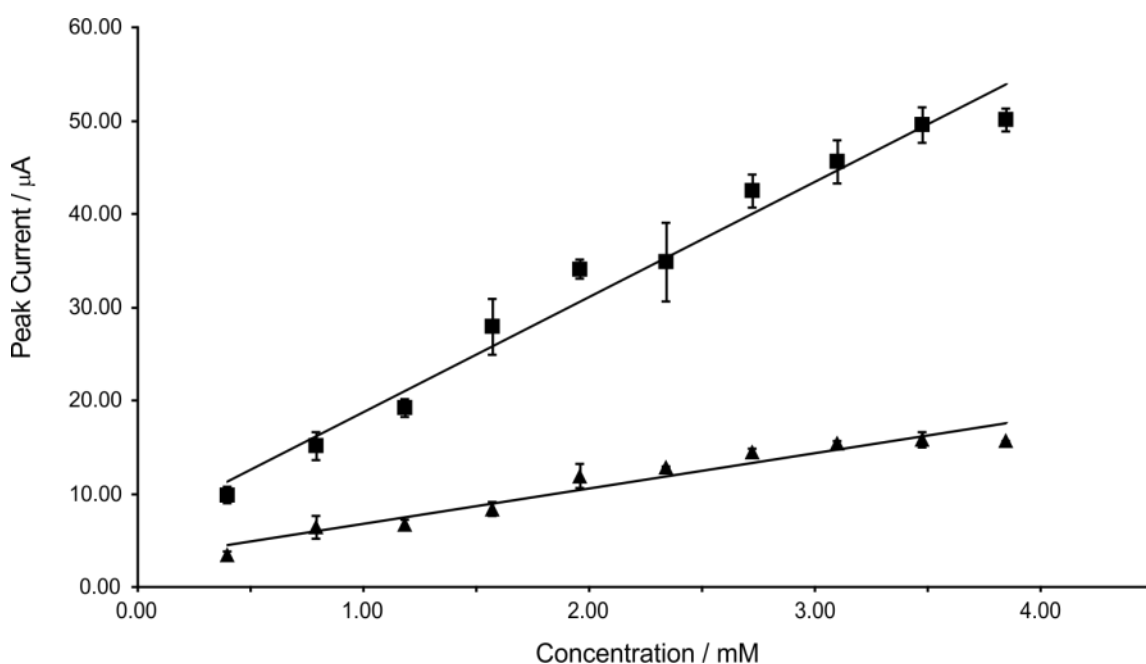


Figure 5-3 Calibration plots for both the GSPE A (Squares) and GPSE B (Triangles) electrodes response to hydrazine over the linear range 400 - 3900 μM . Scan rate 50 mV s^{-1} (vs. Ag/AgCl)

$$(I_p/A = -0.01A/\mu\text{M} + 6.4A; R^2 = 0.97; N = 10);$$

For GSPE A and 0.17 mM,

$$(I_p/A = -0.003A/\mu\text{M} + 2.9A; R^2 = 0.94; N = 10);$$

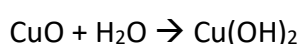
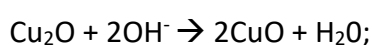
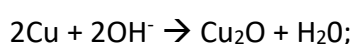
For GSPE B; such responses are electroanalytically useful.

This is strong evidence that graphene SPEs contain metallic impurities which can dominate the observed electrochemical response. The graphenes contained within the two inks are both fabricated differently and at present it is not possible to determine at what stage metallic impurities are introduced into the graphene; either during the fabrication of the graphene or during the ink processing. This work also highlights that hydrazine has utility as an electroactive species to determine metallic impurities present (that interfere with the graphene signal) within graphene inks and fabricate graphene based electrodes used in future electrochemical applications. Another deliberation from this work is that in terms of developing a screen-printed in-the-field sensor, graphene screen-printed electrodes (in their current state), are unsuitable.

5.2 *Regal Electrochemistry: Exploring British Currency as a novel electrochemical sensor*

Electrochemical sensors based upon a British 1 pence coin are utilised to successfully detect 4-MMC and 4-MEC for the first time. This novel electrochemical sensing platform based upon British coinage offers an economical approach to the sensing of NPSs 4-MMC and 4-MEC using a 1 pence coin, where the benefits of a sensor costing 1 pence (each side of the coin is useable) are unmistakeable. This new electrochemical approach is explored in ideal solutions and validated towards a seized street sample that has been independently analysed using HPLC.

The cyclic voltammetric behaviour of 4-MMC using the 1 pence coin (1p-sensor) in aqueous buffer solutions was first explored. Figure 5-4 depicts the voltammetric response obtained in a solution of pH 8.5 acetate buffer (selected so the copper is in the form of an oxide, CuO or Cu₂O, as to provide a useful sensing platform) using a 1p-sensor in the absence and presence of both 4-MMC and 4-MEC scanning anodically from -1.5 V to 0.2 V. Inspection of the resultant cyclic voltammograms reveals two reduction peaks observed at approximately -0.4 V and -0.6 V respectively in order of potential cycling and a single oxidation peak at -0.01 V, all of which are in agreement with the literature regarding the electrochemical behaviour of copper oxidation after the following reactions:²⁶¹



Note: the oxidation peak at -0.01 V is visible in the absence of 4-MMC and is seen to decrease in intensity upon its addition, this can be attributed to the 4-MMC adhering to the surface of the electrode and obstructing its electroactivity; as such the sensing of 4-MMC is an indirect approach. No pre-treatment is required for this adsorption, the only precautionary pre-treatment step taken is the sonication for 2 minutes prior to analysis to provide thorough surface cleaning as mentioned in Chapter 3. As the focus of this

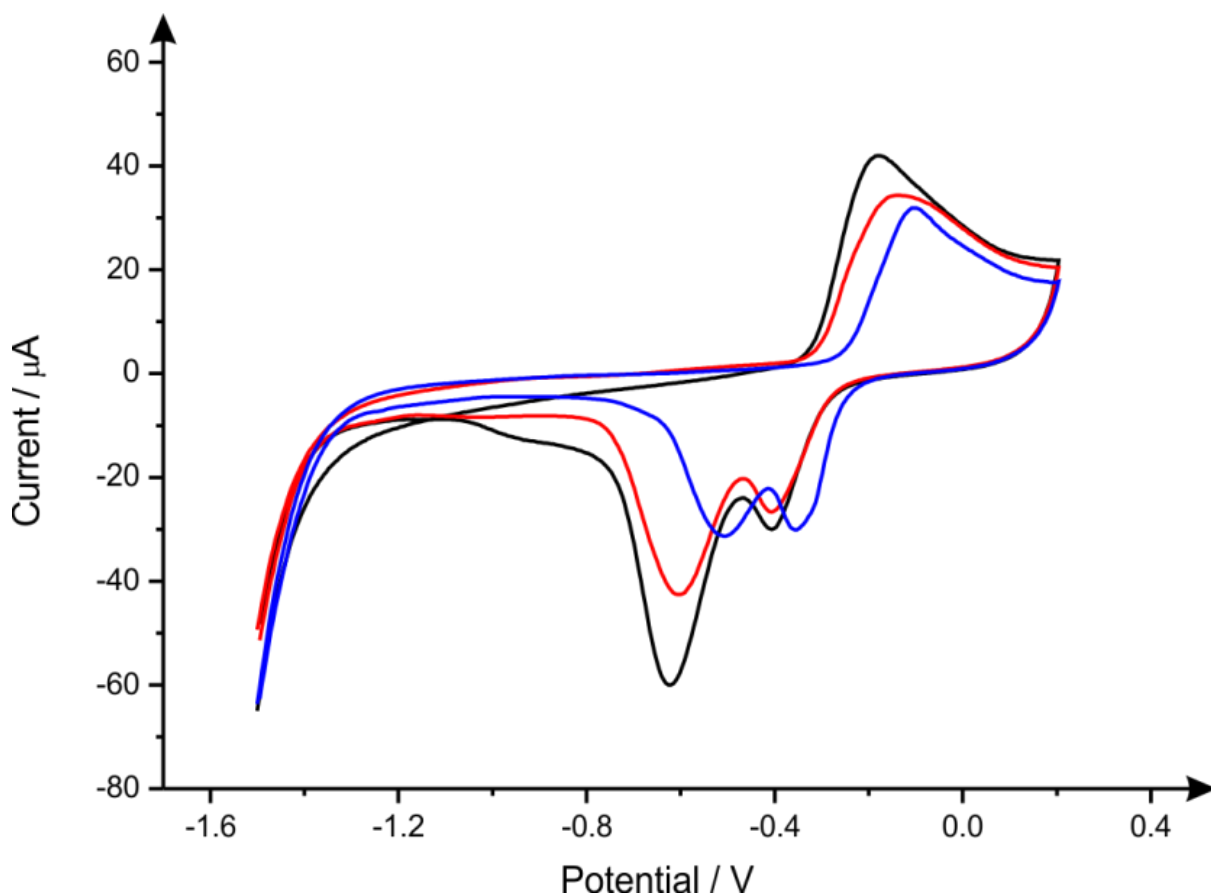


Figure 5-4 Typical cyclic voltammograms using a 1 pence electrochemical sensor in the absence (black) and presence of 4-MMC (red) and 4-MEC (blue) in pH 8.5 acetate buffer. Scan rate: 50 mV s^{-1} (vs. SCE).

research is rapid on-site analysis, investigation into a timely pre-treatment to cause further adsorption was not explored in light of present results satisfying the sensitivity requirements.

The electroanalytical method was explored through additions of 4-MMC into a pH 8.5 acetate buffer using the 1p-sensor; pH 8.5 was chosen since this maintains copper in the form of an oxide (CuO or Cu_2O) which appears useful to provide an indirect sensing platform and is also a pH that ensures that the degradation of the NPs, which occurs at alkaline pH is not significant. As is represented in Figure 5-5, the oxidation peak observed at approximately -0.01 V decreases in magnitude upon the addition of 4-MMC. The corresponding calibration plot (Figure 5-5B) demonstrates the linear response observed

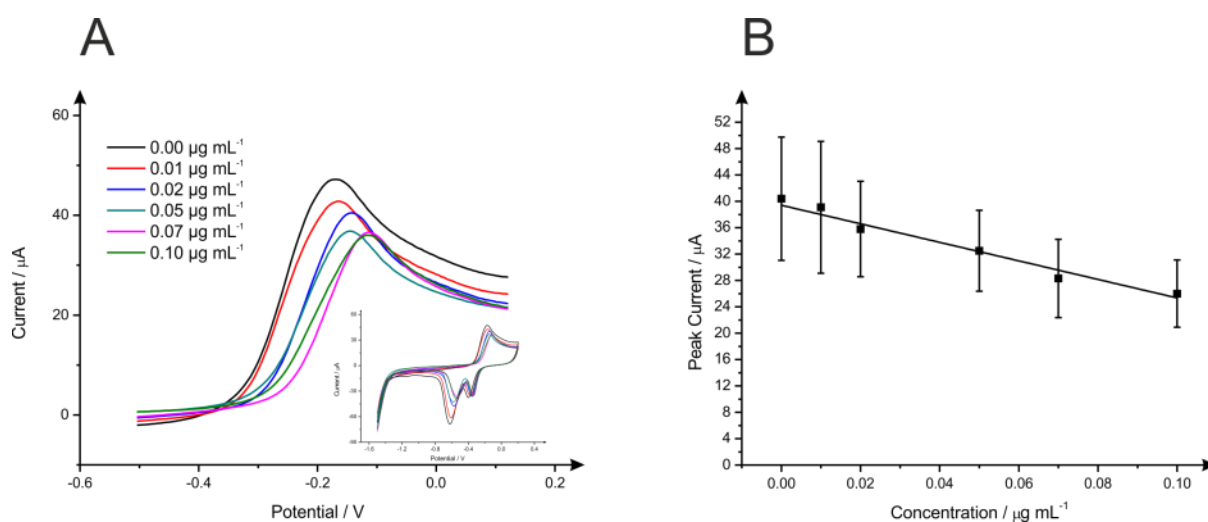


Figure 5-5 A: Typical voltammetric responses between the range -0.5 and $+0.1$ V as a result of increasing concentrations of 4-MMC using the 1p-sensor recorded in a pH 8.5 acetate buffer. Scan rate 50 mV s^{-1} (vs. SCE), using the oxidative peak at approximately -0.1 V as the analytical peak. Inset: typical voltammetric responses (full voltammetric range) as a result of increasing concentrations of 4-MMC. B: Typical calibration resulting from the analysis of voltammetric signatures obtained in the form of a plot of peak height (current) against 4-MMC concentration using a 1p-sensor in a pH 8.5 acetate buffer over a linear range of 0.01 – $0.10 \text{ } \mu\text{g mL}^{-1}$. Scan rate: 50 mV s^{-1} (vs. SCE) ($N = 3$ – average and standard deviation is plotted).

$$(I/\mu\text{A} = 0.1 \times 10^{-3} \text{ A } [\mu\text{g mL}^{-1}] + 4 \times 10^{-5} \text{ A}, R^2 = 0.97, N=3)$$

Over the analytical range studied (1×10^{-3} – $0.1 \text{ } \mu\text{g mL}^{-1}$). The limit of detection (3σ) for 4-MMC utilising the 1 pence sensor was estimated to correspond to $0.56 \text{ } \mu\text{g mL}^{-1}$ which is a large improvement on the work reported in section 4.2.4 which reported a value of $11.80 \text{ } \mu\text{g mL}^{-1}$. Note that this novel proof-of-concept has a substantial error when the average of three different coins is used.

Attention was now turned to another novel psychoactive substance (similar to 4-MMC), 4-MEC (also found in seized street samples)²⁶² wherein the cyclic voltammetric behaviour towards a 1 pence sensor in pH 8.5 acetate buffer is visible in Figure 5-4. A similar response to 4-MMC is observed with again a single oxidation peak at -0.01 V and the two reduction peaks at approximately -0.3 and -0.6 V with the intensity of the oxidation peak again decreasing proportionally to the increasing concentration of 4-MEC. The resultant calibration plot demonstrated a linear response:

$$(I/\mu\text{A} = 0.2 \times 10^{-3} \text{ A } [\mu\text{g mL}^{-1}] + 6 \times 10^{-5} \text{ A}, R^2 = 0.97, N = 3)$$

Over the studied analytical range (1×10^{-3} – $0.1 \mu\text{g mL}^{-1}$), with a limit of detection (3σ) equal to $0.50 \mu\text{g mL}^{-1}$. The electrochemical mechanism is an indirect approach where the electrochemistry of copper oxide is inhibited due to the adsorption of the NPSs under investigation. As with SPEs (Section 4.2.2), there is not a discernible difference between 4-MMC and 4-MEC however, in terms of an on-site low cost qualitative sensor this is of no issue.

As shown in Figure 5-6 and Figure 5-7, Scanning Electron Microscopy-Energy Dispersive X-ray microanalysis (SEM-EDX) shows a higher percentage of copper (and therefore CuO) in the 1 pence coins minted post-1992. Since the underlying mechanism is dependent upon the presence of copper oxide, post-1992 are ideal. This is fortunate given the scarcity of coins minted pre-1992 further justifying the use of post-1992, which are in current circulation.

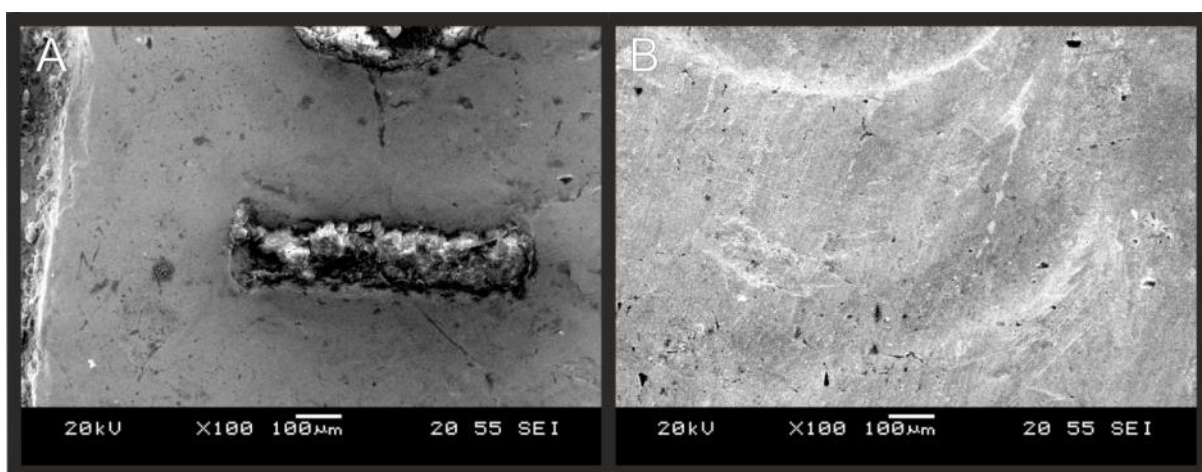


Figure 5-6 SEM of a A: British 1 pence coin minted pre-1992 and B: British 1 pence coin minted post-1992.

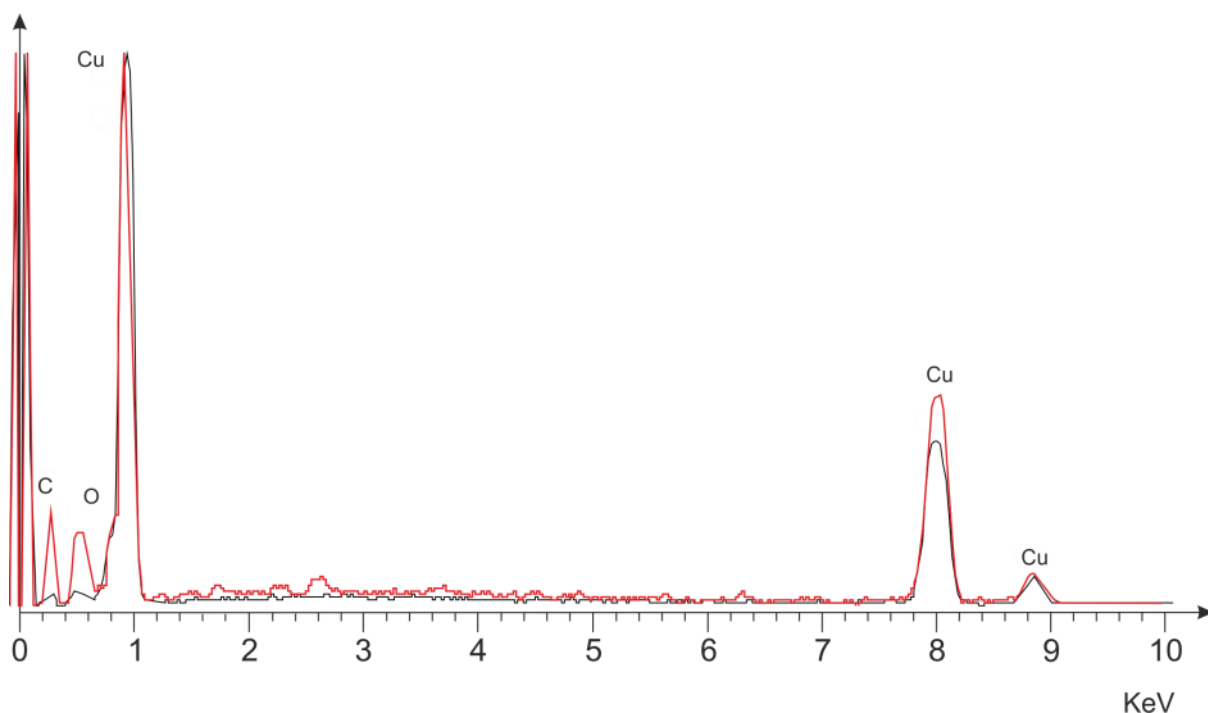


Figure 5-7 EDX spectra obtained from a pre-1992 (red) and post-1992 (black) British 1 pence coin following analysis.

To define the qualities of a 1p-sensor, the analytical protocol was applied to a seized street sample (NRG-2), previously analysed (section 4.2.4) to determine if the 1p-sensor has merit as a potential sensor for the content of 4-MMC within. Note: Previous analysis²⁶² of NRG-2 seized street samples via HPLC has shown their contents comprise of adulterants such as caffeine and benzocaine.²⁶² Seized street sample for analysis in this thesis was known to contain 11.15 % (w/w) 4-MMC and 87.99 % (w/w) caffeine (see section 0 for more details). The standard addition method was utilized in an attempt to quantify the amount of 4-MMC in a street sample and was compared to the previously reported values obtained by cyclic voltammetry (with a carbon screen-printed sensor) and HPLC.²⁰⁷ Following analysis, the standard addition plot revealed a reported 4-MMC content of 10.99 % (w/w) which is in excellent agreement with 11.15% (w/w) obtained via HPLC and 11.32% (w/w) reported previously²⁶² using the carbon based screen-printed sensor and is indicative that an electrochemical sensor using British coinage has analytical merit. Note: the adulterants had no effect on the electrochemical signal suggesting it is a moiety that is unique to synthetic cathinones (Scheme 2-2) that reacts with the copper oxide surface.

The preceding work formed the basis of research manuscripts J. P. Smith, C. W. Foster, J. P. Metters, O. B. Sutcliffe and C. E. Banks, *Electroanalysis*, 2014, **26**, 2429-2433 And F. Tan, J. P. Smith, O. B. Sutcliffe and C. E. Banks, *Anal. Methods*, 2015, **7**, 6470-6474. The next chapter summarises the conclusions and consequent contributions to the scientific community whilst also postulating further work to continue the growth of the niche research area *Forensic Electrochemistry*.

Chapter 6 Conclusions and Future Work

The work presented in this thesis has provided much to the field of *Forensic Electrochemistry*. It is hoped this niche field can continue to expand and provide a genuine solution to a low-cost, in-the-field quantitative sensor. Below is a summary of the contributions to the field and how these can provide a basis for a strong future in *Forensic Electrochemistry*, additionally there are suggestions for future work to ensure its expansion. In brief, the aims and objectives outlined at the beginning of this thesis were successfully met.

6.1 Conclusions

Chapter 4.1 demonstrated for the first time, the electroanalytical oxidation of mephedrone and 4-methylethcathinone (another synthetic cathinone derivative that frequently occurs in “*legal highs*”) using both commercially available solid macroelectrodes (boron-doped diamond, glassy carbon) and disposable screen-printed graphite macroelectrodes. Screen-printed electrodes are favourable since they offer a low cost, single-shot disposable yet highly reproducible and reliable sensing platform for electrochemical measurement of the target analytes.

The analytical parameters realised, in terms of limits of detection and accessible linear range in model solutions are analytically useful. The adulterants likely to be found in such “*legal high*” products, caffeine and benzocaine, were also explored at the optimum electrode material and solution pH. At pH 12 and 2 it is found that there is no electrochemical selectivity over the electrochemical detection of methcathinone, mephedrone (4-MMC) and 4-methylethcathinone (4-MEC) such that a mixture of these cannot be differentiated from. The interesting case of a redox couple being formed in acidic conditions for 4-MMC and 4-MEC offers an additional electrochemical quantification approach however, there is still no selectivity between the two compounds and the adulterants. Consequently, at the pHs studied in section 4.1 and through the use of SPEs, a

portable on the spot sensor for these cathinone classes of “legal highs” is unlikely to be realised using such electrochemical approaches/technology.

In light of the work in section 4.1, the work carried out in 0 reported an improvement on the earlier proof-of-concept work utilizing a different, novel, electrochemical approach. Additionally inspired by Krishnaiah *et al.*²¹⁰ as well as other reports that electroanalytical signals have been improved through the use of bismuth-modified electrodes (though not yet applied to the sensing of NPSs); the use of in situ formed mercury and bismuth film modified graphite screen-printed electrodes were explored for the first time toward the sensing of the substituted cathinones, 4-MMC and 4-MEC.

Consequently demonstrated for the first time, meeting the principal aims of the thesis; the electrochemical reduction of substituted cathinones was shown to be a viable analytical protocol offering a limit of detection (3σ) of $11.80 \mu\text{g mL}^{-1}$ for 4-MMC and $11.60 \mu\text{g mL}^{-1}$ for 4-MEC with no improvement observed using either mercury or bismuth film modified electrodes. This work demonstrated for the first time a rapid, accurate, and sensitive method for quantification of substituted cathinones components found in seized street samples of NRG-2 via the use of an electrochemical protocol utilizing graphite screen-printed electrodes (SPEs) which was independently verified with HPLC. Adulterants that are typically found in street samples were also electrochemically characterized for their potential interference in the simultaneous sensing of 4-MMC and 4-MEC and were found to have no interference unlike that of prior work (4.1). By virtue of SPEs being a low-cost, single-shot, disposable yet highly reproducible and reliable sensing platform, there is a clear forensic application of this electrochemical reduction method to be used “on-site” for the screening, or even quantification, of common synthetic cathinones found within real seized street samples.

Following the successful detection of prevalent NPSs 4-MMC and 4-MEC, attention was directed towards the on-site detection of Rohypnol®. Work in chapter 0 successfully provided an electrochemically sensing methodology for detecting Rohypnol®, a drug reported to be used extensively in the case of “date-rape”. The analytical protocol utilised for the first time screen-printed electrodes allowing Rohypnol® to be readily determined in common beverages, Coca Cola™ and the alcoholic WKD™ without the

requirement of any pH modification or further sample preparation. Notably, the protocol works within coloured beverages that are used to mask the dye present in current Rohypnol® drug tablets and can be used to identify “spiked” beverages. The electrochemical sensing methodology provides a rapid, accurate and sensitive approach for determining Rohypnol® in coloured beverages which has a clear forensic application and can be used for the on-site screening (*i.e.* indicate the drug is there or not) of suspected spiked drinks.

Chapter 5 saw the exploration of other materials for their utility as in-the-field sensors. In summary, it was shown that despite graphene being an exciting material, proof-of-concept that graphene SPEs contain metallic impurities which can dominate the observed electrochemical response was demonstrated. The graphenes contained within the two inks (GSPE A/B) are both fabricated differently and at present it is insurmountable to determine at what stage metallic impurities are introduced into the graphene; it is possible either during the fabrication of the graphene or during the ink processing. This work also highlighted that hydrazine has utility as an electroactive species to determine metallic impurities present within graphene inks and fabricate graphene based electrodes used in future electrochemical applications. Avant-garde work carried out in section 5.1 showed proof-of-concept for the detection of NPSs using a 1 pence coin as a novel electrochemical sensor. This novel approach is extremely cost effective with the sensor costing just 0.5 pence (both sides of the coin can be used), and a PTFE ‘housing’ unit which is readily made using cheap components readily available in university workshops. The proposed protocol was successfully validated against independently performed HPLC in seized street samples. This new, exciting, field coined *Regal Electrochemistry* is an attractive proposition since everyone will have a coin in his or her pocket, which can be readily utilised at low cost with minimal pretreatment and in light of its low cost – can be used as a one shot sensor; this is particularly useful in developing countries.

6.2 Future Work

Given the nature of NPSs and their forever changing structures to evade and circumvent nationwide drug legislation, future work should involve the extension of the validated

protocol in this thesis to a larger number of seized samples and the possible potential development into a portable “legal high” sensor. What’s more, to overcome any limiting issue of overlapping voltammetric waves, HPLC with an electrochemical detector may be able to be utilised. Electrochemistry and HPLC working in tandem could offer a solution to multi-compound quantification in-the-field if scaled down to a micro-fluidic device.

The concept of *Regal Electrochemistry* can also be expanded to other coinage towards a range of target (electro-active) analytes and is another niche area of research that can be expanded to a multitude of applications such as those postured by militaristic operations as well as the already demonstrated detection of NPSs.

Bibliography

1. A. Bard and L. Faulkner, *Electrochemical Methods: Fundamentals and Applications*, John Wiley & Sons, Inc, 2001.
2. C. E. Banks and R. G. Compton, *Understanding Voltammetry*, Imperial College Press, 2008.
3. J. Wang, *Analytical Electrochemistry*, Wiley, 2004.
4. A. C. Fisher, *Electrode Dynamics*, Oxford University Press, 1996.
5. H. Helmholtz, *Annalen der Physik*, 1853, **165**, 353-377.
6. O. Stern, *Zeitschrift für Elektrochemie und angewandte physikalische Chemie*, 1924, **30**, 508-516.
7. D. A. Skoog, D. M. West and F. J. Holler, *Fundamentals of analytical chemistry*, Saunders College Pub., 1996.
8. J. P. Metters, R. O. Kadara, C. E. Banks, *Analyst*, 2012, **137**, 896.
9. C. W. Foster, J. P. Metters and C. E. Banks, *Electroanalysis*, 2013, **25**, 2275-2282.
10. J. P. Metters, F. Tan and C. E. Banks, *Journal of Solid State Electrochemistry*, 2013, **17**, 1553-1562.
11. J. P. Metters, M. Gomez-Mingot, J. Iniesta, R. O. Kadara and C. E. Banks, *Sensors and Actuators B: Chemical*, 2013, **177**, 1043-1052.
12. A. V. Koliopoulos, J. P. Metters and C. E. Banks, *Anal. Methods*, 2013, **5**, 851-856.
13. D. A. C. Brownson, C. W. Foster and C. E. Banks, *Analyst*, 2012, **137**, 1815-1823.
14. M. C. Granger, M. Witek, J. S. Xu, J. Wang, M. Hupert, A. Hanks, M. D. Koppang, J. E. Butler, G. Lucazeau, M. Mermoux, J. W. Strojek and G. M. Swain, *Anal. Chem.*, 2000, **72**, 3793-3804.
15. C. E. Banks, T. J. Davies, G. G. Wildgoose and R. G. Compton, *Chemical Communications*, 2005, 829-841.
16. H. Kahlert, *Journal of Solid State Electrochemistry*, 2008, **12**, 1255-1266.
17. E. Bilici, Z. Yazicigil, M. Tok and Y. Oztekin, *Desalin. Water Treat.*, 2012, **50**, 198-205.
18. V. Suryanarayanan, C.-T. Wu and K.-C. Ho, *Electroanalysis*, 2010, **22**, 1795-1811.
19. L. Wasserman, *All of Statistics: A Concise Course in Statistical Inference*, Springer, 2004.
20. D. Frumkin, A. Wasserstrom, A. Davidson and A. Gravit, *Forensic Science International: Genetics*, **4**, 95-103.
21. E. P. Randviir and C. E. Banks, *TrAC Trends in Analytical Chemistry*, 2015, **64**, 75-85.
22. J. P. Smith, O. B. Sutcliffe and C. E. Banks, *Analyst*, 2015, **140**, 4932-4948.
23. E. Katz and J. Halmek, *Forensic Science: A Multidisciplinary Approach*, Wiley, 2016.

24. C. Banks and J. Birkett, *Anal. Methods*, 2013, **5**, 5375-5375.
25. O. Ramdani, J. P. Metters, L. C. S. Figueiredo-Filho, O. Fatibello-Filho and C. E. Banks, *Analyst*, 2013, **138**, 1053-1059.
26. Chemistry World, <http://www.rsc.org/chemistryworld/2013/09/atropine-belladonna-deadly-nightshade-podcast>.
27. Chemistry World, <http://www.rsc.org/chemistryworld/2012/05/forensic-electrochemistry-detect-firearms-use-0>.
28. M. Vuki, K.-K. Shiu, M. Galik, A. M. O'Mahony and J. Wang, *Analyst*, 2012, **137**, 3265-3270.
29. B. News, Dando appeal based on gun residue, <http://news.bbc.co.uk/1/hi/uk/7078221.stm>, Accessed 2016.
30. F. Nizam, W. Knaap and J. D. Stewart, *Journal of Forensic Identification*, 2012, **62**, 129.
31. M. Zhang and H. H. Girault, *Electrochemistry Communications*, 2007, **9**, 1778-1782.
32. A. Ambrosi and M. Pumera, *Physical Chemistry Chemical Physics*, 2010, **12**, 8943-8947.
33. C. Deng, Y. Xia, C. Xiao, Z. Nie, M. Yang and S. Si, *Biosens Bioelectron*, 2012, **31**, 469-474.
34. Q. Li, C. Batchelor-McAuley and R. G. Compton, *The Journal of Physical Chemistry B*, 2010, **114**, 7423-7428.
35. J. Wang, G. Liu and A. Merkoçi, *Journal of the American Chemical Society*, 2003, **125**, 3214-3215.
36. R. Lindigkeit, A. Boehme, I. Eiserloh, M. Luebbecke, M. Wiggermann, L. Ernst and T. Beuerle, *Forensic Science International*, 2009, **191**, 58-63.
37. L. A. Johnson, R. L. Johnson and R.-B. Portier, *The Journal of Emergency Medicine*, 2013, **44**, 1108-1115.
38. United Nations Office on Drugs and Crime, The Challenge Of New Psychoactive Substances, www.unodc.org/documents/scientific/NPS_2013_SMART.pdf, Accessed April, 2014.
39. S. D. Brandt, H. R. Sumnall, F. Measham and J. Cole, *Drug Testing and Analysis*, 2010, **2**, 377-382.
40. O. Corazza, S. Assi and G. Trincas, *Italian Journal on Addiction*, 2011, **1**, 25-30.
41. European Monitoring Centre for Drugs and Drug Addiction, Europol, EU drug markets report: a strategic analysis, <http://www.emcdda.europa.eu/publications/joint-publications/drug-markets>, Accessed April, 2015.
42. European Monitoring Centre for Drugs and Drug Addiction, Annual report 2011: the state of the drugs problem in Europe, New drugs and emerging trends, <http://www.emcdda.europa.eu/online/annual-report/2011/new-drugs-and-trends/5>, Accessed April, 2015.

43. *New psychoactive substances in Europe. An update from the EU Early Warning System (March 2015)*, 2015.
44. N. V. Cozzi, M. K. Sievert, A. T. Shulgin, P. Jacob, 3rd and A. E. Ruoho, *Eur J Pharmacol*, 1999, **381**, 63-69.
45. J. Kehr, F. Ichinose, S. Yoshitake, M. Goiny, T. Sievertsson, F. Nyberg and T. Yoshitake, *Br. J. Pharmacol.*, 2011, **164**, 1949-1958.
46. M. H. Baumann, M. A. Ayestas, J. S. Partilla, J. R. Sink, A. T. Shulgin, P. F. Daley, S. D. Brandt, R. B. Rothman, A. E. Ruoho and N. V. Cozzi, *Neuropsychopharmacology*, 2012, **37**, 1192-1203.
47. N. V. Cozzi and K. E. Foley, *Pharmacology & Toxicology*, 2003, **93**, 219-225.
48. N. V. Cozzi, M. K. Sievert, A. T. Shulgin, P. Jacob and A. E. Ruoho, *European Journal of Pharmacology*, 1999, **381**, 63-69.
49. K. Morris, *Lancet*, 2010, **375**, 1333-1334.
50. J. A. Fass, A. D. Fass and A. S. Garcia, *Ann. Pharmacother.*, 2012, **46**, 436-441.
51. J. B. Zawilska and J. Wojcieszak, *Forensic science international*, 2013, **231**, 42-53.
52. The Charleston Gazette, Man high on bath salts kills neighbor's goat, police say, <http://www.wvgazette.com/News/201105020871>, Accessed April, 2015.
53. E. M. Sammler, P. L. Foley, G. D. Lauder, S. J. Wilson, A. R. Goudie and J. I. O'Riordan, *Lancet*, 2010, **376**, 742-742.
54. M. Paillet-Loilier, A. Cesbron, R. Le Boisselier, J. Bourguine and D. Debruyne, *Substance abuse and rehabilitation*, 2014, **5**, 37-52.
55. J. R. H. Archer, P. I. Dargan, S. Hudson, S. Davies, M. Puchnarewicz, A. T. Kicman, J. Ramsey, F. Measham, M. Wood, A. Johnston and D. M. Wood, *Journal of Substance Use*, 2014, **19**, 103-107.
56. J. Beyer, F. T. Peters, T. Kraemer and H. H. Maurer, *J. Mass Spectrom.*, 2007, **42**, 150-160.
57. H. Torrance and G. Cooper, *Forensic Science International*, 2010, **202**, E62-E63.
58. E. Y. Santali, A. K. Cadogan, N. N. Daeid, K. A. Savage and O. B. Sutcliffe, *J. Pharm. Biomed. Anal.*, 2011, **56**, 246-255.
59. O. I. G. Khreit, C. Irving, E. Schmidt, J. A. Parkinson, N. Nic Daeid and O. B. Sutcliffe, *J. Pharm. Biomed. Anal.*, 2012, **61**, 122-135.
60. P. M. O'Byrne, P. V. Kavanagh, S. M. McNamara and S. M. Stokes, *J. Anal. Toxicol.*, 2013, **37**, 64-73.
61. M. J. Swortwood, D. M. Boland and A. P. DeCaprio, *Analytical and Bioanalytical Chemistry*, 2013, **405**, 1383-1397.
62. A. Ambrosi, S. Y. Chee, B. Khezri, R. D. Webster, Z. Sofer and M. Pumera, *Angewandte Chemie International Edition*, 2012, **51**, 500-503.
63. B. D. Paul and K. A. Cole, *J. Anal. Toxicol.*, 2001, **25**, 525-530.
64. S. D. Brandt, S. Freeman, H. R. Sumnall, F. Measham and J. Cole, *Drug Testing and Analysis*, 2011, **3**, 569-575.

65. C. Bell, C. George, A. T. Kicman and A. Traynor, *Drug Testing and Analysis*, 2011, **3**, 496-504.
66. P. Jankovics, A. Varadi, L. Tolgyesi, S. Lohner, J. Nemeth-Palotas and H. Koszegi-Szalai, *Forensic Science International*, 2011, **210**, 213-220.
67. L. K. Sorensen, *J. Chromatogr. B*, 2011, **879**, 727-736.
68. S. V. R. C. Rambabu, G. Ramu, A. Biksham Babu, *Rasayan J. Chem.*, 2010, **3**, 796-799.
69. G. Frison, M. Gregio, L. Zamengo, F. Zancanaro, S. Frasson and R. Sciarrone, *Rapid Commun. Mass Spectrom.*, 2011, **25**, 387-390.
70. Y. Al-Saffar, N. N. Stephanson and O. Beck, *J. Chromatogr. B*, 2013, **930**, 112-120.
71. A. J. Pedersen, P. W. Dalsgaard, A. J. Rode, B. S. Rasmussen, I. B. Muller, S. S. Johansen and K. Linnet, *Journal of Separation Science*, 2013, **36**, 2081-2089.
72. E. M. Mwenesongole, L. Gautam, S. W. Hall, J. W. Waterhouse and M. D. Cole, *Anal. Methods*, 2013, **5**, 3248-3254.
73. D. Ammann, J. M. McLaren, D. Gerostamoulos and J. Beyer, *J. Anal. Toxicol.*, 2012, **36**, 381-389.
74. S. Strano-Rossi, L. Anzillotti, E. Castrignano, F. S. Romolo and M. Chiarotti, *Journal of Chromatography A*, 2012, **1258**, 37-42.
75. M. Mayer, A. Benko, A. Huszar, K. Sipos, A. Lajtai, A. Lakatos and Z. Porpaczy, *Journal of chromatographic science*, 2013, **51**, 861-866.
76. N. Nic Daeid, K. A. Savage, D. Ramsay, C. Holland and O. B. Sutcliffe, *Science & justice : journal of the Forensic Science Society*, 2013, **54**, 22-31.
77. E. L. Menzies, S. C. Hudson, P. I. Dargan, M. C. Parkin, D. M. Wood and A. T. Kicman, *Drug Testing and Analysis*, 2014, **6**, 506-515.
78. O. I. G. Khreit, M. H. Grant, T. Zhang, C. Henderson, D. G. Watson and O. B. Sutcliffe, *J. Pharm. Biomed. Anal.*, 2013, **72**, 177-185.
79. M. Taschwer, Y. Seidl, S. Mohr and M. G. Schmid, *Chirality*, 2014, **26**, 411-418.
80. A. M. Leffler, P. B. Smith, A. de Armas and F. L. Dorman, *Forensic Science International*, 2014, **234**, 50-56.
81. U. Khan, A. L. N. van Nuijs, J. Li, W. Maho, P. Du, K. Li, L. Hou, J. Zhang, X. Meng, X. Li and A. Covaci, *Science of The Total Environment*, 2014, **487**, 710-721.
82. A. D. Lesiak, R. A. Musah, R. B. Cody, M. A. Domin, A. J. Dane and J. R. E. Shepard, *Analyst*, 2013, **138**, 3424-3432.
83. R. A. Musah, R. B. Cody, M. A. Domin, A. D. Lesiak, A. J. Dane and J. R. E. Shepard, *Forensic Science International*, 2014, **244**, 42-49.
84. M. Joshi, B. Cetroni, A. Camacho, C. Krueger and A. J. Midey, *Forensic Science International*, 2014, **244**, 196-206.
85. S. Armenta, S. Garrigues, M. de la Guardia, J. Brassier, M. Alcalá, M. Blanco, C. Perez-Alfonso and N. Galipienso, *Drug Testing and Analysis*, 2015, **7**, 280-289.
86. S. Mabbott, A. Eckmann, C. Casiraghi and R. Goodacre, *Analyst*, 2013, **138**, 118-122.

87. S. Mabbott, E. Correa, D. P. Cowcher, J. W. Allwood and R. Goodacre, *Anal. Chem.*, 2013, **85**, 923-931.
88. M. J. Swortwood, W. L. Hearn and A. P. DeCaprio, *Drug Test Anal*, 2014, **6**, 716-727.
89. N. NicDaeid, W. Meier-Augenstein, H. F. Kemp and O. B. Sutcliffe, *Anal Chem*, 2012, **84**, 8691-8696.
90. J. W. Huffman, D. Dai, B. R. Martin and D. R. Compton, *Bioorganic & Medicinal Chemistry Letters*, 1994, **4**, 563-566.
91. S. Dresen, N. Ferreiros, M. Puetz, F. Westphal, R. Zimmermann and V. Auwaerter, *J. Mass Spectrom.*, 2010, **45**, 1186-1194.
92. N. Uchiyama, R. Kikura-Hanajiri, J. Ogata and Y. Goda, *Forensic Sci.Int.*, 2010, **198**, 31-38.
93. J. i. Nakajima, M. Takahashi, T. Seto, C. Kanai, J. Suzuki, M. Yoshida and T. Hamano, *Forensic Toxicology*, 2011, **29**, 95-110.
94. V. Auwärter, P. I. Dargan and D. M. Wood, in *Novel Psychoactive Substances*, ed. P. I. D. M. Wood, Academic Press, Boston, 2013, pp. 317-343.
95. B. K. Atwood, J. Huffman, A. Straiker and K. Mackie, *Br. J. Pharmacol.*, 2010, **160**, 585-593.
96. A. B. Schneir, J. Cullen and B. T. Ly, *J. Emerg. Med.*, 2011, **40**, 296-299.
97. J. Simmons, L. Cookman, C. Kang and C. Skinner, *Clin. Toxicol.*, 2011, **49**, 431-433.
98. J. Cohen, S. Morrison, J. Greenberg and M. Saidinejad, *Pediatrics*, 2012, **129**, E1064-E1067.
99. I. Vardakou, C. Pistos and C. Spiliopoulou, *Toxicology Letters*, 2010, **197**, 157-162.
100. New York: United Nations Office on Drugs and Crime (UNODC), *World Drug Report*, UNODC, 2009.
101. C. E. J. Emanuel, B. Ellison and C. E. Banks, *Anal. Methods*, 2010, **2**, 614-616.
102. V. Auwarter, S. Dresen, W. Weinmann, M. Muller, M. Putz and N. Ferreiros, *J. Mass Spectrom.*, 2009, **44**, 832-837.
103. N. Uchiyama, R. Kikura-Hanajiri, N. Kawahara, Y. Haishima and Y. Goda, *Chem. Pharm. Bull.*, 2009, **57**, 439-441.
104. B. K. Koe, G. M. Milne, A. Weissman, M. R. Johnson and L. S. Melvin, *European Journal of Pharmacology*, 1985, **109**, 201-212.
105. T. Sobolevsky, I. Prasolov and G. Rodchenkov, *Forensic Science International*, 2010, **200**, 141-147.
106. H. J. Penn, L. J. Langman, D. Unold, J. Shields and J. H. Nichols, *Clinical biochemistry*, 2011, **44**, 1163-1165.
107. H. Koskela, U. Hakala, L. Loiske, P. Vanninen and I. Szilvay, *Anal. Methods*, 2011, **3**, 2307-2312.
108. R. A. Musah, M. A. Domin, M. A. Walling and J. R. E. Shepard, *Rapid Commun. Mass Spectrom.*, 2012, **26**, 1109-1114.

109. G. Merola, Z. Aturki, G. D'Orazio, R. Gottardo, T. Macchia, F. Tagliaro and S. Fanali, *J. Pharm. Biomed. Anal.*, 2012, **71**, 45-53.
110. A. O. Cox, R. C. Daw, M. D. Mason, M. Grabenauer, P. G. Pande, K. H. Davis, J. L. Wiley, P. R. Stout, B. F. Thomas and J. W. Huffman, *J. Anal. Toxicol.*, 2012, **36**, 293-302.
111. R. Gottardo, A. Chiarini, I. Dal Pra, C. Seri, C. Rimondo, G. Serpelloni, U. Armato and F. Tagliaro, *J. Mass Spectrom.*, 2012, **47**, 141-146.
112. A. Gregori, F. Damiano, M. Bonavia, V. Mileo, F. Varani and M. Monfreda, *Science & justice : journal of the Forensic Science Society*, 2012.
113. F. Westphal, F. D. Soennichsen and S. Thiemt, *Forensic Science International*, 2012, **215**, 8-13.
114. S. Beuck, I. Moeller, A. Thomas, A. Klose, N. Schloerer, W. Schaenzer and M. Thevis, *Analytical and Bioanalytical Chemistry*, 2011, **401**, 493-505.
115. A. Wohlfarth, K. B. Scheidweiler, X. H. Chen, H. F. Liu and M. A. Huestis, *Anal. Chem.*, 2013, **85**, 3730-3738.
116. D. P. Lovett, E. G. Yanes, T. W. Herbelin, T. A. Knoerzer and J. A. Levisky, *Forensic Science International*, 2013, **226**, 81-87.
117. M. J. Jin, J. Lee, M. K. In and H. H. Yoo, *J. Forensic Sci.*, 2013, **58**, 195-199.
118. A. D. de Jager, J. V. Warner, M. Henman, W. Ferguson and A. Hall, *J. Chromatogr. B*, 2012, **897**, 22-31.
119. U. Kim, M. J. Jin, J. Lee, S. B. Han, M. K. In and H. H. Yoo, *J. Pharm. Biomed. Anal.*, 2012, **64-65**, 26-34.
120. E. G. Yanes and D. P. Lovett, *J. Chromatogr. B*, 2012, **909**, 42-50.
121. C. L. Moran, V.-H. Le, K. C. Chimalakonda, A. L. Smedley, F. D. Lackey, S. N. Owen, P. D. Kennedy, G. W. Endres, F. L. Ciske, J. B. Kramer, A. M. Kornilov, L. D. Bratton, P. J. Dobrowolski, W. D. Wessinger, W. E. Fantegrossi, P. L. Prather, L. P. James, A. Radomska-Pandya and J. H. Moran, *Anal. Chem.*, 2011, **83**, 4228-4236.
122. K. C. Chimalakonda, C. L. Moran, P. D. Kennedy, G. W. Endres, A. Uzieblo, P. J. Dobrowolski, E. K. Fifer, J. Lapoint, L. S. Nelson, R. S. Hoffman, L. P. James, A. Radomska-Pandya and J. H. Moran, *Anal. Chem.*, 2011, **83**, 6381-6388.
123. M. A. Neukamm, T. E. Muerdter, C. Knabbe, H.-D. Wehner and F. Wehner, *Blutalkohol*, 2009, **46**, 373-379.
124. S. Dresen, S. Kneisel, W. Weinmann, R. Zimmermann and V. Auwaerter, *J. Mass Spectrom.*, 2011, **46**, 163-171.
125. J. Teske, J.-P. Weller, A. Fieguth, T. Rothaemel, Y. Schulz and H. D. Troeger, *J. Chromatogr. B*, 2010, **878**, 2659-2663.
126. M. Dziadosz, J.-P. Weller, M. Klintschar and J. Teske, *J Chromatogr B Analyt Technol Biomed Life Sci*, 2013, **929**, 84-89.
127. S. Kneisel and V. Auwarter, *J Mass Spectrom*, 2012, **47**, 825-835.
128. A. Salomone, E. Gerace, F. D'Urso, D. Di Corcia and M. Vincenti, *J. Mass Spectrom.*, 2012, **47**, 604-610.

129. M. Hutter, S. Kneisel, V. Auwarter and M. A. Neukamm, *J. Chromatogr. B*, 2012, **903**, 95-101.
130. R. Heltsley, M. K. Shelby, D. J. Crouch, D. L. Black, T. A. Robert, L. Marshall, C. L. Bender, A. Z. DePriest and M. A. Colello, *J. Anal. Toxicol.*, 2012, **36**, 588-593.
131. A. Arntson, B. Ofsa, D. Lancaster, J. R. Simon, M. McMullin and B. Logan, *J. Anal. Toxicol.*, 2013, **37**, 284-290.
132. Narcotic Testing Supplies & Equipment Store, Synthetic Cannabinoids test (K2, Spice), <http://shop.narcotictests.com/products/narcotic-field-tests/synthetic-cannabinoids-test-k2-spice/details>, Accessed April 2015.
133. A. D. Lesiak, R. A. Musah, M. A. Domin and J. R. E. Shepard, *J Forensic Sci*, 2014, **59**, 337-343.
134. V. Shevyrin, V. Melkozerov, A. Nevero, O. Eltsov and Y. Shafran, *Forensic Science International*, 2013, **232**, 1-10.
135. N. Uchiyama, R. Kikura-Hanajiri, N. Kawahara and Y. Goda, *Forensic Toxicology*, 2009, **27**, 61-66.
136. N. Uchiyama, M. Kawamura, R. Kikura-Hanajiri and Y. Goda, *Forensic Toxicology*, 2011, **29**, 25-37.
137. S. Kneisel, P. Bisel, V. Brecht, S. Broecker, M. Mueller and V. Auwaerter, *Forensic Toxicology*, 2012, **30**, 126-134.
138. J. i. Nakajima, M. Takahashi, R. Nonaka, T. Seto, J. Suzuki, M. Yoshida, C. Kanai and T. Hamano, *Forensic Toxicology*, 2011, **29**, 132-141.
139. L. Ernst, H.-M. Schiebel, C. Theuring, R. Lindigkeit and T. Beuerle, *Forensic Science International*, 2011, **208**, E31-E35.
140. S. Hudson and J. Ramsey, *Drug Testing and Analysis*, 2011, **3**, 466-478.
141. H. Chung, H. Choi, S. Heo, E. Kim and J. Lee, *Forensic Toxicology*, 2014, **32**, 82-88.
142. K. B. Scheidweiler and M. A. Huestis, *Journal of Chromatography A*, 2014, **1327**, 105-117.
143. A. L. Mohr, B. Ofsa, A. M. Keil, J. R. Simon, M. McMullin and B. K. Logan, *J Anal Toxicol*, 2014, **38**, 427-431.
144. M. Wikstrom, P. Holmgren and J. Ahlner, *J. Anal. Toxicol.*, 2004, **28**, 67-70.
145. M. S. Monteiro, M. D. Bastos, P. G. de Pinho and M. Carvalho, *Archives of Toxicology*, 2013, **87**, 929-947.
146. B. M. Z. Cohen and R. Butler, *International Journal of Drug Policy*, 2011, **22**, 95-101.
147. L. Elie, M. Baron, R. Croxton and M. Elie, *Forensic Science International*, 2012, **214**, 182-188.
148. D. M. Wood, J. Button, S. Lidder, J. Ramsey, D. W. Holt and P. I. Dargan, *Journal of medical toxicology : official journal of the American College of Medical Toxicology*, 2008, **4**, 254-257.
149. C. Wilkins and P. Sweetsur, *Drug and Alcohol Dependence*, 2013, **127**, 72-80.
150. S. Elliott and C. Smith, *J. Anal. Toxicol.*, 2008, **32**, 172-177.

151. A. J. Dickson, S. P. Vorce, J. M. Holler and T. P. Lyons, *J. Anal. Toxicol.*, 2010, **34**, 464-469.
152. C. Montesano, M. Sergi, M. Moro, S. Napoletano, F. S. Romolo, M. Del Carlo, D. Compagnone and R. Curini, *J. Mass Spectrom.*, 2013, **48**, 49-59.
153. S. C. Bishop, B. R. McCord, S. R. Gratz, J. R. Loeliger and M. R. Witkowski, *J. Forensic Sci.*, 2005, **50**, 326-335.
154. M. Wada, K. Yamahara, R. Ikeda, R. Kikura-Hanajiri, N. Kuroda and K. Nakashima, *Biomedical Chromatography*, 2012, **26**, 21-25.
155. I. E. D. Moreno, B. M. da Fonseca, M. Barroso, S. Costa, J. A. Queiroz and E. Gallardo, *J. Pharm. Biomed. Anal.*, 2012, **61**, 93-99.
156. M. Takahashi, M. Nagashima, J. Suzuki, T. Seto, I. Yasuda and T. Yoshida, *Talanta*, 2009, **77**, 1245-1272.
157. M. Monteiro, M. Carvalho, M. L. Bastos and P. G. de Pinho, *Toxicology Letters*, 2013, **221**, S185-S186.
158. K. M. Abdel-Hay, J. DeRuiter and C. R. Clark, *Rapid Commun. Mass Spectrom.*, 2013, **27**, 2551-2558.
159. K. M. Abdel-Hay, C. R. Clark and J. DeRuiter, *Forensic Science International*, 2013, **233**, 113-120.
160. R. J. Waite, G. J. Barbante, N. W. Barnett, E. M. Zammit and P. S. Francis, *Talanta*, 2013, **116**, 1067-1072.
161. M. D. Arbo, M. L. Bastos and H. F. Carmo, *Drug and Alcohol Dependence*, 2012, **122**, 174-185.
162. D. de Boer, I. J. Bosman, E. Hidvegi, C. Manzoni, A. A. Benko, L. dos Reys and R. A. A. Maes, *Forensic Science International*, 2001, **121**, 47-56.
163. M. Philp, R. Shimmon, N. Stojanovska, M. Tahtouh and S. L. Fu, *Anal. Methods*, 2013, **5**, 5402-5410.
164. United Nations Office on Drugs and Crime, Details for Aminoindanes, https://www.unodc.org/LSS/SubstanceGroup/Details/8fd64573-c567-4734-a258-76d1d95dca25#_ftn1, Accessed April, 2015.
165. P. D. Sainsbury, A. T. Kicman, R. P. Archer, L. A. King and R. A. Braithwaite, *Drug Testing and Analysis*, 2011, **3**, 479-482.
166. C. T. Gallagher, S. Assi, J. L. Stair, S. Fergus, O. Corazza, J. M. Corkery and F. Schifano, *Human Psychopharmacology-Clinical and Experimental*, 2012, **27**, 106-112.
167. J. Casale and P. Hays, *Microgram Journal*, 2012, **9**, 18-26.
168. O. Grundmann, S. M. Phipps, I. Zadezensky and V. Butterweck, *Planta Med.*, 2007, **73**, 1039-1046.
169. J. W. Gruber, D. J. Siebert, A. H. Der Marderosian and R. S. Hock, *Phytochem. Anal.*, 1999, **10**, 22-25.
170. C. Medana, C. Massolino, M. Pazzi and C. Baiocchi, *Rapid Commun. Mass Spectrom.*, 2005, **20**, 131-136.

171. M. K. Paudel, O. Shirota, K. Sasaki-Tabata, H. Tanaka, S. Sekita and S. Morimoto, *Journal of Natural Products*, 2013, **76**, 1654-1660.
172. R. Capasso, F. Borrelli, M. G. Cascio, G. Aviello, K. Huben, J. K. Zjawiony, P. Marini, B. Romano, V. Di Marzo, F. Capasso and A. A. Izzo, *Br J Pharmacol*, 2008, **155**, 681-689.
173. J. H. Kennedy and J. M. Wiseman, *Rapid Commun Mass Spectrom*, 2010, **24**, 1305-1311.
174. J. D. Jermain and H. K. Evans, *J Forensic Sci*, 2009, **54**, 612-616.
175. S. Pichini, S. Abanades, M. Farre, M. Pellegrini, E. Marchei, R. Pacifici, L. Torre Rde and P. Zuccaro, *Rapid Commun Mass Spectrom*, 2005, **19**, 1649-1656.
176. M. S. Schmidt, T. E. Prisinzano, K. Tidgewell, W. Harding, E. R. Butelman, M. J. Kreek and D. J. Murry, *J. Chromatogr. B: Anal. Technol. Biomed. Life Sci.*, 2005, **818**, 221-225.
177. B. Janchawee, N. Keawpradub, S. Chittrakarn, S. Prasettho, P. Wararatananurak and K. Sawangjareon, *Biomedical Chromatography*, 2007, **21**, 176-183.
178. M. F. Neerman, R. E. Frost and J. Deking, *J Forensic Sci*, 2013, **58 Suppl 1**, S278-279.
179. R. Kikura-Hanajiri, M. Kawamura, T. Maruyama, M. Kitajima, H. Takayama and Y. Goda, *Forensic Toxicology*, 2009, **27**, 67-74.
180. D. Ponglux, S. Wongseripipatana, H. Takayama, M. Kikuchi, M. Kurihara, M. Kitajima, N. Aimi and S. Sakai, *Planta Medica*, 1994, **60**, 580-581.
181. H. Takayama, *Chemical and Pharmaceutical Bulletin*, 2004, **52**, 916-928.
182. K. Matsumoto, M. Mizowaki, T. Suchitra, Y. Murakami, H. Takayama, S. Sakai, N. Aimi and H. Watanabe, *European Journal of Pharmacology*, 1996, **317**, 75-81.
183. M. Tohda, S. Thongpraditchote, K. Matsumoto, Y. Murakami, S. Sakai, N. Aimi, H. Takayama, P. Tongroach and H. Watanabe, *Biological & Pharmaceutical Bulletin*, 1997, **20**, 338-340.
184. S. Thongpradichote, K. Matsumoto, M. Tohda, H. Takayama, N. Aimi, S. Sakai and H. Watanabe, *Life Sciences*, 1998, **62**, 1371-1378.
185. H. Takayama, H. Ishikawa, M. Kurihara, M. Kitajima, N. Aimi, D. Ponglux, F. Koyama, K. Matsumoto, T. Moriyama, L. T. Yamamoto, K. Watanabe, T. Murayama and S. Horie, *Journal of Medicinal Chemistry*, 2002, **45**, 1949-1956.
186. A. A. Philipp, D. K. Wissenbach, S. W. Zoerntlein, O. N. Klein, J. Kanogsunthornrat and H. H. Maurer, *J. Mass Spectrom.*, 2009, **44**, 1249-1261.
187. N. V. de Moraes, R. A. C. Moretti, E. B. Furr, C. R. McCurdy and V. L. Lanchote, *J. Chromatogr. B*, 2009, **877**, 2593-2597.
188. S. J. Lu, B. N. Tran, J. L. Nelsen and K. M. Aldous, *J. Chromatogr. B*, 2009, **877**, 2499-2505.
189. S. Parthasarathy, S. Ramanathan, S. Ismail, M. I. Adenan, S. M. Mansor and V. Murugaiyah, *Analytical and Bioanalytical Chemistry*, 2010, **397**, 2023-2030.
190. A. A. Philipp, D. K. Wissenbach, A. A. Weber, J. Zapp and H. H. Maurer, *J. Mass Spectrom.*, 2010, **45**, 1344-1357.

191. R. Kronstrand, M. Roman, G. Thelander and A. Eriksson, *J. Anal. Toxicol.*, 2011, **35**, 242-247.
192. T. Arndt, U. Claussen, B. Guessregen, S. Schroefel, B. Stuerzer, A. Werle and G. Wolf, *Forensic Science International*, 2011, **208**, 47-52.
193. R. Bowler, T. J. Davies, M. E. Hyde and R. G. Compton, *Anal. Chem.*, 2005, **77**, 1916-1919.
194. L. R. Cumba, C. W. Foster, D. A. C. Brownson, J. P. Smith, J. Iniesta, B. Thakur, D. R. do Carmo and C. E. Banks, *Analyst*, 2016, **141**, 2791-2799.
195. <http://www.haydale.com/>, Accessed June, 2014.
196. O. Ramdani, J. P. Metters, L. C. S. Figueiredo, O. Fatibello and C. E. Banks, *Analyst*, 2013, **138**, 1053-1059.
197. J. P. Metters, R. O. Kadara and C. E. Banks, *Analyst*, 2011, **136**, 1067-1076.
198. Y. V. R. R. V. Krishnaiah, V. Hanuman Reddy, M. Thirupalu Reddy, G. MadhuSudana Rao, *International journal of Scientific Research*, 2012, **1**, 14-17.
199. I. Morales Fuentes and R. Reyes Gil, *Revista de Saude Publica*, 2003, **37**, 266-272.
200. O. InSug, S. Datar, C. J. Koch, I. M. Shapiro and B. J. Shenker, *Toxicology*, 1997, **124**, 211-224.
201. J. A. Marcusson, B. Carlmark and C. Jarstrand, *Environmental research*, 2000, **83**, 123-128.
202. G. Sandborgh-Englund, C. G. Elinder, G. Johanson, B. Lind, I. Skare and J. Ekstrand, *Toxicology and Applied Pharmacology*, 1998, **150**, 146-153.
203. O. World Health, *Concise International Chemical Assessment Document*, 2003, i.
204. D. A. C. Brownson, D. K. Kampouris and C. E. Banks, *Chemical Society Reviews*, 2012, **41**, 6944-6976.
205. J. DeRuiter, L. Hayes, A. Valaer, C. R. Clark and F. T. Noggle, *Journal of chromatographic science*, 1994, **32**, 552-564.
206. E. M. Garrido, J. M. Garrido, N. Milhazes, F. Borges and A. M. Oliveira-Brett, *Bioelectrochemistry (Amsterdam, Netherlands)*, 2010, **79**, 77-83.
207. J. P. Smith, J. P. Metters, C. Irving, O. B. Sutcliffe and C. E. Banks, *Analyst*, 2014, **139**, 389-400.
208. R. N. Goyal, S. Bishnoi and B. Agrawal, *Journal of Electroanalytical Chemistry*, 2011, **655**, 97-102.
209. Š. Komorsky-Lovrić, N. Vukašinić and R. Penovski, *Electroanalysis*, 2003, **15**, 544-547.
210. V. Krishnaiah, Y. V. Rami Reddy, V. Hanuman Reddy, M. Thirupalu Reddy and G. M. Rao, *International journal of Scientific Research*, 2012, **1**, 14-17.
211. K. Pokpas, S. Zbeda, N. Jahed, N. Mohamed, P. G. Baker and E. I. Iwuoha, *International Journal of Electrochemical Science*, 2014, **9**, 736-759.
212. D. L. Lu, J. Wang, C. Le Ninivin, S. Mabic and T. Dimitrakopoulos, *Journal of Electroanalytical Chemistry*, 2011, **651**, 46-49.

213. E. A. Hutton, B. Ogorevc, S. B. Hocevar, F. Weldon, M. R. Smyth and J. Wang, *Electrochemistry Communications*, 2001, **3**, 707-711.
214. J. Wang, U. Anik and J. M. Lu, *Electrochemistry Communications*, 2001, **3**, 703-706.
215. J. F. Wang, C. Bian, J. H. Tong, J. Z. Sun and S. H. Xia, *Chinese Journal of Analytical Chemistry*, 2012, **40**, 1791-1796.
216. J. Wang, J. Lu, Ü. A. Kirgöz, S. B. Hocevar and B. Ogorevc, *Analytica Chimica Acta*, 2001, **434**, 29-34.
217. S. A. B. Shah, N. I. K. Deshmukh, J. Barker, A. Petroczi, P. Cross, R. Archer and D. P. Naughton, *J. Pharm. Biomed. Anal.*, 2012, **61**, 64-69.
218. P. D'Aloise, H. Chen, *Sci. Justice*, 2012, **52**, 2.
219. H. Druid, P. Holmgren, J. Ahlner, *Forensic Sci. Int.*, 2001, **122**, 136.
220. J. P. Gouille, J. P. Anger, *Ther. Drug Monit.*, 2004, **26**, 206.
221. P. Ghosh, M. M. K. Reddy, V. B. Ramteke, B. S. Rao, *Anal. Chim. Acta*, 2004, **508**, 31.
222. M. P. Juhascik, A. Negrusz, D. Gaugno, L. Ledray, P. Greene, A. Lindner, B. Haner, R. E. Gaensslen, *J. Forensic Sci.*, 2007, **52**, 1396.
223. A. Negrusz, C. M. Moore, K. B. Hinkel, T. L. Stockham, M. Verma, M. J. Strong, P. G. Janicak, *J. Forensic Sci.*, 2001, **46**, 1143.
224. D. Anglin, K. L. Spears, H. R. Hutson, *Adameic Emergency Medicine*, 1997, **4**, 323.
225. T. McKibben, *J. Forensic Sci.*, 1999, **44**, 396.
226. R. H. Schwartz, A. B. Weaver, *Clinical Pediatrics*, 1998, 321.
227. L. R. Brenneisen and S. S. (Eds.), 2001, *Benzodiazepines and GHB: Detection and Pharmacology*, (Totowata, NJ).
228. C. Lledo-Fernandez, C. E. Banks, *Anal. Methods*, 2011, **3**, 1227.
229. K. C. Honeychurch, J. P. Hart, *J. Solid State Electrochem.*, 2008, **12**, 1317.
230. K. C. Honeychurch, A. T. Chong, K. Elamin, J. P. Hart, *Anal. Methods*, 2012, **4**, 132.
231. M. J. Bogusz, R.-D. Maier, K.-D. Krüger and W. Früchtnicht, *Journal of Chromatography B: Biomedical Sciences and Applications*, 1998, **713**, 361-369.
232. A. W. Jones, A. Holmgren and F. C. Kugelberg, *Ther. Drug. Monit.*, 2007, **29**, 248.
233. M. D. Robertson and O. H. Drummer, *J. For. Sci.*, 1998, **43**, 5.
234. M. R. Fuh, S. W. Lin, L. L. Chen and T. Y. Lin, *Talanta*, 2007, **72**, 1329.
235. N. Leesakul, S. Pongampai, P. Kanatharana, P. Sudkeaw, Y. Tantirungrotechai, C. Buramachai, *J. Lumin.*, 2013, **28**, 76.
236. SHS Drinks, <http://www.shs-drinks.co.uk/mainpage.aspx>; Accessed May 2013.
237. N. Samyn, G. D. Boeck, V. Cirimele, A. Verstraete and P. Kintz, *J. Anal. Toxicol.*, 2002, **26**, 211.
238. M. J. Bogusz, R.-D. Maier, K.-D. Kruger and W. Fruchtnicht, *J. Chromatogr. B*, 1988, **713**, 361.
239. I. Deinl, G. Mahr and L. v. Meyer, *J. Anal. Toxicol.*, 1988, **22**, 197.

240. F. Berthault, P. Kintz and P. Mangin, *J. Chromatogr. B*, 1996, **685**, 383.
241. D. B. Faber, R. M. Kok and E. M. R.-V. Dijk, *J. Chromatogr. A*, 1977, **133**, 319.
242. W. Song, X. Ji, W. Deng, Q. Chen, C. Shen and C. E. Banks, *Physical Chemistry Chemical Physics*, 2013, **15**, 4799-4803.
243. W. Deng, X. Ji, M. Gomez-Mingot, F. Lu, Q. Chen and C. E. Banks, *Chemical Communications*, 2012, **48**, 2770-2772.
244. D. A. C. Brownson, L. J. Munro, D. K. Kampouris and C. E. Banks, *Rsc Advances*, 2011, **1**, 978-988.
245. D. A. Brownson and C. E. Banks, Springer, 2014.
246. D. A. C. Brownson, S. A. Varey, F. Hussain, S. J. Haigh and C. E. Banks, *Nanoscale*, 2014, **6**, 1607-1621.
247. D. A. Brownson, D. K. Kampouris and C. E. Banks, *Chemical Society reviews*, 2012, **41**, 6944-6976.
248. A. Ambrosi, C. K. Chua, B. Khezri, Z. Sofer, R. D. Webster and M. Pumera, *Proceedings of the National Academy of Sciences*, 2012, **109**, 12899-12904.
249. C. H. A. Wong, C. K. Chua, B. Khezri, R. D. Webster and M. Pumera, *Angewandte Chemie International Edition*, 2013, **52**, 8476-8476.
250. A. Ambrosi and M. Pumera, *Nanoscale*, 2014, **6**, 472-476.
251. X. Yang, X. Li, X. Ma, L. Jia and L. Zhu, *Electroanalysis*, 2014, **26**, 139-146.
252. E. B. Secor, P. L. Prabhumirashi, K. Puntambekar, M. L. Geier and M. C. Hersam, *The Journal of Physical Chemistry Letters*, 2013, **4**, 1347-1351.
253. E. P. Randviir, D. A. C. Brownson, J. P. Metters, R. O. Kadara and C. E. Banks, *Physical Chemistry Chemical Physics*, 2014, **16**, 4598-4611.
254. A. C. Ferrari, J. C. Meyer, V. Scardaci, C. Casiraghi, M. Lazzeri, F. Mauri, S. Piscanec, D. Jiang, K. S. Novoselov, S. Roth and A. K. Geim, *Physical Review Letters*, 2006, **97**, 187401.
255. F. Tuinstra and J. L. Koenig, *Journal of Chemical Physics*, 1970, **53**, 1126-&.
256. L. C. S. Figueiredo-Filho, D. A. C. Brownson, O. Fatibello-Filho and C. E. Banks, *Analyst*, 2013, **138**, 4436-4442.
257. C. E. Banks, A. Crossley, C. Salter, S. J. Wilkins and R. G. Compton, *Angewandte Chemie International Edition*, 2006, **45**, 2533-2537.
258. B. Šljukić, C. E. Banks and R. G. Compton, *Nano Letters*, 2006, **6**, 1556-1558.
259. M. Pumera and Y. Miyahara, *Nanoscale*, 2009, **1**, 260-265.
260. L. Wang, A. Ambrosi and M. Pumera, *Angewandte Chemie International Edition*, 2013, **52**, 13818-13821.
261. A. Paracchino, V. Laporte, K. Sivula, M. Grätzel and E. Thimsen, *Nat Mater*, 2011, **10**, 456-461.
262. J. P. Smith, J. P. Metters, O. I. G. Khreit, O. B. Sutcliffe and C. E. Banks, *Anal. Chem.*, 2014, **86**, 9985-9992.

263. D. M. Kalendra and B. R. Sickles, *The Journal of organic chemistry*, 2003, **68**, 1594-1596.

Appendix

6.1 The following experimental was performed by a 3rd party:

6.1.1 Characterisation

NMR spectra were acquired on both JEOL AS-400 (JEOL, Tokyo, Japan) and Bruker Avance 400 (Bruker, Karlsruhe, Germany) NMR spectrometers operating at a proton resonance frequency of 400 MHz. Infrared spectra were obtained in the range 4000–400 cm^{-1} using a ThermoScientific Nicolet iS10ATR-FTIR instrument (ThermoScientific, Rochester, USA). Mass spectra were recorded on a ThermoScientific LTQ ORBITRAP mass spectrometer (ThermoScientific, Rochester, USA) using electrospray ionisation. Ultraviolet spectra were obtained using a Unicam 300 UV spectrophotometer (ThermoScientific, Rochester, USA). Thin-Layer Chromatography (TLC) was carried out on aluminium-backed SiO_2 plates (Merck, Darmstadt, Germany) and spots were visualised using ultra-violet light (254 nm). Microanalysis was carried out using a PerkinElmer 2400 Series II elemental analyser (PerkinElmer, San Jose, USA). Melting points were determined using differential scanning calorimetry (DSC; Netzsch STA449 C, Netzsch-Gerätebau, Wolverhampton, UK). Optical rotation values $[\alpha]_{\text{D}}^{22}$ ($10^{-1} \text{ deg cm}^2 \text{ g}^{-1}$) were performed on a Bellingham & Stanley ADP-220 polarimeter (Bellingham & Stanley, Tunbridge Wells, UK).

X-ray Photoelectron Spectroscopy (XPS) measurements were performed with a Kratos Axis Ultra spectrometer using monochromatic Al K X-rays (1486.6 eV) (independently by CERAM). For each sample, the aim was to analyse as large an area as possible within the circular region of interest in order to provide an averaged response over the entire graphene domain.

6.1.2 Chromatography

Liquid chromatography–mass spectrometry (LC–MS) data were acquired using a Finnigan LTQ Orbitrap instrument (Thermo-Fisher Corporation, Hemel Hempstead, UK). Sample analysis was carried out in positive ion (ESI) detection mode. The mass scanning range was 50–1250 m/z , while the capillary temperature was 250 °C and the sheath and auxiliary gas flow rates were 30 and 10, respectively (units not specified by the manufacturer). The LC–MS system (controlled by Xcalibur Ver. 2.0, Thermo-Fisher Corporation, Hemel Hempstead, UK) was run in binary gradient mode. Solvent A was aqueous ammonium formate buffer (10 mM, pH 3.5 ± 0.02) and solvent B was methanol; the flow rate was 0.3 mL min⁻¹. An ACE 3 C18 (150 mm × 4.6 mm i.d., particle size: 3 μm) column (HiChrom Limited, Reading, UK) was used for all analyses. The gradient programme was as follows: 10% B (0 min) to 60% B at 7 min to 60% B at 20 min to 10% B at 25 min. Test solutions: four samples of NRG-2 were obtained from four independent Internet vendors as white crystalline powders in clear zip-lock bags. 5.0 mg of each substance was weighed (in triplicate) accurately into a 100.0 mL clear glass volumetric flask and diluted to volume with deionised water. This solution was then further diluted (1:10) with deionised water to give the test solution.

High Performance Liquid Chromatography (HPLC): Reverse phase high-performance liquid chromatography was performed with an integrated Agilent HP Series 1100 Liquid Chromatograph (Agilent Technologies, Wokingham, UK) fitted with an in-line degasser, 100-place autoinjector and single channel, tunable UV absorbance detector (264 nm). Data analysis was carried out using ChemStation for LC (Ver. 10.02) software (Agilent Technologies, Wokingham, UK). The HPLC system was run in binary gradient mode. Solvent A was aqueous ammonium formate buffer (10 mM, pH 3.5 ± 0.02) and solvent B was methanol; the flow rate was 0.8 mL min⁻¹ with an injection volume of 10 μL. Six replicate injections of each calibration standard were performed. The stationary phase (ACE 3 C18, 150 mm × 4.6 mm i.d., particle size: 3 μm) used in the study was obtained from HiChrom Limited (Reading, UK). The column was fitted with a guard cartridge (ACE 3 C18) and maintained at an isothermal temperature of 22 °C with an Agilent S3 HP Series 1100 column oven with a programmable controller (Agilent Technologies, Wokingham, UK). The gradient

programme was as follows: 30% B (0 min) to 60% B at 7 min to 60% B at 12 min to 30% B at 18 min.

6.1.3 Synthesis

6.1.3.1 Synthesis of 2-bromopropiophenone and 2-bromo-4'-methylpropiophenone

The pre-requisite α -bromoketones were prepared using the method reported by Kalendra *et al.*²⁶³ to a solution of the desired ketone in dichloromethane (50 mL) was added one drop of hydrobromic acid (48% aqueous solution) and one drop of bromine. The mixture was stirred at room temperature until the bromine colour was discharged (*circa.* 30 seconds) and additional bromine (100 mmol total including the original drop) was introduced drop wise with stirring. The mixture was stirred for 1 h and then concentrated *in vacuo* to give a dark orange oils (yield: 95–99%). The α -bromoketones were used in the subsequent step without further purification.

6.1.3.2 2-Bromopropiophenone

Yield = 95.7%; R_f [SiO₂, EtOAc–*n*-hexane (1 : 3)] = 0.81; ¹H-NMR (400 MHz, 25 °C, CDCl₃) δ^1 H (ppm) = 8.02 (2H, dd, J = 7.4 and 1.5 Hz, Ar-H), 7.59 (1H, tt, J = 7.4 and 1.5 Hz, Ar-H), 7.49 (2H, t, J = 7.4 Hz, Ar-H), 5.30 (1H, q, J = 7.0 Hz, CH(Br)CH₃) and 1.91 (3H, d, J = 7.0 Hz, CH(Br)CH₃); ¹³C-NMR (400 MHz, 25 °C, CDCl₃) δ^{13} C (ppm) = 193.2 (C=O), 134.0 (ArCH), 133.6 (ArC), 128.9 (2 \times ArCH), 128.7 (2 \times ArCH), 41.4 (CH(Br)CH₃) and 20.1 (CH(Br)CH₃); m/z (EI, 70 eV) 215 (2, [M⁸¹Br]⁺), 213 (2, [M⁷⁹Br]⁺), 105 (100) and 77 (36%).

6.1.3.3 4'-Methyl-2-bromopropiophenone

Yield = 99.4%; R_f [SiO₂, EtOAc–*n*-hexane (1 : 3)] = 0.79; ¹H-NMR (400 MHz, 25 °C, CDCl₃) δ^1 H (ppm) = 7.91 (2H, d, J = 8.3 Hz, AA'BB'), 7.27 (2H, d, J = 8.3 Hz, AA'BB'), 5.28 (1H, q, J = 7.0 Hz, CH(Br)CH₃), 2.42 (3H, s, ArCH₃) and 1.86 (3H, d, J = 7.0 Hz, CH(Br)CH₃); ¹³C-NMR (400 MHz, 25 °C, CDCl₃) δ^{13} C (ppm) = 193.1 (C=O), 144.8 (ArC), 131.6 (ArC), 129.5 (2 \times ArCH),

O, C1), 134.2 (ArC, C4'), 132.9 (ArC, C1'), 128.8 (2 × ArCH, C3'/C5'), 128.4 (2 × ArCH, C2'/C6'), 57.9 (CHCH₃, C2), 30.4 (NH₂⁺CH₃) and 15.1 (CHCH₃, C3); LRMS (ESI+, 70 eV): *m/z* = 164 (100, [M + H]⁺), 146 (42), 131 (4) and 105 (1%); HRMS (ESI+, 70 eV) calculated for [M + H] C₁₀H₁₄NO: 164.1070, found: 164.1069.

6.1.3.6 4'-Methylmethcathinone hydrochloride [mephedrone hydrochloride] (4-MMC):

Yield = 51.2% (from 4'-Methyl-2-bromopropiophenone); Mpt. (acetone) 251.18 °C; *R_f* [SiO₂, EtOAc-*n*-hexane (1 : 3)] = 0.11; [α]^{22_b} = 0 (*c* = 0.5 g per 100 mL in MeOH); found: C, 61.81; H, 7.52; N, 6.57. C₁₁H₁₆ClNO requires C, 61.82; H, 7.55 and N, 6.55%; UV (EtOH): λ_{max} = 259.5 nm (*A* = 0.735, *c* = 9.95 × 10⁻⁴ g per 100 mL); IR (ATR-FTIR): 2717.5 (NH₂⁺), 1689.5 (C=O), 1606.3 cm⁻¹ (C=C); ¹H NMR (400 MHz, 60 °C, *d*₆-DMSO) δ¹H (ppm) = 9.35 (2H, br s, CH(NH₂⁺CH₃)CH₃); 7.96 (2H, d, *J* = 8.3 Hz, AA'BB'), 7.41 (2H, d, *J* = 8.3 Hz, AA'BB'), 5.08 (1H, q, *J* = 7.2 Hz, CH(NH₂⁺CH₃)CH₃), 2.59 (3H, s, CH(NH₂⁺CH₃)CH₃), 2.41 (3H, s, ArCH₃) and 1.46 (3H, d, *J* = 7.2 Hz, CH(NH₂⁺CH₃)CH₃); ¹³C NMR (400 MHz, 60 °C, *d*₆-DMSO) δ¹³C (ppm) = 195.8 (C=O, C1), 145.5 (ArC, C4'), 130.4 (ArC, C1'), 129.7 (2 × ArCH, C3'/C5'), 128.9 (2 × ArCH, C2'/C6'), 58.1 (CHCH₃, C2), 30.6 (NH₂⁺CH₃), 21.2 (ArCH₃, C7') and 15.5 (CHCH₃, C3); LRMS (ESI+, 70 eV): *m/z* = 178 (6, [M + H]⁺), 160 (47), 145 (100), 130 (7), 119 (16) and 91 (5%); HRMS (ESI+, 70 eV) calculated for [M + H] C₁₁H₁₆NO: 178.1226, found: 178.1226.

6.1.3.7 4'-Methyl-N-ethylcathinone hydrobromide (4-MEC):

Yield = 41.5% (from 4'-Methyl-2-bromopropiophenone); Mpt. (acetone) 206.08 °C; *R_f* [SiO₂, EtOAc-*n*-hexane (1 : 3)] = 0.10; [α]^{22_b} = 0 (*c* = 0.5 g per 100 mL, MeOH); found: C, 52.90; H, 6.65; N, 4.95. C₁₂H₁₈BrNO requires C, 52.95; H, 6.67 and N, 5.15%; UV (EtOH): λ_{max} = 260.0 nm (*A* = 0.693, *c* = 1.02 × 10⁻³ g per 100 mL); IR (ATR-FTIR): 2735.4 (NH₂⁺), 1687.3 (C=O), 1605.4 cm⁻¹ (C=C); ¹H NMR (400 MHz, 60 °C, *d*₆-DMSO) δ¹H (ppm) = 8.92 (2H, br s, CH(NH₂⁺CH₂CH₃)CH₃); 7.98 (2H, d, *J* = 8.4 Hz, AA'BB'), 7.41 (2H, d, *J* = 8.4 Hz, AA'BB'), 5.21 (1H, q, *J* = 6.8 Hz, CH(NH₂⁺CH₂CH₃)CH₃), 3.04 (2H, dq, *J* = 12.4, 7.2 Hz, CH(NH₂⁺CH₂CH₃)CH₃), 2.42 (3H, s, ArCH₃), 1.53 (3H, d, *J* = 7.2 Hz, CH(NH₂⁺CH₂CH₃)CH₃) and 1.28 ppm (3H, t, *J* = 7.2 Hz, CH(NH₂⁺CH₂CH₃)CH₃); ¹³C NMR (100 MHz, 60 °C, *d*₆-DMSO) δ¹³C (ppm) = 195.5 (C=O, C1), 145.2 (ArC, C4'), 130.2 (ArC, C1'), 129.4 (2 × ArC, C3'/C5'), 128.6 (2 × ArCH, C2'/C6'), 56.5

(CHCH₃, C2), 40.2 (NH₂⁺CH₂CH₃, C4); 20.9 (ArCH₃, C7'), 15.7 (CHCH₃, C3) and 10.8 ppm (NH₂⁺CH₂CH₃, C5); LRMS (ESI+, 70 eV): *m/z* = 192 (34, [M + H]⁺), 174 (100), 159 (30), 145 (57), 131 (16), 119 (25) and 91 (6%); HRMS (ESI+, 70 eV) calculated for [M + H] C₁₂H₁₈NO: 192.1383, found: 192.1381.

Once again, thank you Mum and Dad.